

RE-CONFIGURABLE MICROSTRIP PATCH ANTENNAS  
CONTROLLED BY RF MEMS SWITCHES

A THESIS SUBMITTED TO  
THE GRADUATE SCHOOL OF APPLIED AND NATURAL SCIENCES  
OF  
THE MIDDLE EAST TECHNICAL UNIVERSITY

BY

SİNAN ONAT

IN PARTIAL FULFILMENT OF THE REQUIREMENTS THE DEGREE OF  
MASTER OF SCIENCE  
IN  
ELECTRICAL AND ELECTRONICS ENGINEERING

DECEMBER 2006

Approval of Graduate School of Natural and Applied Sciences

---

Prof. Dr. Canan ÖZGEN  
Director

I certify that this thesis satisfies all the requirements as a thesis for the degree of Master of Science.

---

Prof. Dr. İsmet ERKMEN  
Head of Department

This is to certify that we have read this thesis and that in our opinion it is fully adequate, in scope and quality, as a thesis for the degree of Master of Science.

---

Asst. Prof. Dr. Lale ALATAN  
Co-Supervisor

---

Assoc. Prof. Dr. Şimşek DEMİR  
Supervisor

Examining Committee Members

Prof. Dr. Altunkan HIZAL (METU, EEE) \_\_\_\_\_

Assoc. Prof. Dr. Şimşek DEMİR (METU, EEE) \_\_\_\_\_

Asst. Prof. Dr. Lale ALATAN (METU, EEE) \_\_\_\_\_

Assoc. Prof. Dr. Özlem Aydın ÇİVİ (METU, EEE) \_\_\_\_\_

Assoc. Prof. Dr. Vakur B. ERTÜRK BİLKENT UNI., EE) \_\_\_\_\_

**I hereby declare that all information in this document has been obtained and presented in accordance with academic rules and ethical conduct. I also declare that, as required by these rules and conduct, I have fully cited and referenced all material and results that are not original to this work.**

Sinan ONAT

## **ABSTRACT**

### **RE-CONFIGURABLE MICROSTRIP PATCH ANTENNAS CONTROLLED BY RF MEMS SWITCHES**

ONAT, Sinan

M. Sc., Department of Electrical and Electronics Engineering

Supervisor: Assoc. Prof. Dr. Şimşek DEMİR

Co-Supervisor: Asst. Prof. Dr. Lale ALATAN

August 2006, 92 pages

This thesis presents design, fabrication and testing of a number of multi-frequency band microstrip-fed re-configurable microstrip patch antennas. All re-configurable antennas are designed to change from one resonance frequency to another by an electronic control of RF MEMS switches, one at a time. Besides a fixed size slot on the patch, switches are placed in insets for satisfying better input match at each resonance frequency individually. Also some switches are placed into the slot for adding another resonance frequency to change the effective slot-length like effective inset length changing.

To actuate the RF MEMS switches in the configured way, DC-stubs are also designed to apply required potential difference between switch ports and the carrier. These stubs exhibit RF-open at switch side to prevent any RF leakage, and DC-ground on the other side. That RF short-to-open conversion is accomplished together with feed structure; with a taper depending on the feed network selected.

All devices introduced here are built by Microwave Research Group in Electrical and Electronics Department, Middle East Technical University. Depending on the sensitivity of structure, some devices are built by RF MEMS group in Microelectronic Production Plant for MEMS (METU – MET) during the thesis study. Therefore this study is the continuation of the first national work on fabrication of RF MEMS devices.

Keywords: Re-configurable, microstrip patch antennas, RF MEMS switches.

## ÖZ

### RF MEMS ANAHTARLAR İLE KONTROL EDİLEBİLİR TEKRAR-AYARLANABİLİR MİKROŞERİT YAMA ANTENLER

ONAT, Sinan

Yüksek Lisans, Elektrik ve Elektronik Mühendisliği Bölümü

Tez Yöneticisi: Doç. Dr. Şimşek DEMİR

Ortak Tez Yöneticisi: Yrd. Doç. Dr. Lale ALATAN

Ağustos 2006, 92 sayfa

Bu tez birkaç çoklu-frekanslı mikroşerit-beslemeli tekrar-ayarlanabilir mikroşerit yama anten yapılarının tasarım, üretim ve ölçümünü sunmaktadır. Tasarlanan tüm tekrar-ayarlanabilir antenler RF MEMS anahtarlarla elektriksel kontrol edilerek uyumlu rezonans sağlayıp bir rezonans frekansından diğerine atlayacak şekilde tasarlanmıştır. Yama antene açılan sabit yarığın yanı sıra, her bir rezonans frekansında daha iyi giriş empedans uyumunu sağlamak üzere girintilere anahtarlar yerleştirilmiştir. Ayrıca gerektiğinde, yapıya başka bir rezonans frekans eklemek için açılan yarığa anahtar yerleştirilip yarığın-etkin-uzunluğu tıpkı girinti-etkin-uzunluğu gibi değiştirilmiştir.

RF MEMS anahtarları düzenlenen mimaride çalıştırmak için, DA-hatları da tasarlanarak anahtarların uçları ile taşıyıcısı arasında gereken potansiyel fark sağlanmıştır. Bu hatlar anahtarlar ucunda RF-açık devre sağlayıp, herhangi RF kaçağı önler, diğer ucunda ise DA-topraklamayı sağlar. Söz konusu RF-açık devreden kısa devre çevrimi besleme düzeneği ile birlikte sağlanır, bazen de seçilen besleme çeşidine göre ise geçişle da birlikte sağlanabilir.

Burada tanıtılan tüm yapılar Elektrik ve Elektronik Mühendisliği, Orta Doğu Teknik Üniversitesi bünyesindeki Mikrodalga Araştırma Grubu tarafından üretilmiştir. Yapıların üretim hassasiyetine bağlı olarak bazı yapılar MEMS için Mikroelektronik Tesislerinde (ODTU – MET) tez çalışması süresince RF MEMS grubu tarafından üretilmiştir. Dolayısıyla bu çalışma RF MEMS aygıtların üretimi üzerine yapılan ilk ulusal çalışmanın devamıdır.

Anahtar kelimeler: Tekrar-ayarlanabilir, mikroşerit yama antenler, RF MEMS anahtarlar.

*To my professors who made this opportunity possible for me...*

## ACKNOWLEDGEMENTS

I would like to sincerely thank my advisors Prof. Lale ALATAN and Prof. Şimşek DEMİR for their sincere friendship, support and extremely kind attitude towards me besides their great technical guidance together with the encouragement. I owe so much to both of them, also for both providing studying-working facilities within and outside the university, and keeping their trust with patience in my hard times.

I also would like to thank Prof. Vakur B. ERTÜRK for his inspiration during last two years in my undergraduate study in Bilkent University, and supplying a reference letter to my graduate study application. In addition, special thanks to Prof. Özlem Aydın ÇİVİ for accepting me to RF MEMS group as a researcher during a few projects sponsored by TÜBİTAK and DPT.

Being a part of RF MEMS group in Department of Electrical and Electronics Engineering, Middle East Technical University, was a great honour for me. I am very grateful to Hüseyin SAĞKOL, the teacher, for sharing his great experience in RF MEMS, and creating my ambition on being a part of RF MEMS technology during this thesis. Also, thanks to all RF MEMS group members for their friendship. I would like to express my special appreciation to Kağan TOPALLI, Mehmet ÜNLÜ and Mustafa SEÇMEN for their great supervising efforts in design tools and manufacturing of my designs.

My frank thanks would go to all sincere people who supported, trusted me, and still keep existing in my life without leaving, during this thesis study.

## TABLE OF CONTENTS

<b>PLAGIARISM</b> .....	<b>iii</b>
<b>ABSTRACT</b> .....	<b>iv</b>
<b>ÖZ</b> .....	<b>vi</b>
<b>DEDICATION</b> .....	<b>viii</b>
<b>ACKNOWLEDGEMENTS</b> .....	<b>ix</b>
<b>TABLE OF CONTENTS</b> .....	<b>x</b>
<b>LIST OF TABLES</b> .....	<b>xii</b>
<b>LIST OF FIGURES</b> .....	<b>xiii</b>
<b>CHAPTERS</b> .....	<b>1</b>
<b>1. INTRODUCTION</b> .....	<b>1</b>
<b>2. DESIGN STUDIES ON MICROSTRIP ANTENNAS</b> .....	<b>7</b>
2.1. Design Studies on Microstrip Patch Antennas.....	7
2.1.1. Miniaturization in Microstrip Patch Antennas .....	7
2.1.2. Dual Frequency in Microstrip Patch Antennas .....	8
2.1.3. Multi Frequency in Microstrip Patch Antennas .....	15
2.2. Summary .....	15
<b>3. DESIGN STUDIES ON RF MEMS SWITCHES</b> .....	<b>17</b>
3.1. Coplanar Waveguide (CPW) Series Connected Capacitive Switch.....	23
3.2. Microstrip Line Series Connected Capacitive (T-Wing) Switch .....	24
3.3. Manufacturing Process.....	26
<b>4. INTEGRATED RE-CONFIGURABLE (DUAL FREQUENCY)</b> <b>MICROSTRIP PATCH ANTENNA</b> .....	<b>29</b>
4.1. Antenna Design Details.....	33
4.1.1. Microstrip-Feed.....	34

4.1.2.	CPW-Fed.....	34
4.2.	RF MEMS Switch Design Details .....	38
4.2.1.	Single Switch Approach.....	41
4.2.2.	Double (Parallel) Switches Approach.....	41
4.3.	Simulation and Measurement Results .....	44
4.3.1.	CPW-Fed.....	44
4.3.2.	Microstrip-Fed.....	47
4.4.	Summary .....	52
<b>5.</b>	<b>HYBRID RE-CONFIGURABLE (TRIPLE FREQUENCY)</b>	
	<b>MICROSTRIP PATCH ANTENNA .....</b>	<b>55</b>
5.1.	Antenna Design Details.....	56
5.1.1.	Single Stub Configuration.....	59
5.1.2.	Double Stub Configuration .....	64
5.2.	RF MEMS Switch Design Details .....	68
5.2.1.	Slot Switches .....	70
5.2.2.	Inset Switches.....	72
5.3.	Manufacturing Details.....	74
5.3.1.	RF MEMS Fabrication.....	74
5.3.2.	Microstrip-patch Manufacturing .....	75
5.3.3.	Hybridizing the Structure.....	77
5.4.	Simulation and Measurement Results .....	78
5.4.1.	Single Stub Configuration.....	78
5.4.2.	Double Stub Configuration .....	81
5.5.	Summary .....	82
<b>6.</b>	<b>CONCLUSION AND FUTURE WORK .....</b>	<b>85</b>
	<b>REFERENCES.....</b>	<b>88</b>

## LIST OF TABLES

Table 2.1: Suggested miniaturized antenna configuration simulation results.....	8
Table 2.2: Simulation results for different slot shaped antenna configurations.....	9
Table 2.3: Simulation results for different slot shaped (enlarged) antenna configurations.....	14
Table 4.1: Simulated gain results of integrated re-configurable dual-frequency microstrip-fed microstrip patch antenna. ....	51
Table 4.2: 3-dB bandwidth measurement results of integrated re-configurable dual-frequency microstrip-fed microstrip patch antenna. ....	52
Table 5.1: Dimensions of stubs in slot.....	62
Table 5.2: Dimensions of stubs in inset.....	63
Table 5.3: Dimensions of stubs in slot and inset.....	67

## LIST OF FIGURES

Figure 2.1: Highlighted antenna structures with different slot shapes.....	10
Figure 2.2: Interpreted signal flow in dual frequency inset-fed microstrip patch antennas, at (a) Lower frequency, (b) Higher frequency. ....	12
Figure 2.3: Pictures of manufactured different slot shaped antenna configurations. ....	12
Figure 2.4: Simulation and measurement results of manufactured different slot shaped antenna configurations. (a) Design 1-Enlarged, (b) Design 2-Enlarged,.....	13
Figure 3.1: OFF and ON state of switches in the inset. ....	18
Figure 3.2: Single-Pole-Single-Throw (SPST) Switch .....	19
Figure 3.3: Air Bridge (Membrane) Switch.....	20
Figure 3.4: Switch Models, (a) Series Switch (b) Parallel (Shunt) Switch.....	20
Figure 3.5: T-Wing Switch.....	21
Figure 3.6: Single-Pole-Double-Throw (SPDT) Switch.....	21
Figure 3.7: Capacitive Contact Switch (a) ON state (b) OFF state;.....	22
Figure 3.8: SPST Design Pictures .....	23
Figure 3.9: CoventorWare schematic of the CPW-capacitive SPST switch at.....	24
Figure 3.10: RF MEMS switch (a) side view, (b) top view,.....	25
Figure 3.11: Design schematics of T-Wing SPDT switches, by CoventorWare. ....	25
Figure 3.12: Design schematics of T-Wing SPDT switches.....	26
Figure 3.13: Fabrication process steps of RF MEMS switches in this study.....	27
Figure 4.1: Patch with a 0.2 mm x 10 mm sized rectangular slot.....	33
Figure 4.2: The integrated Microstrip-fed Re-Configurable (Dual Frequency) Microstrip Patch Antenna Structure (dimensions are not scaled).....	34
Figure 4.3: Schematic of taper .....	35
Figure 4.4: RF characteristics of taper .....	36

Figure 4.5: The integrated CPW-fed Re-Configurable (Dual Frequency) Microstrip Patch Antenna Structure (dimensions are not scaled).....	37
Figure 4.6: Electrical characteristic goal determination study results .....	39
Figure 4.7: Electrical Schematic and Electrical Performance of suggested switch structure in Single Switch Approach.....	40
Figure 4.8: Suggested switch structure in Double Switch Approach.....	42
Figure 4.9: Designed and manufactured .....	43
Figure 4.10: Simulation results of integrated re-configurable dual-frequency CPW-fed microstrip patch antenna. (a) Close look around 6.5 GHz,.....	45
Figure 4.11: Comparison of Optimized and Un-Optimized CPW-Fed Configuration .....	47
Figure 4.12: Simulation and measurement results of integrated re-configurable dual-frequency microstrip-fed microstrip patch antenna. ....	48
Figure 4.13: Radiation pattern simulation and measurement results of integrated re-configurable dual-frequency microstrip-fed microstrip patch antenna. ....	50
Figure 5.1: Hybrid Re-Configurable (Triple Frequency) Microstrip Patch Antenna .....	55
Figure 5.2: ON state metal strip model performance of two inset width alternatives. ....	57
Figure 5.3: S11 performance of ideal antenna structure resonating at 1.9 GHz. ....	58
Figure 5.4: Slot switch grounding stub alternatives investigated in the study,.....	60
Figure 5.5: Impact of chosen radial stub .....	61
Figure 5.6: Phase performance of slot stub .....	62
Figure 5.7: Inset stub in single stub in configuration.....	63
Figure 5.8: Phase performances of inset stub.....	64
Figure 5.9: Metal strip model driven design goals of triple-frequency antenna. ....	65
Figure 5.10: Close look into proposed inset structure in double stub configuration. ....	66
Figure 5.11: The proposed inset whole structure in double stub configuration.....	66
Figure 5.12: Overall proposed hybrid re-configurable (triple-frequency) microstrip patch antenna with double stub configuration.....	67

Figure 5.13: Inset switch alternatives (a) Single SPST, (b) Serial connected SPSTs, .....	68
Figure 5.14: Switch type alternative simulation results to be used in antenna structure.....	69
Figure 5.15: Designed slot switches (1.9 GHz) for double stub configuration of hybrid re-configurable (triple-frequency) microstrip patch antenna.....	71
Figure 5.16: Designed inset switches (1.9 GHz) for double stub configuration of hybrid re-configurable (triple-frequency) microstrip patch antenna.....	72
Figure 5.17: Designed inset switches (2.4 GHz) for double stub configuration of hybrid re-configurable (triple-frequency) microstrip patch antenna.....	73
Figure 5.18: Manufactured double stub RF MEMS switches.....	75
Figure 5.19: Manufactured double stub configuration of hybrid re-configurable (triple-frequency) microstrip patch antenna.....	76
Figure 5.20: Simulation and measurement results of optimized hybrid re- configurable (triple-frequency) microstrip patch antenna single stub configuration with metal strip modelling. (a) At 1.8 GHz state (all switches are at OFF state) ....	79
Figure 5.21: Radiation pattern simulation results optimized hybrid re-configurable (triple-frequency) microstrip patch antenna single stub configuration with metal strip modelling, .....	80
Figure 5.22: Simulation results of optimized hybrid re-configurable (triple- frequency) microstrip patch antenna double stub configuration including RF MEMS switches at 2.4 GHz state (all switches are at ON state) .....	82

# CHAPTER I

## INTRODUCTION

One of the important developments in communication technologies is the integration of several applications like cellular phones, satellite communications and wireless local area networks (WLAN) into a single and compact system. Since each application operates in a different frequency band with different types of polarization and radiation characteristics, these complex systems require the design of different antennas. Due to the limitations on the physical size of these systems it is not practical to construct separate antennas for each application. Therefore, the design of multi-function antennas, which could incorporate different radiation characteristics in a single antenna element, has become an important research area for antenna engineers.

In this thesis study, at first, various modifications are practised on a patch microstrip antenna for different functions, with a desire for compactness, mostly either antenna miniaturizing or enhancing antenna performances while not increasing the dimensions. In the literature it is well known that, placing pins on a patch at some distant from the feed would miniaturize the patch antenna up to 50% [1 – 2]. Other than using shorting pins; opening slots such as L-, E- or U-shaped slots on a patch antenna is also widely preferred in literature for both miniaturizing and obtaining wide bandwidth enhancements [2 – 8]. In addition, simply a rectangular slot could be used to get another resonance, in multi-frequency manner [9 – 11]. A complete design study within this thesis work about dual-frequency microstrip patch antenna

by opening different shaped slots is explained in Chapter 2. Together with design results, also measurement results are given in detail within the same chapter.

Generally, the cost of compactness is requiring much finer tuning in the design and much more sensitivity to manufacturing tolerances. It is a great challenge to increase all electrical characteristics at the same time, or improve some of them while keeping the others same. Usually compactness results with degradation in some other performance parameters. Therefore other than implementing compactness into any device, to increase the performance by multi-functioning or in other words using “re-configurability” becomes an alternative. Re-configurability of a device is adapting or adjusting itself for improving the selected performance while keeping the other characteristics un-degraded based on certain and different scenarios. This offers some additional higher performance one at a time in stead of having the same performance at all times [12 – 18]. For example, a re-configurable dual frequency antenna, which is a type of multi-function antennas, operates at two separate frequency bands one at a time with the same input impedance, polarization, directivity and all the other radiation characteristics within these bands [19 – 21].

This thesis is mostly focused on frequency re-configurability of microstrip patch antennas. This topic is determined while studying on several examples among multi-function (mostly multi-frequency) antennas in the literature [12 – 21]. The major trouble observed was regenerating the specified accurate performances in journals also by EM simulators (Ansoft Ensemble and Ansoft HFSS) in different situations. Unfortunately, it has been observed that the dimensions and sizes of those studied antennas were generally so fine tuned that it was unlikely to re-achieve the assigned performance; especially in the case of multi-frequency antennas [2]. Therefore the use of re-configurability is found the most convenient way to implement multi-frequency function on a microstrip patch antenna while keeping the standard level of easiness of manufacturing and design repeatability.

There are many published journals in the literature on multi-frequency re-configurable antennas by the year of 2006. The most common two ways of

implementing re-configurability (switching between modes / states) on a microstrip patch antenna, is either using purely electronic (PIN diodes or FET transistors) or micro-electro-mechanical-systems (RF MEMS) switches. There are some pros and cons for both approaches [22 – 27]. RF MEMS technology was a new technology at the time this thesis study started (in 2002), the second method preferred is PIN diode switching. Some of the similar novel studies could be listed as [28 – 31].

In [28], patch antennas with switchable slots (PASS) are introduced; concepts, designs and applications of a PASS antenna are described. A probe fed antenna is selected as the default structure to realize all re-configurability functions. At first, the authors implemented multi-frequency approach by opening a single slot, and placing a PIN diode (HPND-4005) within that slot. They also observed that when the frequency ratio of those switched resonance frequencies are getting bigger, an impedance tuning is required to have valid and useful radiations in both frequencies. Other than frequency switching, with this novel technique, polarization switching between right-hand and left-hand circular polarization (CP) is implemented. This feature is again implemented on probe-fed antenna, by using two perpendicular intersecting slots, with each having oppositely directed diodes on themselves. By applying enough positive or negative voltages, one of the diodes are activated and make its own slot ineffective. Therefore either LHCP or RHCP is achieved. The authors also refer to RF MEMS switch applications as a possible alternative to their suggested applications.

In [29], a study on re-configurable aperture (RECAP) antennas, is presented, which proposes the design methodology of a planar array of electrically small, 120 metallic patches that are interconnected by FET transistor switches together with the model (FDTD) and measurement results. The manufactured antenna (in Georgia Tech Research Institute, Georgia Institute of Technology) is good for resonance bandwidth enhancement and beam steering. The re-configurability, interconnection diagram within 120 patches are successfully created by a genetic algorithm. Here in this paper, the power consumption and timing performance of used FET transistors

are also highlighted, where RF MEMS switches are recommended for future such studies based on improved characteristics.

In [30], a fully integrated solution providing scan-beam capability with a single antenna is presented. The proposed two probe-fed antennas include a set of MEMS switches, which are monotonically integrated and packaged onto the same substrate. Simply these antennas (both printed on printed circuit board - PCB and quartz) change radiation pattern based on the states of their RF MEMS switches. Here one of the most important design guidelines is using separate voltage sources for each capacitive membrane type RF MEMS switch, to actuate them individually. In the feeding structure, also there is a radial stub to prevent some leakage through the RF signal path.

[31] is a novel study on re-configurable patch antennas using RF MEMS switches. In this research ohmic contact cantilever RF MEMS switches are integrated with self-similar planar antennas to provide a re-configurable antenna system that radiates similar patterns by integrating the MEMS switches. In the paper design procedure, simulation and measurement results of the bow-tie antenna consisting of several triangular patches are given. Especially compared to the previous research [29], the radiation pattern degradation based on power - losses of FET transistors are not observed in this study. In the paper, it is also pointed out that one of the most important steps in the design procedure is satisfying the matching for selected studied frequencies (8.3 GHz, 15 GHz, and 25 GHz) at each switch state.

As demonstrated in literature examples above, opening a slot on the patch gives two resonance frequencies, in general. But keeping the same feed structure does not result in satisfactory matching levels at both of the frequency bands, because of the frequency dependent behaviour of the patch. In this thesis, as a solution to this problem, changing the feed location of a microstrip line fed patch antenna by electronically controlling the length of the inset through the use of RF MEMS T-Wing switches is suggested. Placing RF MEMS T-Wing switches across the inset, combined structure provides two states. When switches are at ON state, they do

conduct and shorten the inset length; and when the switches are at OFF state, they do not conduct and antenna operates as if there is nothing in the inset. In summary, ON and OFF states of switches correspond to the shorter and the longer inset lengths respectively which provide better and deeper resonance one at a time, respectively.

This thesis is composed of six chapters. After this introduction chapter, a detailed compact microstrip patch antenna structure design study is summarized. Some major topics in the presented part of the study are slot shape effects in microstrip antennas, miniaturization of patch antennas, dual- and multi-frequency microstrip patch antennas. Some measurement results are also shown at the end of that chapter, to demonstrate the agreements on compact antenna design simulation and measurement results. Then, in Chapter 3, some design works on RF MEMS switches are presented. These design efforts are spent both in electro-magnetic and electro-mechanical perspectives, which are specified briefly in that chapter. These designs are also validated by measurements after fabrication in METU facilities by RF MEMS group.

In the beginning of Chapter 4, the detailed design methodology is listed for easiness to follow the whole procedure. Other than that, complete design, fabrication and measurement phases of two integrated re-configurable dual-frequency microstrip patch antennas are explained. One of these antennas is CPW-fed and the other is microstrip-fed. They are both optimized during the design for the best performance and manufactured (by Kağan Topallı, Mehmet Ünlü, Halil İbrahim Atasoy, İpek İstanbulluoğlu, Ufuk Temoçin) to observe the both real-life input return loss and radiation characteristics.

Next, in the fifth Chapter, a different multi-frequency microstrip patch antenna design is presented. This antenna is a triple-frequency antenna, implemented by an additional couple of switches on the slot to change effective length of the slot. Another change in this antenna compared to the one in the previous chapter is its hybrid structure. The switches are manufactured through MEMS fabrication;

however patch and all stubs are manufactured (by Mustafa Seçmen) through regular microstrip patch fabrication. And then these two different scaled objects are connected through wire-bond. The detailed explanation regarding to the design and fabrication together with simulation and measurement results regarding this type of structure are shown in Chapter 5.

Lastly, conclusion and future works are presented in Chapter 6. In this chapter, the contribution of this research work is also summarized.

## CHAPTER II

### DESIGN STUDIES ON MICROSTRIP ANTENNAS

In this thesis, microstrip patch antennas are the primary research subject. To have a deeper insight on microstrip patch antennas, a number of different configurations are analyzed. Especially microstrip inset-fed antennas are studied from several design point of views. These analyses are performed by a 2.5D EM simulator: Ansoft Ensemble v8.0. In this chapter, the design work during the literature survey phase is being introduced in detail.

#### 2.1. Design Studies on Microstrip Patch Antennas

Antennas are designed for some functional goals, such as a specific radiation type, polarization, resonance frequency, directivity etc. In this section, a few examples of such antenna designs are going to be introduced. These design efforts are discrete individual studies for better understanding of microstrip antennas. In the first part, a miniaturized antenna structure is designed using shorting pins (via) to ground; in the second part, different slot shaped dual-frequency antenna structure behaviour is investigated including the consideration of current distribution on the patch. In the third section, multi-frequency structures are explained shortly.

##### 2.1.1. Miniaturization in Microstrip Patch Antennas

There are several methods to miniaturize microstrip patch antennas. In this study, a microstrip patch antenna having a resonance at 2.0 GHz is studied. The antenna is

**Table 2.1:** Suggested miniaturized antenna configuration simulation results.

<b>Antenna with</b>	<b>Resonance Frequency</b>	<b>Via Radius</b>	<b>Inset Dimensions</b>
<b>No pins</b>	2.00 GHz	N / A	15.5 mm x 1.0 mm
<b>9 Pins</b>	1.05 GHz	2.0 mm	15.5 mm x 1.0 mm
<b>15 Pins</b>	1.08 GHz	1.0 mm	15.5 mm x 1.0 mm
<b>27 Pins</b>	1.09 GHz	0.5 mm	15.5 mm x 1.0 mm

placed on a 1.52 mm thick RO 4003 substrate and the patch dimensions are 40.56 mm x 40.56 mm. After placing a number of pins, resonance frequency of the miniaturized antenna is obtained around 1.0 GHz, which is shortening in both axes.

The simulation results of configurations with several number of shorting pins (via) on the radiating side of the patch antenna are shown in Table 2.1.

### **2.1.2. Dual Frequency in Microstrip Patch Antennas**

Another common functional modification on microstrip antennas is inserting a second resonance while slightly changing the other. This type of function can be easily achieved by placing via(s) or slot(s) on appropriate positions of the inset-fed patch, as mentioned briefly before. The objective in both approaches is creating a second possible path for signal to flow from the antenna input to the radiating edge of the patch, while changing the default one a little.

Because of possible implementation and manufacturing realization difficulties in vertical axis, inset-fed structures are the preferred patch antenna structures in this work. Also placing slot(s) on proper positions on the patch are determined as the most convenient way. An extensive study on the effect of shape of a single slot on a patch is introduced below in detail.

Opening slot is one of the simplest modifications that could be implemented on the microstrip patch. That effect on a patch is modelled by adding admittance in circuit model [32]. The area of the slot is the dominant parameter on determining that

admittance. However the shape of the slot is also very important. These two dependencies were centre of the interest in this particular study.

An antenna with RO 4003 substrate resonating at 7.73 GHz and having patch dimensions of 9 mm x 10 mm is examined for determining slot shape effect on antenna resonance frequency. Slot length is defined as 9.5 mm, and width is 0.2 mm maximum in all configurations; except Designs 9 – 11. Those designs have 0.1 mm x 9.5 mm sized rectangular shaped slots (similar but smaller than the corresponding dimensions in Design 1). Those narrower slots differ from each other due to their exact horizontal slot positioning. D10 could be interpreted as having a slot such that left half of the slot in D1, where as D11 has the right half of D1. And D9 is a patch having a slot just the centre of the slot of D1. Some of the studied antenna structure schematics and corresponding simulation results are shown in Table 2.2 and Figure 2.1, respectively.

**Table 2.2:** Simulation results for different slot shaped antenna configurations.

<b>Design no:</b>	<b>f<sub>1</sub> (GHz)</b>	<b>f<sub>2</sub> (GHz)</b>	<b>Ratio (f<sub>2</sub> / f<sub>1</sub>)</b>
<b>D1</b>	6.939	9.055	1.305
<b>D2</b>	6.937	8.725	1.258
<b>D3</b>	7.191	9.328	1.297
<b>D4</b>	7.097	9.387	1.323
<b>D5</b>	6.777	8.730	1.288
<b>D6</b>	6.629	8.756	1.321
<b>D7</b>	6.935	8.967	1.293
<b>D8</b>	7.039	9.039	1.284
<b>D9</b>	6.989	8.997	1.287
<b>D10</b>	6.888	9.042	1.313
<b>D11</b>	7.056	8.992	1.274

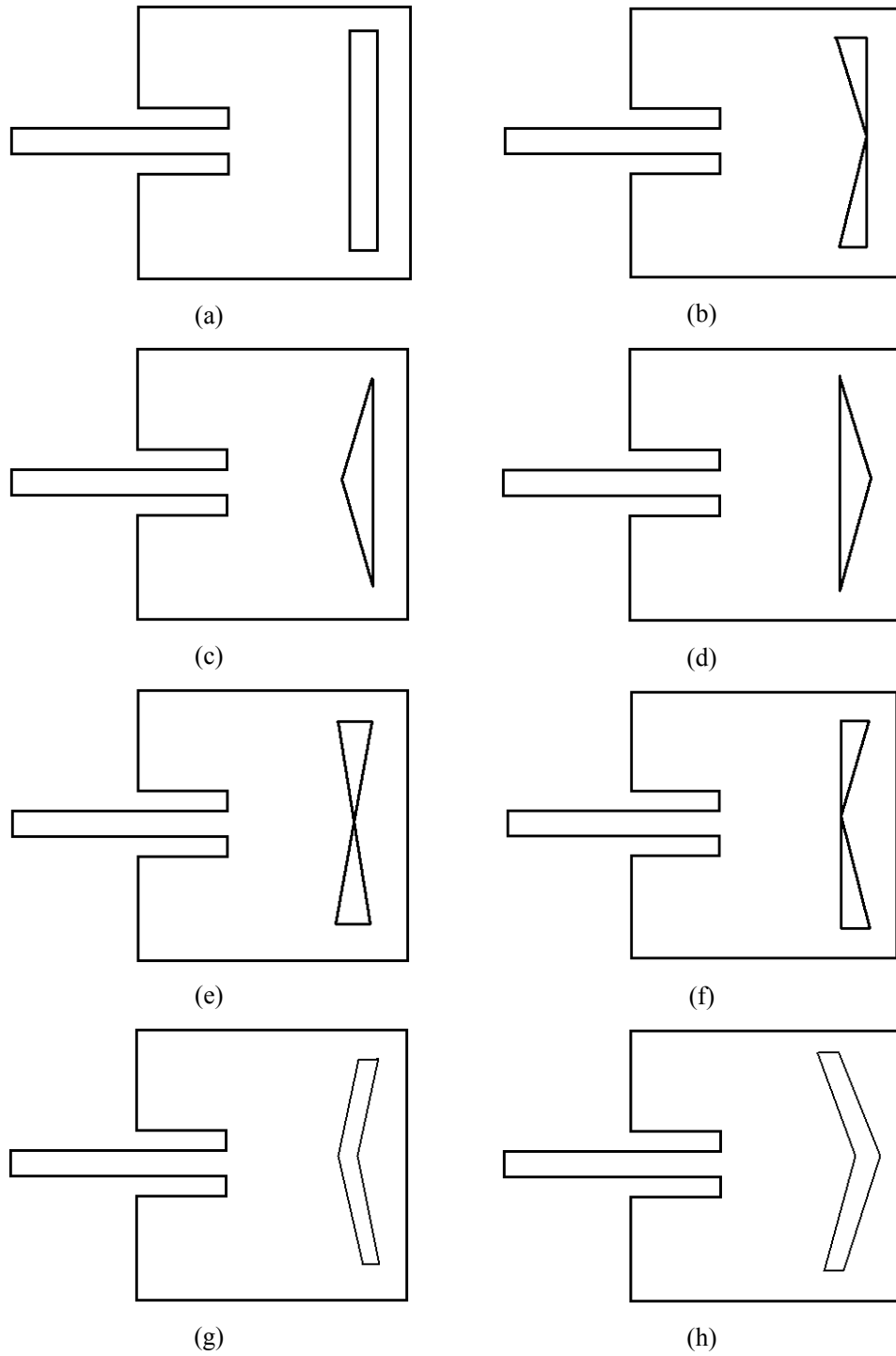


**Figure 2.1:** Highlighted antenna structures with different slot shapes.

(a) - (h) Design 1 – 8.

As it can be observed from Table 2.2, resonances are mainly around 7 GHz and 9 GHz. In addition, resonance frequencies change in 600 – 700 MHz band at each frequency, based on the shape of the slot. These changes resulted with frequency ratios from 1.25 to 1.32.

Current distribution on the patch is also investigated for better understanding the slot shape effect. As specified before, patch without any slot on it has a resonance frequency of 7.73 GHz. Rectangular shaped slot (D1) lowers that frequency to  $f_1 = 6.94$  GHz, which is explained as the increase in the signal flow path around the slot by a certain slot length and width. Similar  $f_1$  value for Design 2 proves that, low resonance frequency has less dependence on left-side shape of slot. However, in the 5<sup>th</sup> and the 6<sup>th</sup> designs, due to mid-section shrinking structures of slot, the space between slot and radiating edge of the patch is increased. This causes indirect arrival of the signal to the radiating edge, resulting with the lowest  $f_1$  value. Based on the same reason, designs 3 and 4 have the highest  $f_1$ , because shrinking slot-width allow the signal to pass around corner of slot quicker and finally to arrive the radiating edge among the shortest path distance.

The comparisons of upper frequency of specified designs are commented relative to the  $f_2$  value of the rectangular shaped slot design (D1). This value decreases in the 2<sup>nd</sup>, 5<sup>th</sup> and 6<sup>th</sup> designs; but increases in the 3<sup>rd</sup> and 4<sup>th</sup> designs, in an order of 300 MHz. When current distributions are examined at upper resonances, increasing effective-slot-distances are observed due to concave, straight and convex shapes; respectively. In addition, current weighted distances cause little variations in the 2<sup>nd</sup> – 5<sup>th</sup> – 6<sup>th</sup> and 3<sup>rd</sup> – 4<sup>th</sup> designs, in order.

Based on comparisons between explained designs (D1 – D6), some prospective (Design 7 – 11) studies are also made and great agreement is observed between estimated and achieved simulation results, due to above reasoning [33].

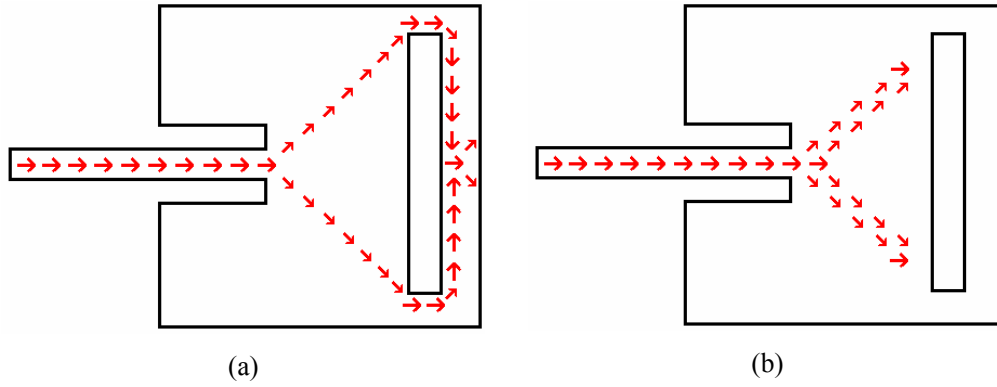


**Figure 2.2:** Interpreted signal flow in dual frequency inset-fed microstrip patch antennas, at (a) Lower frequency, (b) Higher frequency.

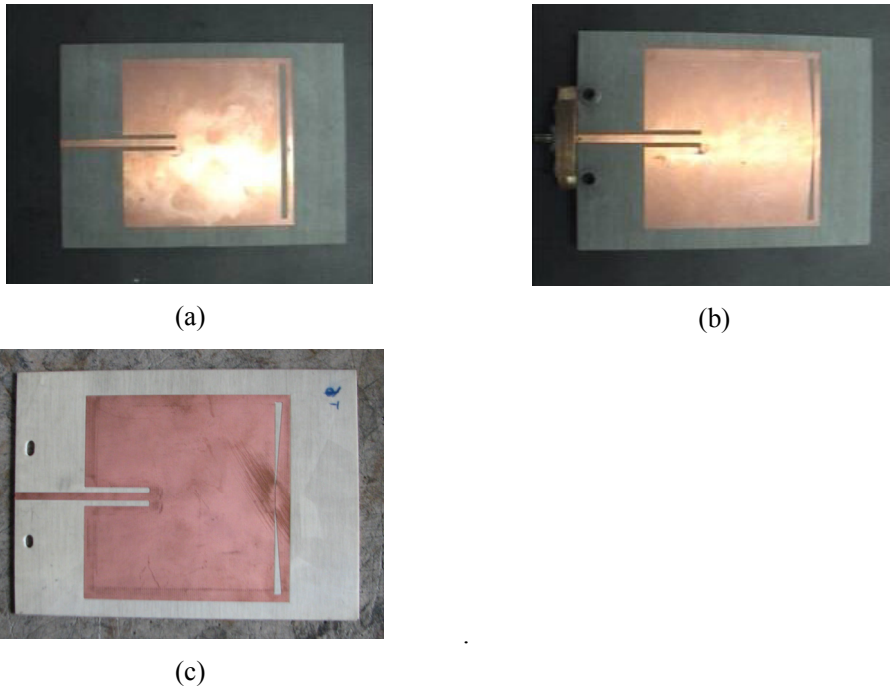
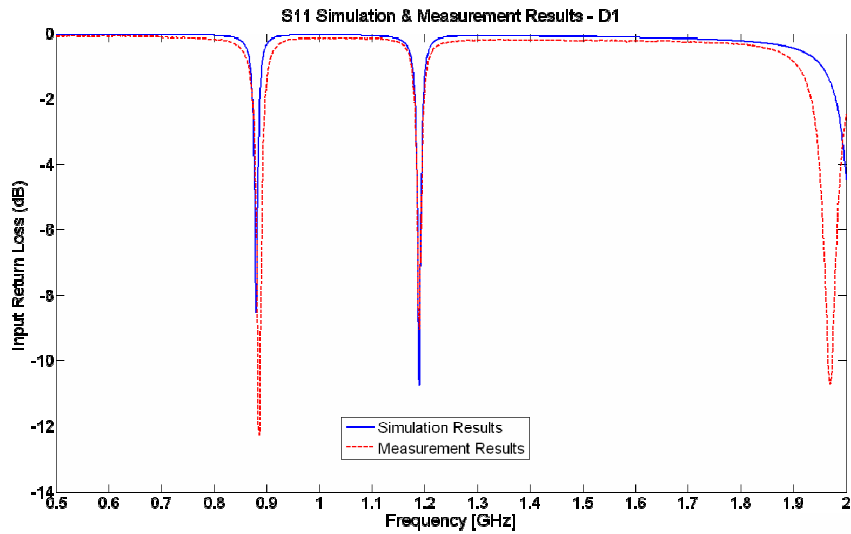


**Figure 2.3:** Pictures of manufactured different slot shaped antenna configurations. (a) Design 1-Enlarged, (b) Design 2-Enlarged, (c) Design 6-Enlarged

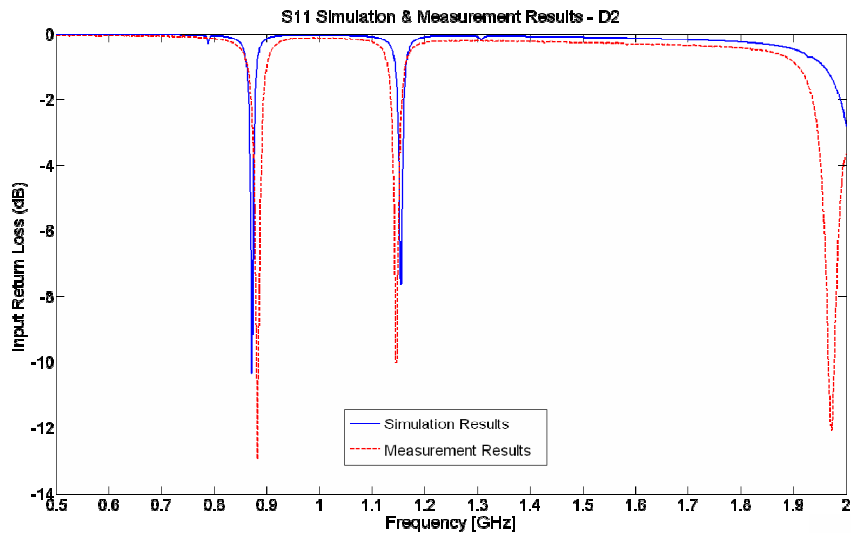
As a conclusion, the suggested signal flow paths that make the patch resonate at two different frequencies are shown in Figure 2.2.

To validate the obtained simulation results with measurement results, some selected designs are decided to be manufactured in METU EEE Department Microwave Laboratory. Unfortunately because of slot shapes being so thin, it was hard to give

such shapes in manufacturing, especially at those sizes. That's why antenna configurations are enlarged to resonate around 1 GHz, in stead of 7.73 GHz plain patch resonance frequency. Due to this change, patch dimensions and slot width are increased to 81 mm x 81 mm, and 3 mm, respectively. Also, slot spacing from the edges are increased from 0.25 mm to 3.0 mm in that enlarged structure (Figure 2.3).

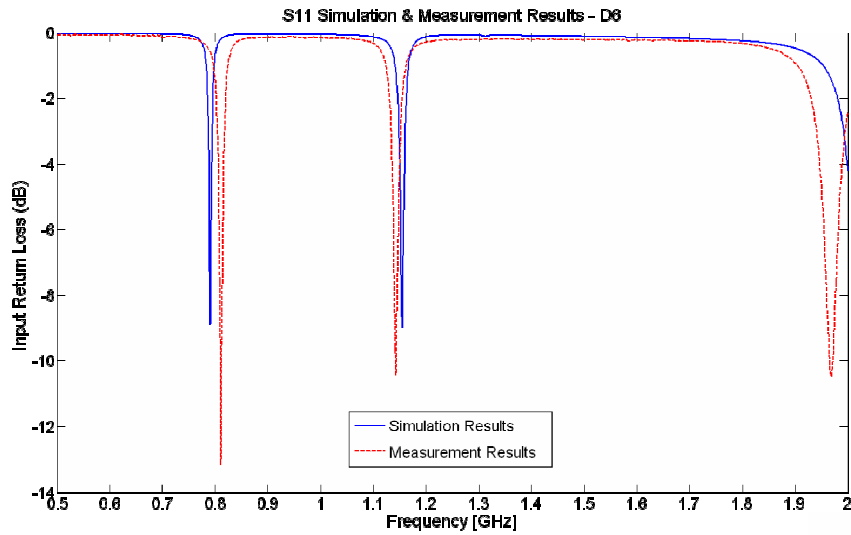


(a)



(b)

**Figure 2.4:** Simulation and measurement results of manufactured different slot shaped antenna configurations. (a) Design 1-Enlarged, (b) Design 2-Enlarged,



(c)

**Figure 2.4 (cont'd):** Simulation and measurement results of manufactured different slot shaped antenna configurations. (c) Design 6-Enlarged.

**Table 2.3:** Simulation results for different slot shaped (enlarged) antenna configurations.

Design no:	$f_1$ (GHz)	$f_2$ (GHz)	Ratio ( $f_2 / f_1$ )
<b>D1-Enlarged (Simulation)</b>	0.882	1.193	1.352
<b>D2-Enlarged (Simulation)</b>	0.886	1.164	1.313
<b>D6-Enlarged (Simulation)</b>	0.805	1.158	1.438
<b>D1-Enlarged (Measurement)</b>	0.886	1.190	1.343
<b>D2-Enlarged (Measurement)</b>	0.882	1.145	1.298
<b>D6-Enlarged (Measurement)</b>	0.811	1.143	1.410

Same-shaped but enlarged structure simulation and measurement results are listed in Table 2.3, input return loss curves are shown in Figure 2.4. In the graphs, input matching of all configurations is only around -10 dB; it is because of the fix inset length, which was determined as the best match for both frequencies at the same time.

From the results, it could be observed that frequency variations and corresponding variations are different than the previous table. The main objective here is to show the increase or decrease tendency of resonance frequency due to different shape of slots opened at the same location on the patch. The changes are all in the same direction; increases or decreases are as expected. Therefore the explanation provided in the first section are demonstrated, that is the prospective designs are validated by those last measurement results. In all plots, the simulation and measurement results are just varied for a few MHz. Although the structures are simple, the slot shapes were not easy to open. The slots are drawn by the automated machine but the connections are opened manually, with a knife by hand. So these differences could be reasoned by manufacturing inaccuracies.

### **2.1.3. Multi Frequency in Microstrip Patch Antennas**

Similar to dual-frequency microstrip antennas explained in previous sections, more than two resonance frequencies at the same time are also achievable by complicating the microstrip antenna structure. Many modifications (via, slot, loading etc.) could be applied at the same time on the upper metal layer of the patch antenna [2]. In fact, a good match at all those resonance frequencies at the same instant; needs very challenging design and also a precise manufacturing.

## **2.2. Summary**

In this part of thesis, some designs inspired from literature survey are studied to observe more about resonance characteristics of microstrip patch antennas. Two major implementations on a patch are focused on: effects of shorting pins (via) to the ground layer and opening slots on the radiating edge. Some of the observed effects were miniaturization, dual-frequency. Both modifications had a recognizable effect on resonance characteristics as well as radiation characteristics. Therefore there is no mean to determine the one better than the other. However the selection among them is made depending on the fabrication capability, preference or sensitivity (resolution) of manufacturer, and some feeding architecture in the design

if needed. Slots and shorting pins could also be implemented at the same time; there are several papers in the literature about such designs result with multi-frequency or enhanced bandwidth, but to distinguish individual effects. Those types of structures are not studied here, in stead they are studied individually.

## CHAPTER III

### DESIGN STUDIES ON RF MEMS SWITCHES

In this study, the purpose of utilizing RF MEMS switches is to impose re-configurability function to microstrip patch antennas. By using RF MEMS switches the shape of the microstrip antenna will be re-configured to obtain multi-frequency operation. Opening a slot on a microstrip patch antenna is a very common way to achieve dual frequency operation, as discussed in the previous chapter. Although two separate resonances may be observed by opening a slot on the patch, it may not be possible to obtain satisfactory matching levels for both of the frequency bands, because of the frequency dependence of the patch.

It is well known that the input matching of a microstrip antenna can be achieved by adjusting the position of the feed. However the best input matches for two separate frequencies might correspond to different feed positions. Since it is not practical to change the feed location, usually a compromise is made and sub-optimum input return loss values (much worse than -20 dB levels) are obtained for both of the frequency bands with a single feed location. As a solution to this problem, changing the feed location of a microstrip line fed patch antenna by electronically controlling the length of the inset through the use of RF MEMS switches is suggested.

Placing RF MEMS switches across the inset provides two states. When switches are at ON state, they do conduct and shorten the inset length; and when the switches are at OFF state, they do not conduct and antenna operates as if there is nothing in the inset. In summary, ON and OFF states of switches correspond to the shorter and the

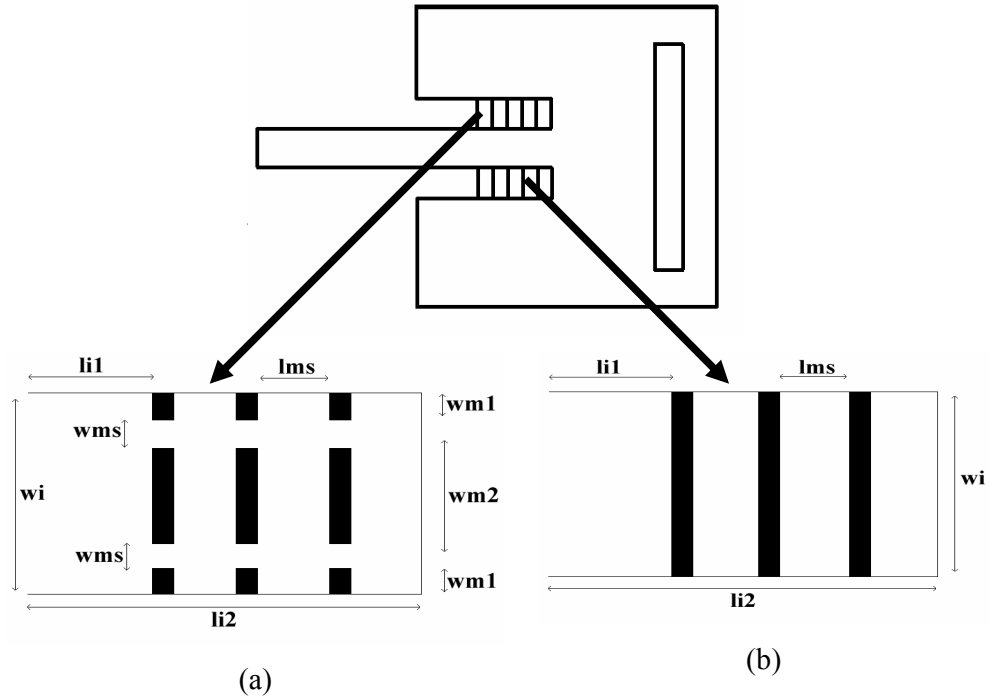


**Figure 3.1:** OFF and ON state of switches in the inset.

(a) OFF State, (b) ON State

longer inset lengths which provide better deeper resonance one at a time, respectively (Figure 3.1).

The insertion loss in the ON state, the isolation in the OFF state and the return loss in both states are the important performance parameter that needs to be optimized in the design of RF switches. The switching of RF MEMS switches between the ON and OFF states is achieved through the mechanical actuation of a metallic segment by applying a DC voltage. The design of RF MEMS switches needs a detailed study to realize the required performance as there are also some mechanical and electrical restrictions for each suggested structure. First of all, any proposed mechanical configuration should be evaluated in terms of possible fabrication processes. Secondly, the materials used in the design should be chosen properly to avoid mechanical problems like stiction where parts of the MEMS device are bonded together upon physical contact. In addition to that, while optimizing the dimensions of the metallic segments that are actuated, the limitations on the DC voltage values should be considered as well as other performance parameters. Finally, the problems

related to the routing of the DC bias lines needs to be resolved during the design of printed structures with integrated RF MEMS switches.

The RF MEMS switches can be categorized by the following three characteristics [34, 40 – 42]:

- a) mechanical structure
- b) RF circuit configuration
- c) form of contact

**a) Mechanical Structure**

The most common mechanical structures are the cantilever and the air bridge. The basic cantilever structure is shown in Figure 3.2. Input side is connected to output side by a one-corner-twistable-cantilever-beam whenever enough voltage is applied between the beam and the centre conductor. The post height is adjusted according to the required capacitance between the beam and the centre conductor.

The air bridge (membrane) type switch is not only different from others structurally but also mechanically. In structure point of view, beams of cantilever type switches are hanging about a single post; however membrane switches hang about two posts as shown in Figure 3.3. The difference related to the mechanics is such that, when a DC voltage is applied, the middle of the air bridge collapses whereas the corner of the beam twists in a cantilever type switch.

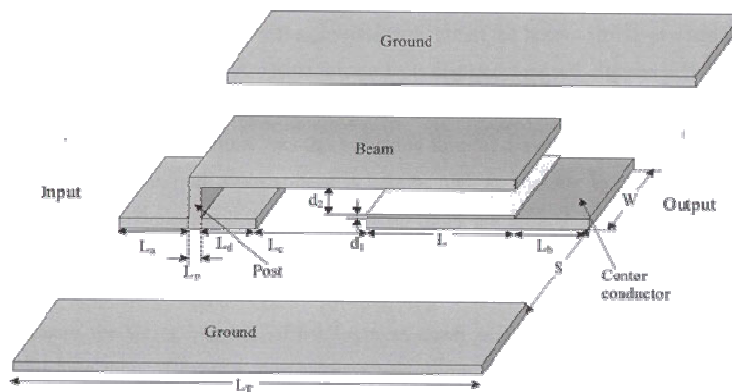


**Figure 3.2:** Single-Pole-Single-Throw (SPST) Switch

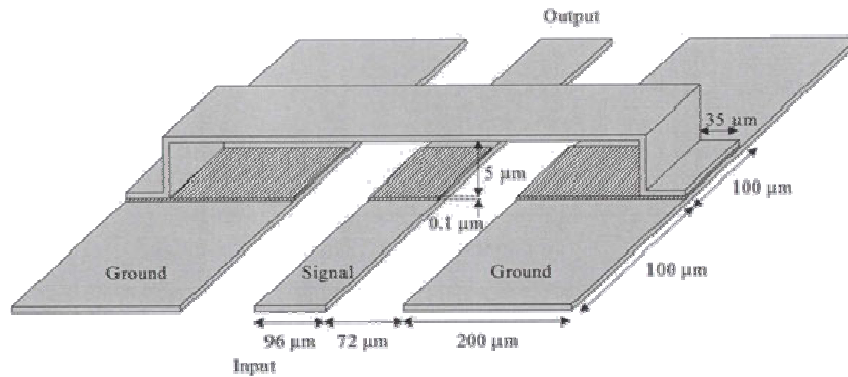


**Figure 3.3:** Air Bridge (Membrane) Switch

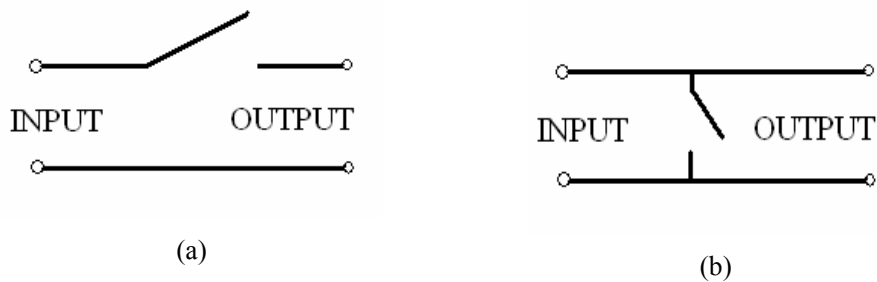


**Figure 3.4:** Switch Models, (a) Series Switch (b) Parallel (Shunt) Switch

### b) RF Circuit Configuration

RF circuit configuration is also subcategorized by the type of connection (series or parallel) and the number of input and output ports.

Series switches are switches that have series connection with input and output as shown in Figure 3.4 (a). If switch is down, the signal flows from input to output. Conversely when switch is up, the line is open circuited and signal cannot pass to the output. On the other hand, parallel switch is connected shunt to the input and output as shown in Figure 3.4 (b). Thus, when the switch is up, signal travels from input to output directly. However, when the switch is down, signal flows through the switch to the ground.

Cantilever beam type switches are, in general, series switches whereas air bridge type switches are parallel switches. By making some modifications in the structure

of the switch, it is possible to obtain parallel cantilever type switches like the T-wing switch shown in Figure 3.5 .

The switch types discussed so far are Single-Pole-Single-Throw (SPST) switches. They are usually preferred due to their simple structures. Single-Pole-Double-Throw (SPDT) switches are a little more complex than SPST switches in structure because this type of switches has two paths for signal flow. A cantilever beam SPDT switch structure is shown in Figure 3.6, in which the two alternative output ports are connected to the twistable corner of the cantilever beam. The output port is determined according to the DC voltage values applied to either side of the cantilever beam.

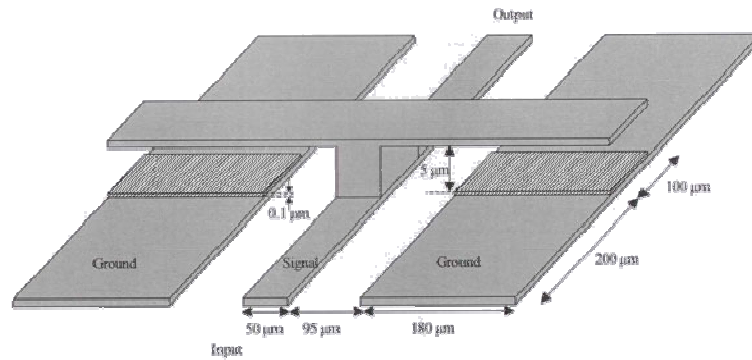


**Figure 3.5:** T-Wing Switch

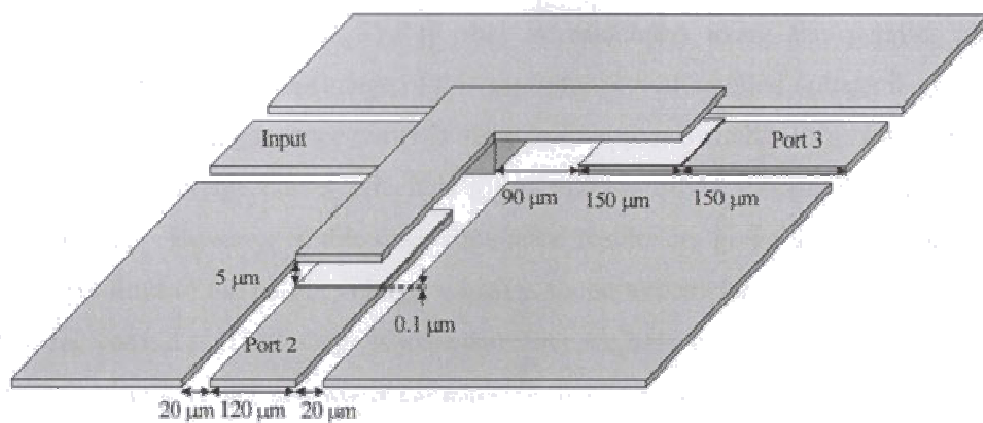


**Figure 3.6:** Single-Pole-Double-Throw (SPDT) Switch

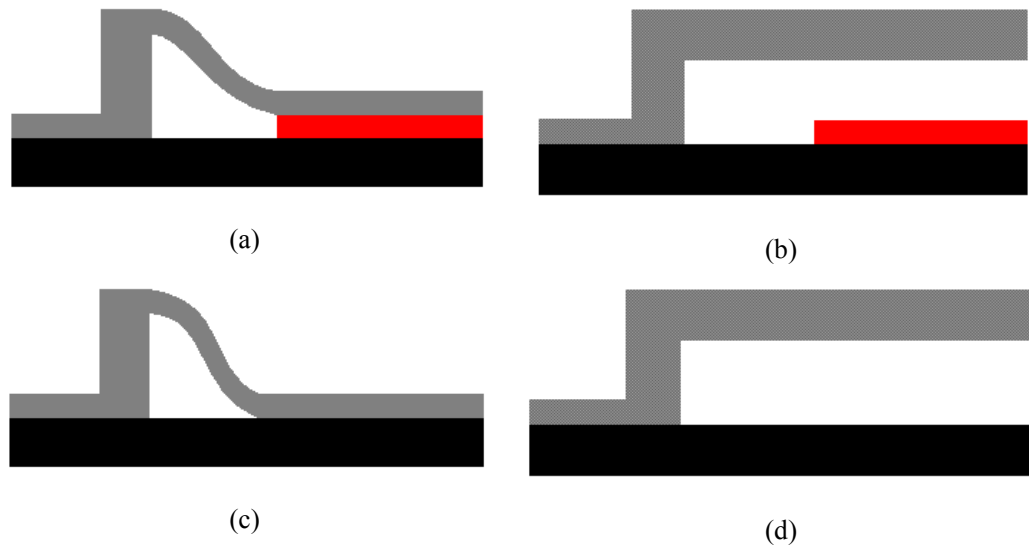


**Figure 3.7:** Capacitive Contact Switch (a) ON state (b) OFF state;  
Resistive Contact Switch (c) ON state, (d) OFF state.

**c) Form of Contact**

The common contact forms are capacitive and resistive contacts. Capacitive contact type switches have metal-to-dielectric layer contact between its cantilever beam and centre conductor as shown in Figure 3.7 (a-b). There is an isolation dielectric layer plated on centre conductor, which prevents DC short circuit for the RF signal. Capacitive contact switches are preferable for 10 – 120 GHz applications. Resistive contact type switches are switches that have metal-to-metal contact between signal line and centre conductor. The main structural discrepancy is due to the need of an extra actuation pad, different than the centre conductor, to actuate the beam and to prevent DC short circuit. These types of switches are generally used from DC to 60 GHz applications.

After summarizing the classification of RF MEMS switches, the design procedure and the simulation results for two different types of switches used in this thesis are presented in the following sections.

### 3.1. Coplanar Waveguide (CPW) Series Connected Capacitive Switch

One of the series connected SPST MEMS switches considered in this thesis is CPW-type capacitive RF MEMS switches designed by RF MEMS group in METU EEE Department, in 2002. Those switches are designed using Ansoft HFSS, also modelled and manufactured in the department [35]. The design schematics for both OFF and ON states are shown in Figure 3.8.

OFF and ON state electrical performances of the switch are characterized by 3D EM simulator HFSS by Ansoft. It should be noted that the thicknesses of all layers (wafer substrate, both metal layers, and dielectric substrate) are determined at the beginning of the design based on the fabrication technology and capabilities. Then the planar (x-y plane) dimensions are optimized through EM simulations to obtain the required electrical characteristics. The proposed switch is on Corning Glass (wafer) material, of dimensions:  $L_a=103\ \mu\text{m}$ ,  $L_b=110\ \mu\text{m}$ ,  $L_c=50\ \mu\text{m}$ ,  $L_d=105\ \mu\text{m}$ ,  $L_p=2\ \mu\text{m}$ ,  $L_T=845\ \mu\text{m}$ ,  $L=475\ \mu\text{m}$ ,  $W=120\ \mu\text{m}$ ,  $S=20\ \mu\text{m}$ ,  $d_1=0.1\ \mu\text{m}$ ,  $d_2=5\ \mu\text{m}$  (Figure 3.2).

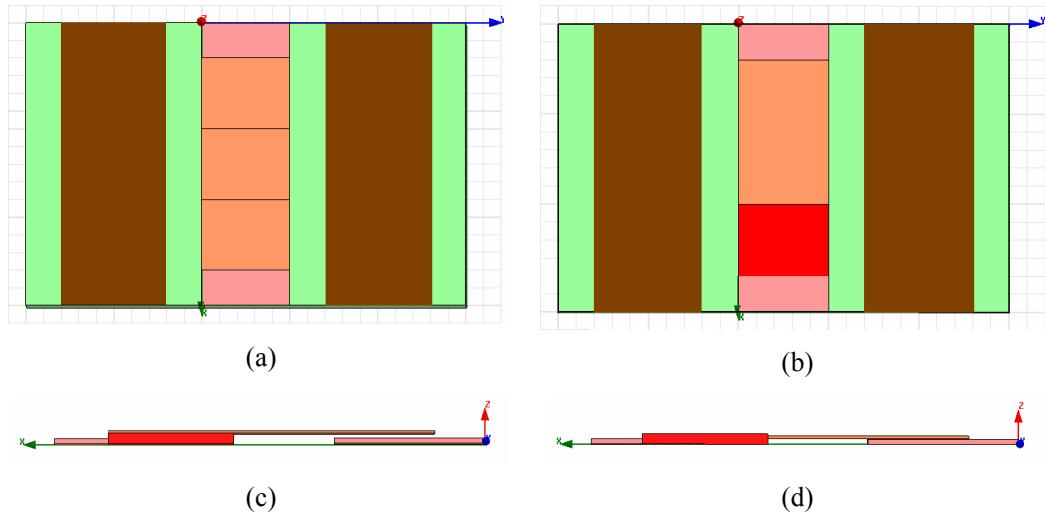


**Figure 3.8:** SPST Design Pictures

(a) OFF State Top-, (b) ON State Top-, (c) OFF State Side-, (d) ON State Side-view

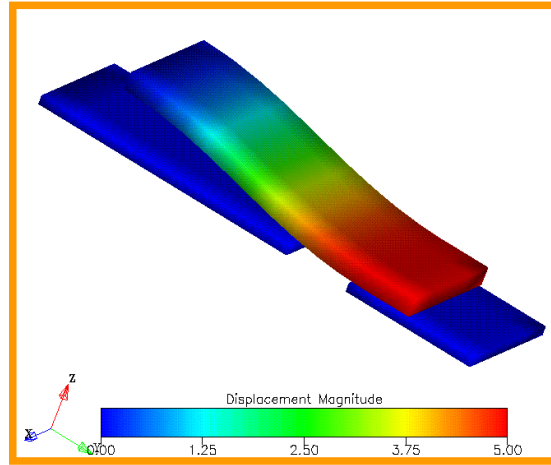


**Figure 3.9:** CoventorWare schematic of the CPW-capacitive SPST switch at ON-State (when DC is applied)

After characterising the switch structure in 3D EM simulator, RF MEMS switches are also simulated in a 3D mechanical simulator (CoventorWare) to investigate the mechanical response when several DC voltage values are applied. According to the mechanical simulation results, the actuation voltage value corresponding to a specific insertion loss could be estimated. In EM simulator, to simplify the numerical analysis, bending of the cantilever beam is not considered and the beam is assumed to be planar both in the ON and OFF states. On the other hand, in the mechanical simulator the exact 3D structure is modelled as shown in Figure 3.9.

### 3.2. Microstrip Line Series Connected Capacitive (T-Wing) Switch

This thesis uses RF MEMS switches for electrically either shortening both sides of the inset, or remain it open. For this particular purpose, capacitive T-Wing structure is preferred to be used as the most significant issue is determined as the isolation. So that, both the number of switches are decreased and sufficient space-wise compactness is achieved compared to two serially placed regular in-line switches.

In Figure 3.10, the thicknesses of each layer that are determined according to the available RF MEMS switch manufacturing technology in 2003 at METU are shown.

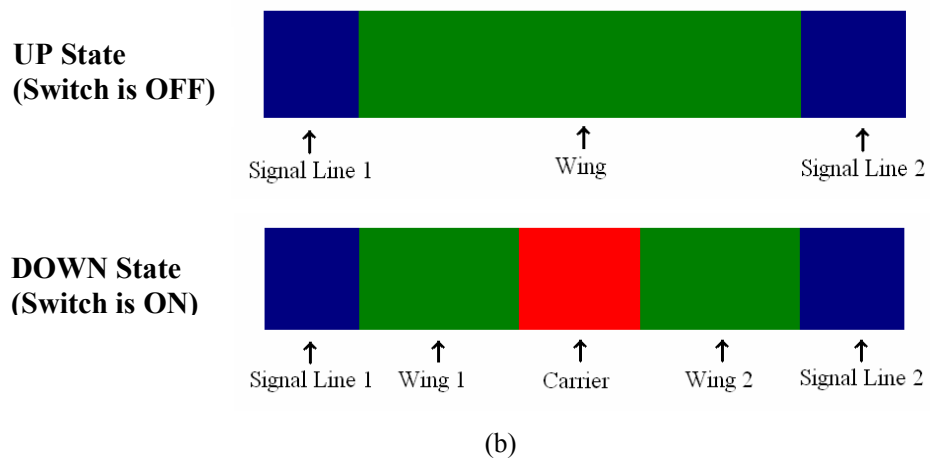
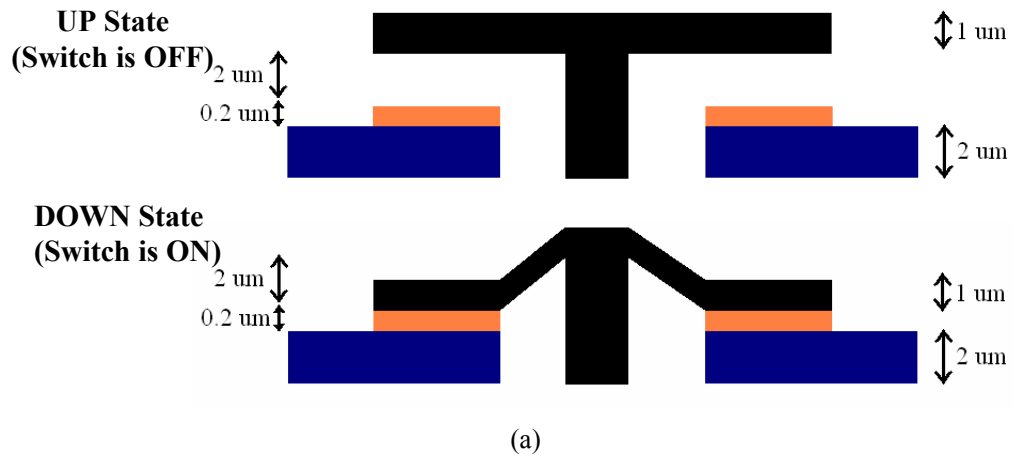


**Figure 3.10:** RF MEMS switch (a) side view, (b) top view,  
 (Orange colour represents the dielectric substrate ( $\text{Si}_3\text{N}_4$ ) and all others are gold).

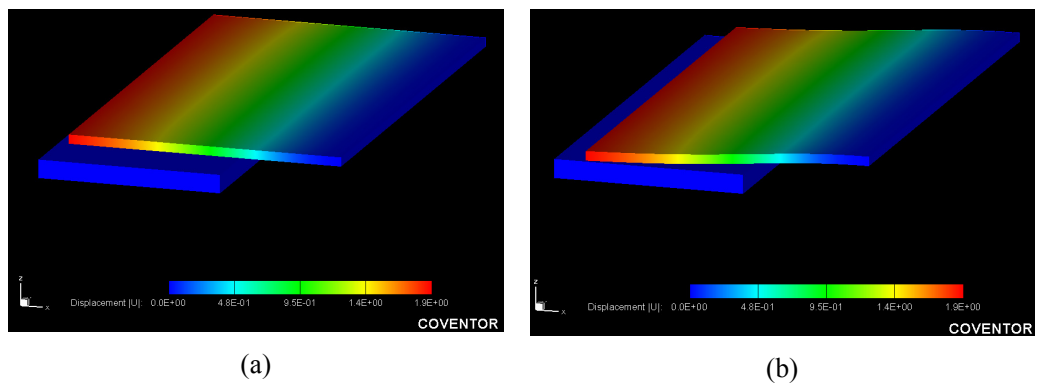


**Figure 3.11:** Design schematics of T-Wing SPDT switches, by CoventorWare.  
 (a) OFF State (without any DC-actuation) (b) ON State (when DC is applied)

The design procedure outlined in the previous section is carried out. The actuation voltage estimate values are obtained by mechanical simulation with the model shown in Figure 3.11, and the dimensions of the switch are optimized through EM simulations by using the ON and OFF state models shown in Figure 3.12 respectively.

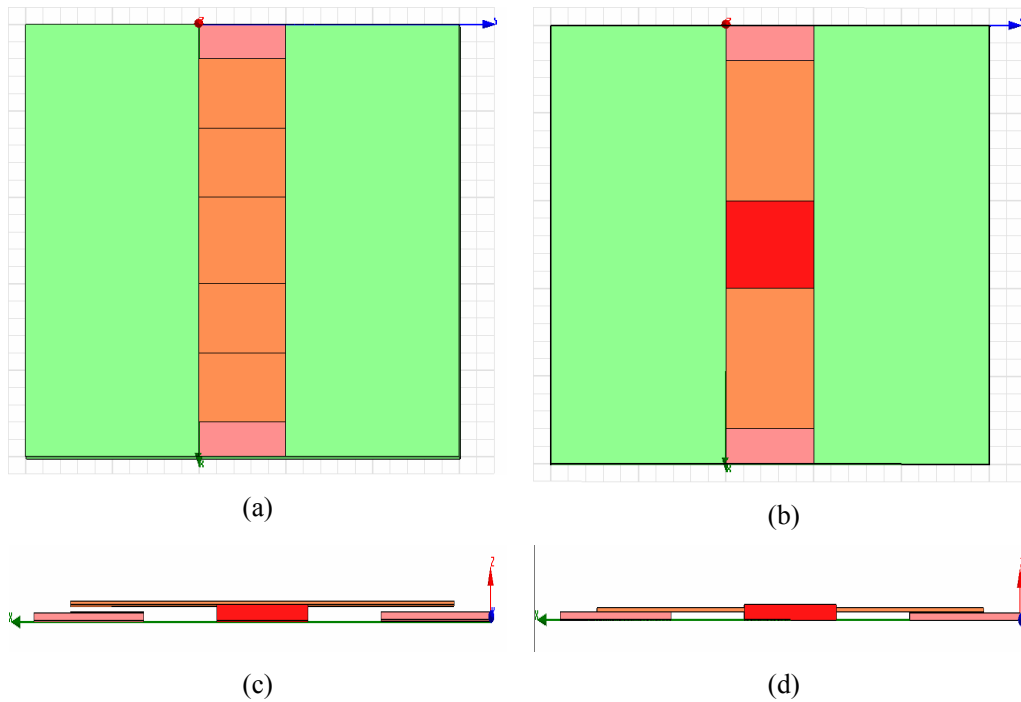


**Figure 3.12:** Design schematics of T-Wing SPDT switches.

(a) OFF State Top view in HFSS, (b) ON State Top view in HFSS,  
 (c) OFF State Side view in HFSS, (d) ON State Side view in HFSS,

### 3.3. Manufacturing Process

The designed MEMS switches are fabricated in METU – MET facilities by RF MEMS team in Electrical Electronics Engineering Department of METU.

Fabrication process flow of microstrip-line series connected capacitive (T-Wing) switch can be presented in the below figure.

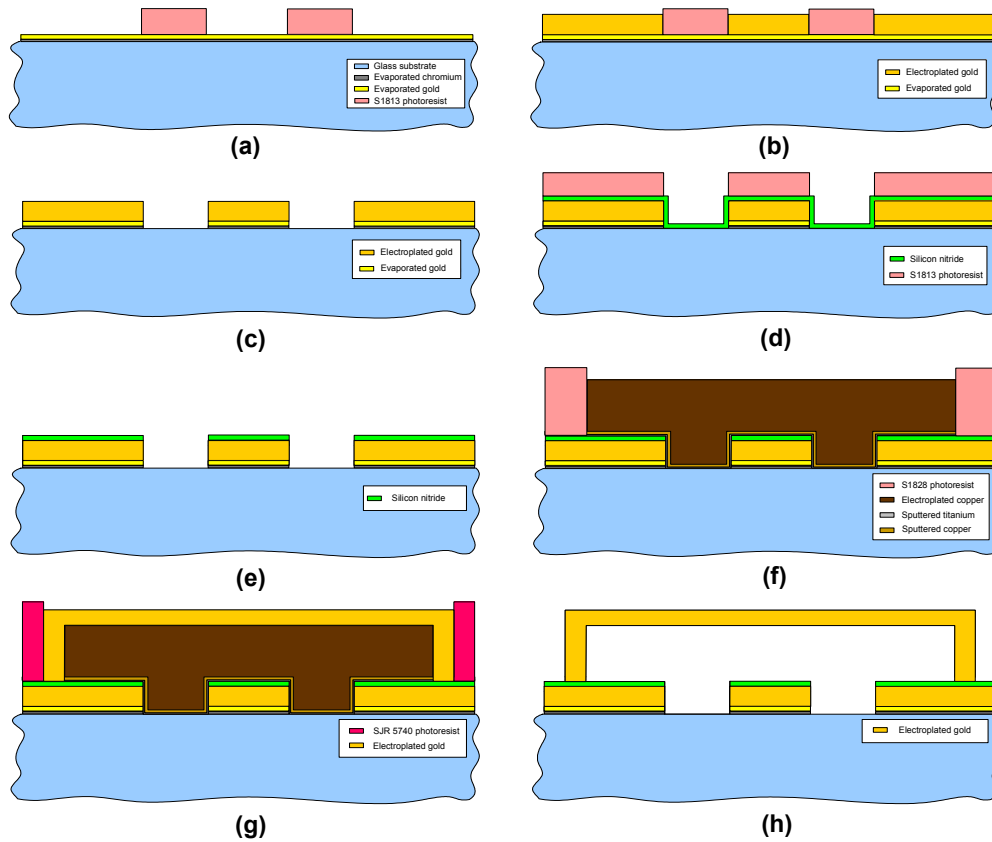


**Figure 3.13:** Fabrication process steps of RF MEMS switches in this study.

In more detail, the main steps of process flow are: (a) 300/3000 Å Cr/Au is evaporated which is required for electroplating of Au. Cr layer is used to promote stiction of Au to the glass surface which is pre-treated with buffered HF to increase roughness. The area that will be electroplated Au is determined by thick photo-resist (SJR 5740) which is compatible to the cyanide gold electroplating bath. (b) Au is coated using the electroplating technique inside the regions defined by mold SJR 5740 photo-resist. (c) SJR 5740 mold photo-resist is removed in acetone and the excessive seed layer to be etched is defined with a lithography using S1828 photo-resist. Cr/Au layers are etched using wet etching with selective Au and Cr etchants. (d) Si<sub>3</sub>N<sub>4</sub> layer is coated as the isolation layer using plasma enhanced chemical vapor deposition technique (PECVD). S1828 photo-resist is coated for patterning of Si<sub>3</sub>N<sub>4</sub>. (e) Si<sub>3</sub>N<sub>4</sub> is patterned using the reactive ion etching (RIE) technique. S1828 photo-resist is removed with acetone after Si<sub>3</sub>N<sub>4</sub> is removed. (f) 125/2500 Å Ti/Cu

layer is sputtered as the seed layer for sacrificial layer plating. Ti/Cu layer in the anchor regions are etched after the patterning of these regions with a lithography using S1828 photo-resist. The removal of Ti/Cu layer inside the anchor regions will ensure the direct contact of base metal to the structural (bridge) metal. Otherwise, the sacrificial layer removal process will not be a secure process due to the undercut of the copper etching towards the anchor regions. The photo-resist used for anchor etch is removed using acetone. The areas to be Cu plated are defined with a lithography using S1828 photo-resist. Deposition of copper sacrificial layer is implemented in copper sulfamate electroplating bath. The photo-resist used as sacrificial layer mold is removed using acetone. (g) The areas to be gold plated for bridge formation is defined with a lithography using SJR 5740 photo-resist. Au gold plating is completed in cyanide gold electroplating bath using the proper current density to obtain stress free bridges after release. The photo-resist used as structural layer mold is removed using acetone. (h) The sacrificial layer is etched and the structures are released. The drying process is performed using critical point drying equipment.

To sum up, the RF MEMS fabricated structures (all switches, stubs and the patch) have a 1  $\mu\text{m}$  high first metal layer. However switches have two additional solid layers, which are dielectric ( $\text{Si}_3\text{N}_4$ ) and second metal layer, with  $\sim 0.2 \mu\text{m}$  ( $0.5 \mu\text{m}$  @ 2002 year productions) and 1  $\mu\text{m}$ , respectively. And there is an empty (air-filled) layer for wings to bend easily. In the structure, as it can be observed easily, the smallest size is dielectric height. Unfortunately that is also one of the most critical parameter in switch design. In current manufacturing technology, that thickness may vary from 0.2  $\mu\text{m}$  to 0.4  $\mu\text{m}$  within each fabrication. Therefore, dielectric thickness of 0.3  $\mu\text{m}$  is preferred to be used in the structure final optimizations. Also, under the first metal layer, there is also another dielectric layer, which is also the antenna substrate (Corning Glass), having a height of 0.5 mm. This is the wafer substrate to start with. In addition, all used wafers used in this study are back-side electroplated, for patch ground.

## CHAPTER IV

### INTEGRATED RE-CONFIGURABLE (DUAL FREQUENCY) MICROSTRIP PATCH ANTENNA

In this chapter the complete design and manufacturing details of two re-configurable dual-frequency microstrip patch antennas are introduced. The major difference between these antennas is inset-feeding types, one is CPW inset-fed and the other is microstrip-fed patch. This difference has some effects on the integrated structure, which are all explained in this chapter. The operating frequency bands of these linearly polarized antennas are selected to be C – X bands, 6.5 GHz and 8.5 GHz.

Design steps in multi-frequency microstrip patch antenna controlled by RF MEMS switches study:

1. Determine slot size and position for demanded resonance frequencies.
2. Match the antenna by changing inset length for each resonance, one at a time.
3. Do OFF and ON state metal strip modelling for all possible switch positions.
4. Define electrical requirements of switches for performance goals.
5. Design and / or determine switches to be used and how they would be placed.
6. Insert switches either as 3D structures or S-parameter files within the left gaps.
7. Design stub(s) for switches' DC-actuation (DC bias or DC-ground).
8. Insert stubs into the patch structure. Do final tuning of slot position and size together with optimization on inset effective-lengths.

This eight stepped procedure is summarizing a complete multi-frequency microstrip patch antenna design. However there are some remarks to be noticed during this work. These could be explained briefly as follows.

In the 1<sup>st</sup> and 2<sup>nd</sup> step, each configuration (the demanded resonances) needs to be studied individually. The only crucial thing is the slot position. This is not applicable for dual-frequency antennas as the only change is applied to inset for matching purposes. However if there is going to be an additional resonance due to a change in effective-slot-length, then designer needs to fix the slot position from the beginning of the design work. The length of slot can change and also may need some more tuning in further procedure steps, but position needs to be as fixed as possible from the beginning for all frequencies.

In the 3<sup>rd</sup> step, metal strip modelling at both OFF and ON states are needed especially for determining the type, approximate width, possible placing architecture of the switch (or switch sets) that is (are) going to be used. In the related studies, T-Wing switches are preferred rather than series single-pole-single-throw (SPST) switches based on OFF state metal strip modelling performance. The number of switches is always kept as few as possible. Besides, inset widths could be optimized in this phase to minimize the impact of possible switch frequency shift impact compared to ideal model determined in the 2<sup>nd</sup> step.

The 4<sup>th</sup> step is implemented together with the complete antenna structure. The switch or switch set performance requirements are not necessarily defined through ‘metal strip modelling’ two port results. Metal strip model is a kind of ideal model, by itself as a two port component. However worse but still enough performance might satisfy all resonances of multi-frequency microstrip patch antenna, after a little tuning.

There are two major alternatives in the 5<sup>th</sup> step; either designing a brand new switch (sets) for the antenna, or using pre-manufactured switches. This choice is up to designer. Both methods are implemented in this thesis. If a brand new switch is

preferred to be used, then designer needs to concern the switches' actuation voltage while meeting the electrical requirements. By this way, number of switches might be decreased to one, depending on the switch requirements. Otherwise, if pre-manufactured switches are preferred to be used, then to meet the electrical requirements, a number of those switches could be placed parallel. This number of switches increases as more incompatible as switches are, at the resonance frequencies of the microstrip patch antenna. If there are more than a couple of switches to be used for the structure, than it is recommended to place switches separated by some distance from each other. This separation needs to be determined by iteration for obtaining the best performance.

When switches or their S-parameter files that are reflecting their end-to-end electrical characteristics are inserted to the complete antenna structure (6<sup>th</sup> step); all designs goals in each antenna configurations shall be satisfied. If 3D structures are inserted, there must be a complete touch between surfaces (signal line and inner side of inset or slot). In S-parameter inserting case, the two port characteristics are defined similarly from one to the other inner side of the inset or the slot. Among these simulations, there still may be some degradation in input return loss. Unless there is additional frequency shift due to the switch performance in the slot, it is not necessary to re-tune the complete structure in this step.

Stub design (Step 7) is one of the most critical parts of RF MEMS switch controlled multi-frequency microstrip patch antenna, because stubs are both assuring DC actuation of switches and preventing any possible RF signal leakage. The first is simply a true DC grounding so that there would always be a potential difference between inset-feed and wings of switches when actuated. RF-wise goal in these stubs is prevention of any signal leakage that might affect resonance and mismatch when that connection is established. In other words, at the switch – stub connection, an RF open but DC short is desired for not changing the resonance performance of the patch by an additional loading. Such a grounded line should be odd multiplies of quarter-wavelength long for satisfying both DC and RF requirements. Rectangular stubs used in this thesis might be ended by a radial stub, for a wider bandwidth of

open-circuit response. The ending of stubs also depends to feeding structure, such as microstrip or CPW feed line.

The stubs are preferred to be rectangular within the inset and slot, for keeping the distance from the boundary of gaps where they are placed, the same. This distance is determined by a trade off between coupling and stub sensitivity. Thicker stub would be closer to inset or slot inner sides, therefore coupling would increase. Thinner stub would be more difficult to manufacture and even in design phase, the sensitivity on that width increase. Other than that, stubs need to have a smoother shape to avoid any possible scattering from corners, if there are any.

Another concern regarding the shape and position trade-off of stubs is their distance to radiating edges of antennas. Regardless of adjusting the length properly to avoid any RF-leakage to DC-ground that degrades antenna performance; there still exist some recognizable current flow on the line. That flow creates two reasons for cross-polarization; one is coupling with the radiation edge and the other is a perpendicular current flow to the current flow on the patch. To prevent these, stubs are placed as far as possible from radiating edges with as small slopes as possible, till a level that there would not be any dominant coupling effect to the input feed line.

The final, 8<sup>th</sup>, step is introducing the designed stubs to the microstrip antenna already including the RF MEMS switches. When this whole structure is simulated all together, most of the time there would be a significant amount of frequency shift and that's why a matching problem occurs. During this step, final tuning on slot position and size is carefully done, for each switch (set) configuration. Similar to the case in the complete design procedure, slot position and size are still designer's key parameters until the last optimization in inset switch positions. After resonance frequency values are acquired, inset switch positions are updated for a good matching.

Another important remark here is that, when complete structure is implemented together, all inset stub lengths needs to be verified or tuned for the best matching

performance. For slot switch stubs, the stub-performance change could be observed as unexpected frequency shift, when stubs are implemented.

As a general methodology in this study, the antenna design starts in Ensemble 2.5D platform. After the design reaches to a mature level, 3D analysis is performed in HFSS v9.2. Commonly, the switch integrations are also first simulated by inserting black box S-parameters to the inset ports in Ensemble, for hybrid structures. But again fine tuning and optimization is done in HFSS, by actual switch, stub and patch dimensions. Also as stated before during the switch simulations, switch wings are assumed to be flat just on the top of the dielectric.

#### 4.1. Antenna Design Details

In this integrated structure, since both the antenna and MEMS switches will be manufactured on same substrate, Corning Glass ( $\epsilon_r = 4.6$ , Loss Tangent = 0.005), with thickness of 0.5 mm is chosen to be the dielectric material. The optimized dimensions of the dual frequency patch antenna are given in Figure 4.1. Optimized inset lengths ( $l_i$ ) are found as 4.25 mm for 6.48 GHz, and 2.6 mm for 8.52 GHz. With those inset lengths, return losses decreased around to -25 dB and -23 dB, respectively.

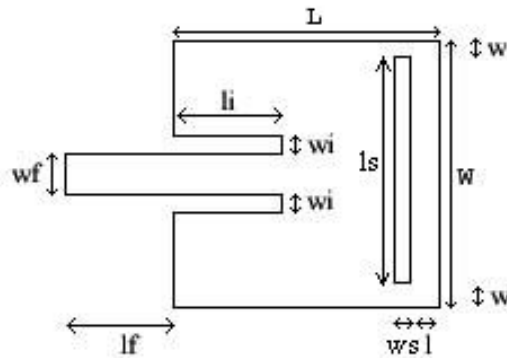


**Figure 4.1:** Patch with a 0.2 mm x 10 mm sized rectangular slot

$L = 9.6$  mm,  $W = 10.5$  mm,  $w_i = 0.25$  mm,  $l_f = 7.6$  mm,  $w_f = 0.92$  mm,  $w = 0.25$  mm,  
 $l = 0.3$  mm,  $l_s = 10$  mm,  $w_s = 0.2$  mm.

### 4.1.1. Microstrip-Feed

At first, one quarter-wave long microstrip is considered for DC-grounding. However, this length is calculated to be, more or less, the same as the inset length. This dimensional conflict and also a risk of degradation on radiation pattern forwarded the design to use three quarter wave-length rather than single quarter-wave long stub. Therefore, the stub became longer and less effect on radiation characteristic of antenna is expected. As an unfavourable impact of this longer microstrip rectangular stub, phase matching became more sensitive to the stub dimensions, both length and width. On the other hand, long and narrow (50  $\mu\text{m}$  wide) stub used for fitting in inset properly, introduced more sensitivity to the width. In this approach, during the simulations stubs are again grounded to bottom layer through (20  $\mu\text{m}$  radii) via at the very end of stubs.

As seen from the Figure 4.2, the rectangular stub has been buckled only once. The position of that corner is another important issue, because a possible scattering from

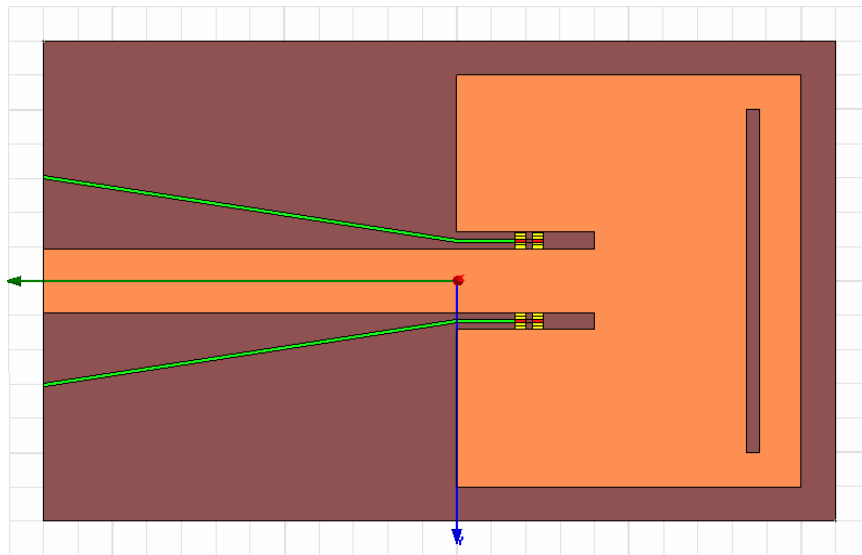


**Figure 4.2:** The integrated Microstrip-fed Re-Configurable (Dual Frequency) Microstrip Patch Antenna Structure (dimensions are not scaled)

there might affect either the radiation pattern or feeding of the antenna. Therefore it shall be placed far enough from both radiation edges and feed line of the patch. The tilt here is designed as  $23^\circ$  to have 5 mm spacing from the signal line at the edge of the substrate.

#### 4.1.2. CPW-Fed

Inset-fed patch antenna has microstrip line feed by its nature. However, the feeding can be changed to some other line type if needed. Especially based on laboratory – facility technology or available input sources (devices, probes or connectors), the device under test (DUT) feed can be modified time to time. Here, in this study,  $1450\ \mu\text{m} - 140\ \mu\text{m} - 1450\ \mu\text{m}$  wide CPW (Ground – Signal – Ground) probe-feed is decided to be used, therefore required microstrip to CPW taper in front of the patch input and based on that taper the rectangular stubs are designed (Figure 4.3).

The length of microstrip-to-CPW taper is one of the most effective parameters in the taper design. The taper width on the CPW side is probe, and taper width on the microstrip side is patch driven, respectively. The metal thickness is set as  $2\ \mu\text{m}$  by MEMS fabrication, for whole integrated structure in this particular fabrication. The taper length shall not be less than some critical value for preventing undesired reflections. A simulation comparison between 11 mm and 5.5 mm long tapers are

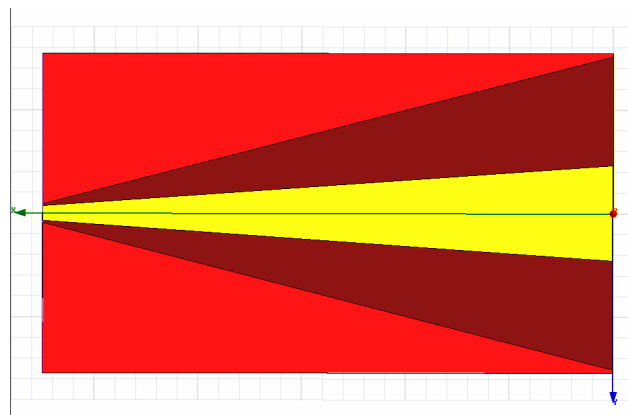


**Figure 4.3:** Schematic of taper

shown in Figure 4.3 (a)-(b), respectively. From the plots, it is observed that when taper shortens, signal would face with new structure width quicker, which results in higher values of return loss and VSWR. However when the taper is longer, those curves become smoother along the frequency band, which means smaller changes in input return losses in both ports. Also, the phase change is increased in the longer taper. Here the comparison is between 11 mm and 5.5 mm long tapers, therefore the phase slope varied two times of the other, as shown in Figure 4.4 (c)-(d). While optimizing the whole structure that phase contribution will be taken into account seriously. An upper limit of taper length is obsessed by MEMS manufacturing technology and maintainability. Briefly, this kind of manufacturing avoids huge aspect ratios between dimensions. Thus there is a trade-off in size optimization.

There are also many other taper types studied in literature [36, 43]. Here a linear taper is preferred to be used because of its easiness to change its own dimensions; although it is known that polynomial tapers have better (smoother even in short

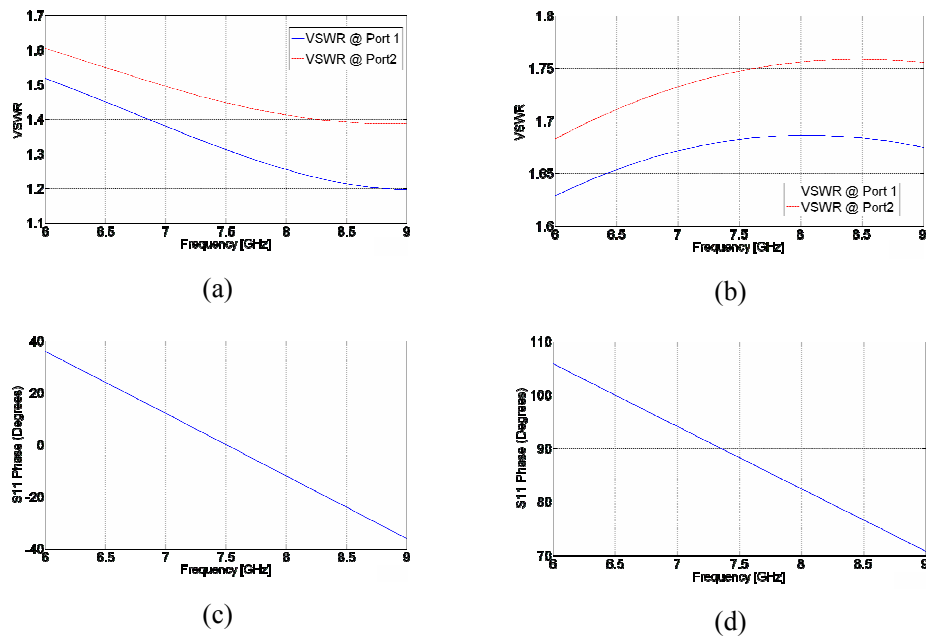


**Figure 4.4:** RF characteristics of taper

(a) VSWR of 11 mm long, (b) VSWR of 5.5 mm long,  
(c) Phase of 11 mm long, (d) Phase of 5.5 mm long, taper.

distances) electrical performance, such as input reflection characteristics in wide bandwidths. Length of taper also reflects the phase change of the signal, as shown in Figure 4.4. In the taper design, when the left-hand side was grounded, phase is aimed to be around 90-degrees.

This portion of the optimization can be done when analyzing the whole structure. In whole structure analysis, the ground-end of CPW is grounded along via as shown in Figure 4.5. These via have 0.5 mm radius, and are placed at the very end of CPW-ground portion to assure the ground effect.

In this design the tilt on rectangular stub is determined as  $6^\circ$ , because of bigger weight on radiation pattern degradation than input-feed coupling. The input-feed coupling deficiency (additional capacitance and inductance reasoned admittance change) is overcome by adjusting the stub length properly, as best as possible.

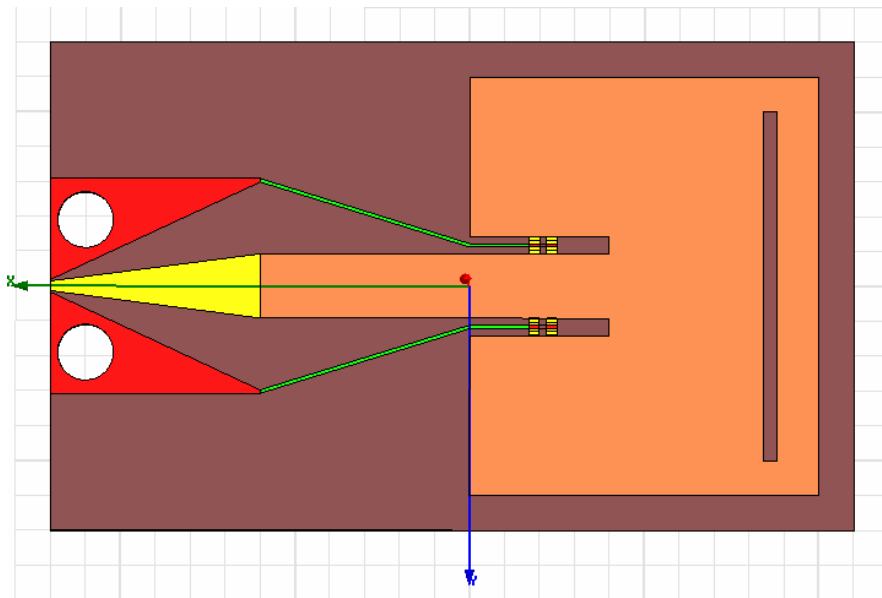


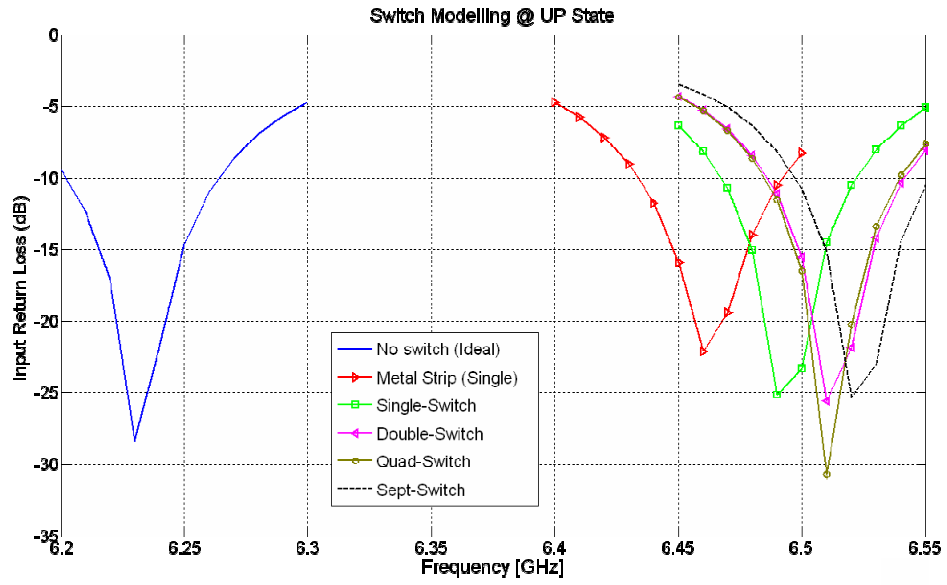
**Figure 4.5:** The integrated CPW-fed Re-Configurable (Dual Frequency) Microstrip Patch Antenna Structure (dimensions are not scaled)

## 4.2. RF MEMS Switch Design Details

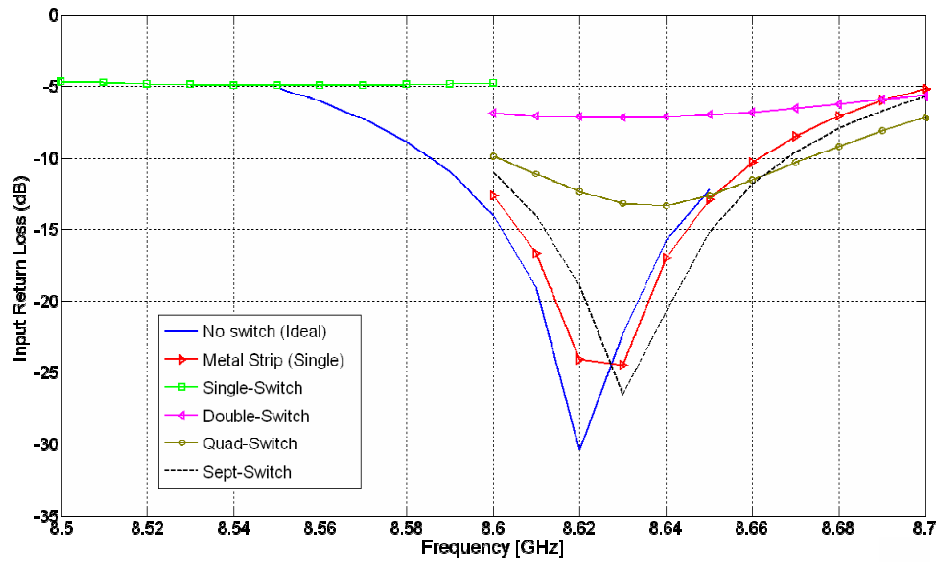
In this part of study, a brand new switch set is designed, and manufactured together with the patch as an integrated structure. The benefit of integrated production would be expectation of a perfect connection between switches and the patch, as well as switches and the stubs.

The RF MEMS Switch design in this study started with defining the requirements. At first metal strip modelling is done, which is placing a single long metal strip to model conducting ON state, or placing three metal strip pieces (as signal line – carrier – signal line, respectively) to model isolation OFF state, as shown in Figure 3.1. These metal strips are placed on the position that shortest inset length (that is 2.6 mm for 8.5 GHz resonance) points, where as the true inset length of microstrip patch is longer, 4.25 mm for 6.5 GHz resonance.

When the inset lengths are re-generated by metal strip modelling, the required insertion loss and isolation characteristics of switches are determined. The methodology was first designing a ‘sample reference’ switch, which had capacitive cross-section area of  $50\ \mu\text{m} \times 40\ \mu\text{m}$  sizes under each side of the wing. And then this switch is placed into the inset, the antenna performance is observed. Next more and more switches are placed in parallel until a close antenna resonance performance to both ideal and metal strip models is observed. As soon as a satisfactory matching between models and switch-set integrated performance, the switch set is pulled out and investigated separately from the antenna. In the study, the antenna including eight parallel ‘sample reference’ switches is observed to be the closest one to the ideal metal strip model (Figure 4.6). Thus goal of switch electrical characteristics, over the selected frequency bands is defined as isolation around 11 dB at lower frequency (@ 6.5 GHz), and insertion loss less than 0.7 dB at higher frequency (@ 8.5 GHz).



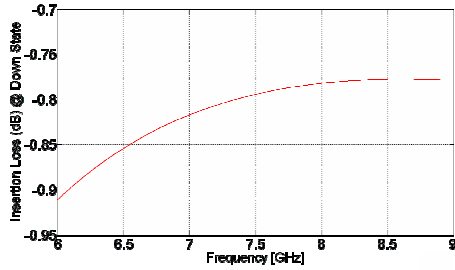
(a)



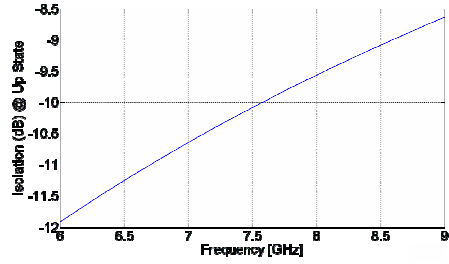
(b)

**Figure 4.6:** Electrical characteristic goal determination study results

(a) Antenna with up stated switches, (b) Antenna with down stated switches,



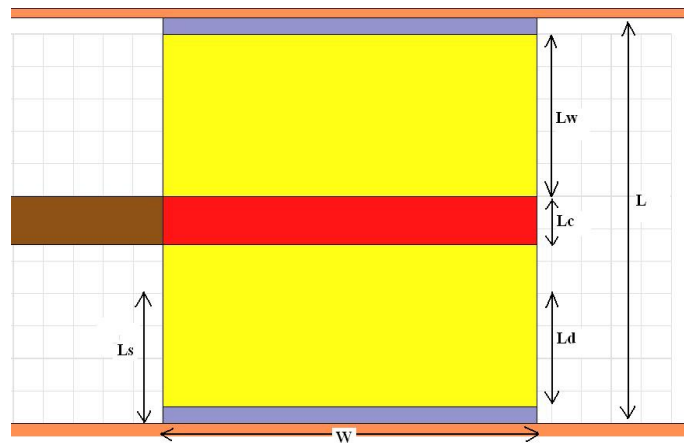
(c)



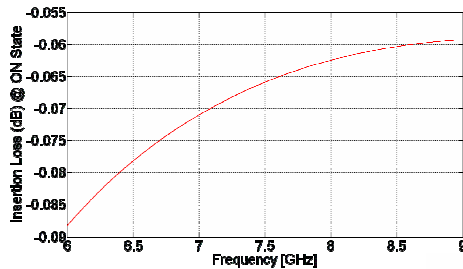
(d)

**Figure 4.6 (cont'd):** Electrical characteristic goal determination study results

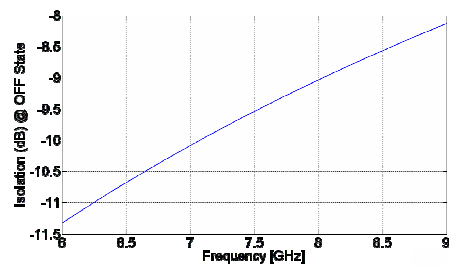
(c) Insertion loss of 8-parallel switches, (d) Isolation of 8-parallel switches.



(a)



(b)



(c)

**Figure 4.7:** Electrical Schematic and Electrical Performance of suggested switch structure in Single Switch Approach

(b) Insertion Loss in ON State, (c) Isolation in OFF State,

where  $W = 250 \mu\text{m}$ ,  $L = 250 \mu\text{m}$ ,  $L_c = 30 \mu\text{m}$ ,  $L_s = 70 \mu\text{m}$ ,  $L_w = 100 \mu\text{m}$ ,  $L_d = 60 \mu\text{m}$ .

### **4.2.1. Single Switch Approach**

All required electrical (insertion loss and isolation) requirements are achieved after a number of iterations, by a single switch. The dimensions of the designed switch are shown in Figure 4.7.

This particular single switch is satisfying the requirements quite well, but this switch is not preferred to be used, because the actuation voltage of this switch is too high. The principle of actuation of T-Wing switches are explained in Chapter 2 in detail. Briefly, there should be a potential difference between the wings (or carrier as they are directly contacted to each other) and the signal lines to actuate switch to bend the wing. A rule of thumb on actuation voltage is that, as the cross section area between the wing and the signal line (the capacitive field faces) increase, the actuation voltage increases. In this switch, that actuation voltage is calculated as approximately 110 V.

However the switches designed in this study are selected as capacitive switches; therefore there is a thin (around 0.2  $\mu\text{m}$ ) dielectric substrate. When switches are loaded with a DC voltage, the dielectric layers interface that potential only with a little loss in either wing or signal line. If this voltage is high, that may cause charging in the dielectric material. As density increases in some portions of the dielectric, breakdown occurs. This defects the dielectric material characteristics once for all. This is called as ‘burn’ of switch. The dielectric has a breakdown voltage around 90 V – 100 V, this particular switch is expected to ‘burn’ when it is actuated. Yet, it is decided to increase the switch number and design a new switch set, even though that was satisfying the electrical requirement.

### **4.2.2. Double (Parallel) Switches Approach**

Another way to meet the electrical requirements expected from RF MEMS switches in this structure is using parallel placed switches in each inset. Hence the switch (wing and capacitive-cross-section area) sizes are expected to be much smaller.

Especially decrease in capacitive cross-section area brings lower actuation voltage. By using the same methodology explained in the previous section; similar electrical requirements are met with following switch set (Figure 4.8).

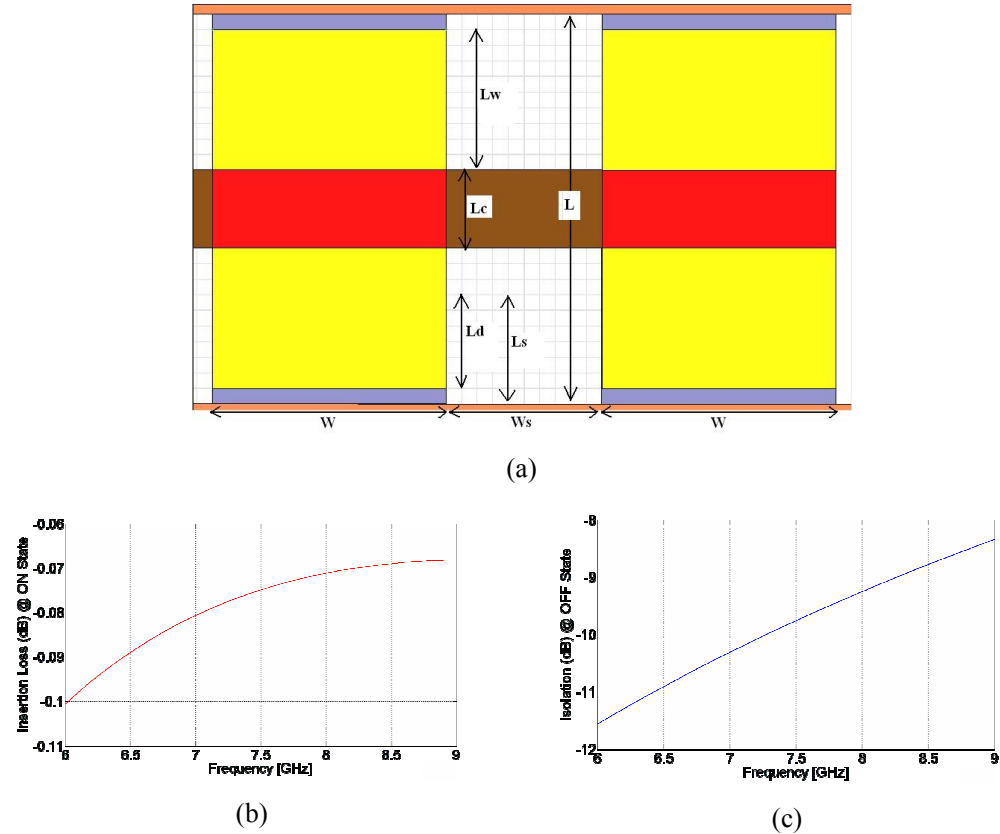
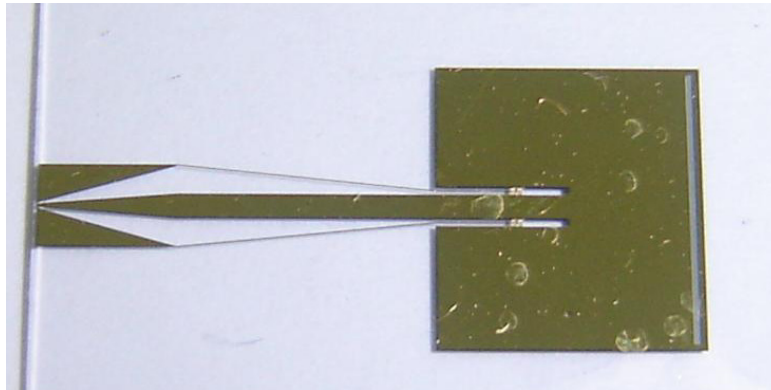


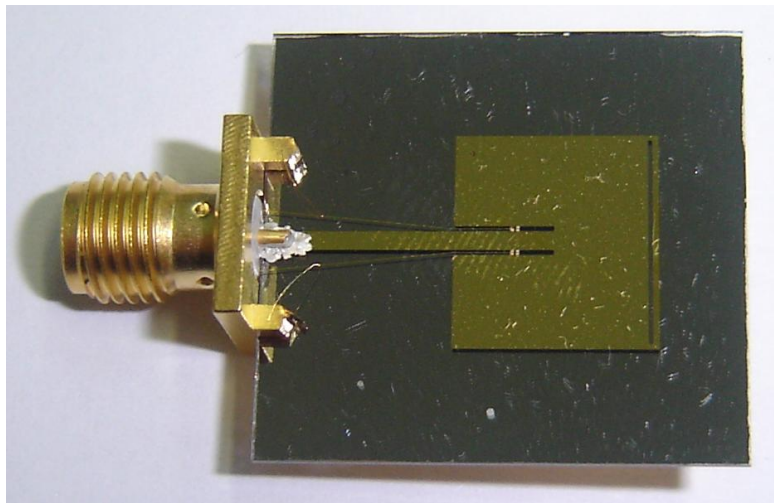
**Figure 4.8:** Suggested switch structure in Double Switch Approach

Schematic, (b) Insertion Loss in ON State, (c) Isolation in OFF State, where  $W = 150 \mu\text{m}$ ,  $L = 250 \mu\text{m}$ ,  $L_c = 50 \mu\text{m}$ ,  $L_s = 60 \mu\text{m}$ ,  $L_w = 90 \mu\text{m}$ ,  $L_d = 50 \mu\text{m}$ ,  $W_s = 100 \mu\text{m}$ .

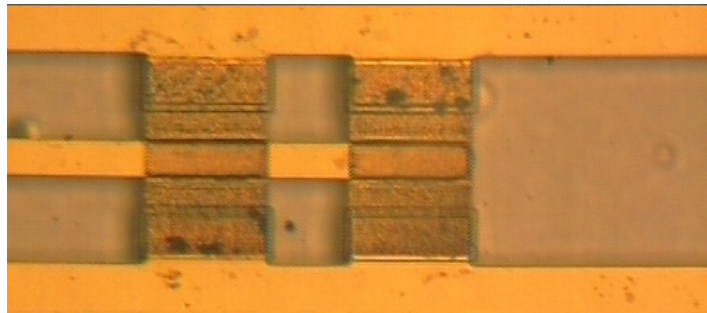
Now, there are two switches in each inset, to be DC-grounded but also RF-open; the centre point is used for reference. From that  $W_s / 2$  point, three-quarter wavelength point is calculated and the stub is designed. The estimated actuation voltage for switches in this switch set was around 70 V, so breakdown is not expected. The only disadvantage is the number of switches in the patch, which was not the design preference in the beginning. In Figure 4.9 there are some pictures of manufactured antennas their connectors, and RF MEMS switches.



(a)



(b)



(c)

**Figure 4.9:** Designed and manufactured

- (a) Integrated re-configurable dual-frequency CPW-fed microstrip patch antenna,
- (b) Integrated re-configurable dual-frequency microstrip-fed microstrip patch antenna,
- (c) RF MEMS T-Wing switches used in the antennas.

### 4.3. Simulation and Measurement Results

Design phase of re-configurable dual-frequency microstrip patch antennas are followed by manufacturing and then measurements.

In the measurement phase, basically two major measurements are aimed to be made on these integrated structures; input return loss ( $S_{11}$ ) and radiation characteristics (such as patterns at E- and H-planes, 3-dB bandwidths, and peak power levels) measurements. Unfortunately via type grounding in the design could not be realized for CPW-fed structure because of the incapability on drilling glass; therefore the structure was not measured. Glass is a material, which is very hard to drill without any cracks. But for microstrip-fed antenna SMA type connector is used, to measure the electrical performance through HP8270D model network analyzer.

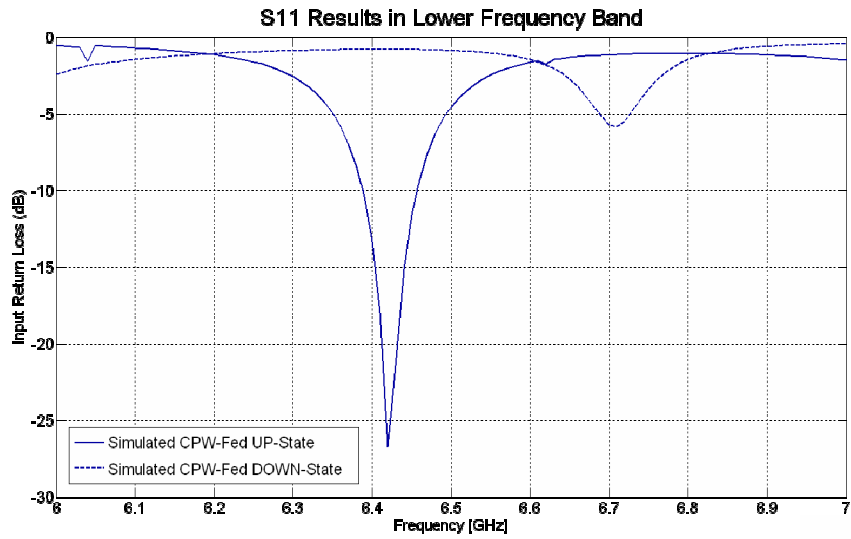
Also radiation characteristics at resonance frequencies of integrated re-configurable dual-frequency microstrip-fed microstrip patch antenna are measured (by Kağan Topallı, Mustafa Seçmen) in anechoic chamber in microwave lab in METU EEE Department. In this last section, simulation and measurement results are given, and measurements are going to be discussed based on differences and similarities to the corresponding simulation results.

#### 4.3.1. CPW-Fed

Two operating frequency of this structure is aimed to be at 6.5 GHz and 8.5 GHz, respectively. When switches are at default OFF state, antenna has a resonance at 6.42 GHz. When switches are actuated, at ON state, antenna re-configures itself to a better resonance at 8.6 GHz. The 10-dB bandwidths at these resonances are 69 MHz (1.07%) and 74.6 MHz (0.87%) at OFF and ON states, respectively. Figure 4.10 shows the simulation results of integrated re-configurable dual-frequency CPW-fed microstrip patch antenna.

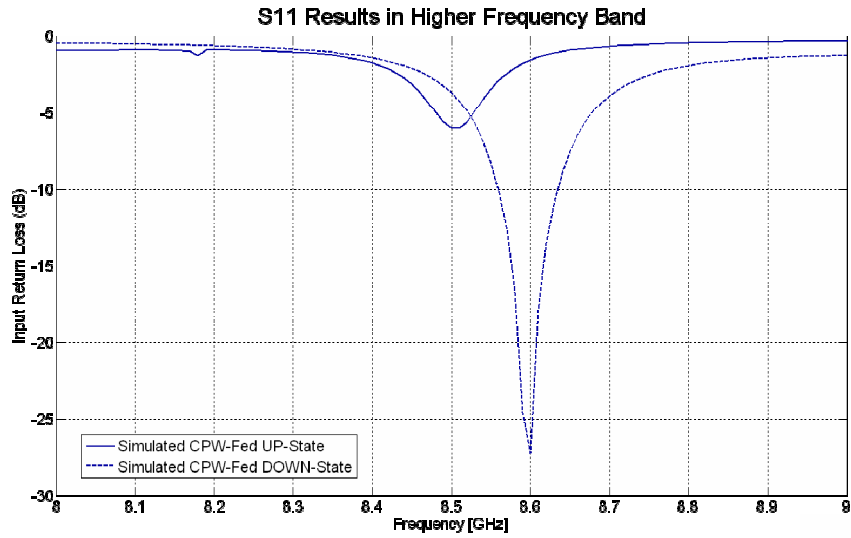
There are also dominant but rarely used parameters, such as slot or patch dimensions. The basic reason for those parameters not preferred in the final tuning

is, they are dominant in defining resonance frequency. The inset and stub lengths mainly change the value of input return loss but resonance frequency. If the aim is to move or adjust the resonance frequency, then slot and patch dimensions need to be adjusted, as that implementation is going to be explained in Chapter 5.

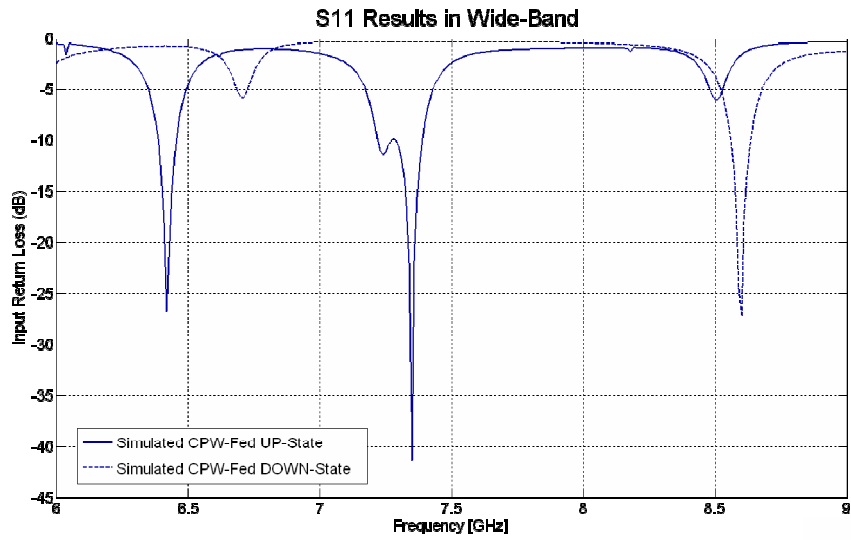


(a)

**Figure 4.10:** Simulation results of integrated re-configurable dual-frequency CPW-fed microstrip patch antenna. (a) Close look around 6.5 GHz,



(b)



(c)

**Figure 4.10 (cont'd):** Simulation results of integrated re-configurable dual-frequency CPW-fed microstrip patch antenna.

(b) Close look around 8.5 GHz, (c) Wide-band response at OFF and ON States.

As a general remark; slot dimension – position tuning at first, is recommended as it is a ‘fine-tuning’. If antenna designer still can not get the resonance at requested

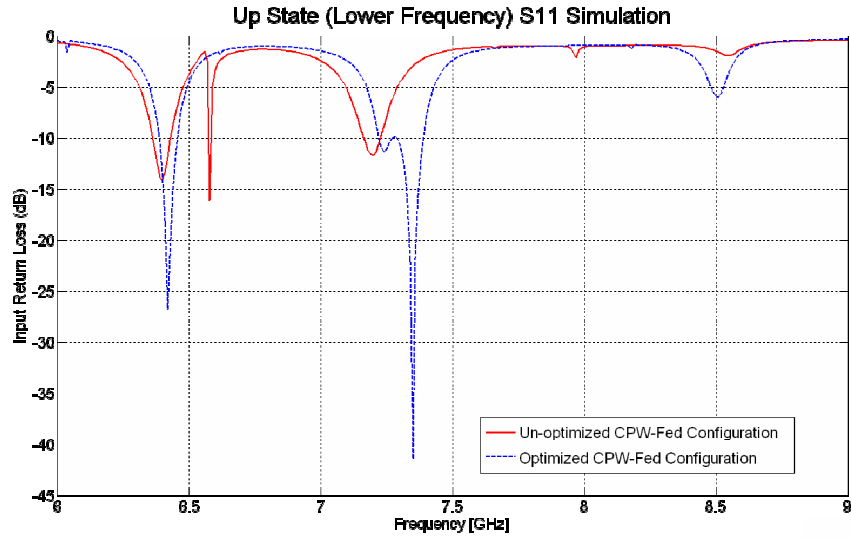


**Figure 4.11:** Comparison of Optimized and Un-Optimized CPW-Fed Configuration

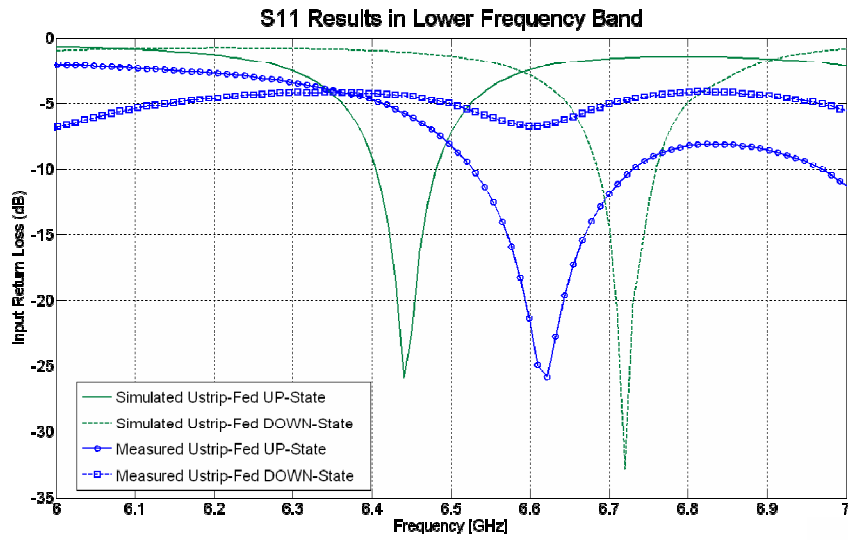
frequency, then tuning of patch dimension is advised. In Figure 4.11, input return loss of the current CPW-Fed antenna, before and after stub length optimization is shown.

### 4.3.2. Microstrip-Fed

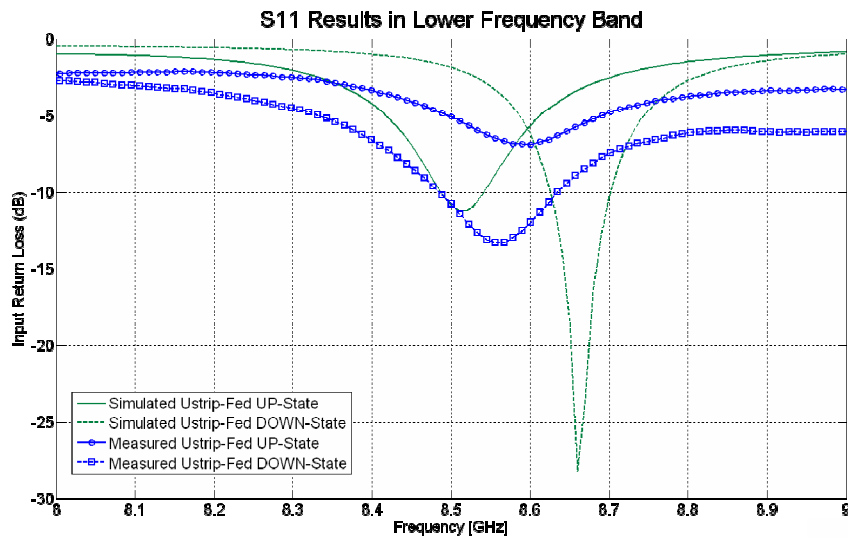
Similar design simulation effort spent to the integrated re-configurable dual-frequency microstrip-fed microstrip patch antenna for same resonance frequency goals. When switches are at default OFF state, antenna has a resonance at 6.621 GHz. And when switches are actuated, at ON state, antenna re-configures itself to a better resonance at 8.556 GHz. The 10-dB bandwidths for these resonances are 203 MHz (3.06%) and 150 MHz (1.75%) at OFF and ON states, respectively. Figure 4.12 shows the simulation and measurement results of integrated re-configurable dual-frequency microstrip-fed microstrip patch antenna.

The radiation pattern measurements are done in anechoic chamber, as mentioned before. Unfortunately in chamber there is not any DC-line to activate the switches, therefore radiation measurements could only be done only at default OFF state.

Some simulation (at both OFF and ON states) by HFSS, and measurement (only at OFF state) results are shown in Figure 4.13. Measurement scale is 5 dB per division.



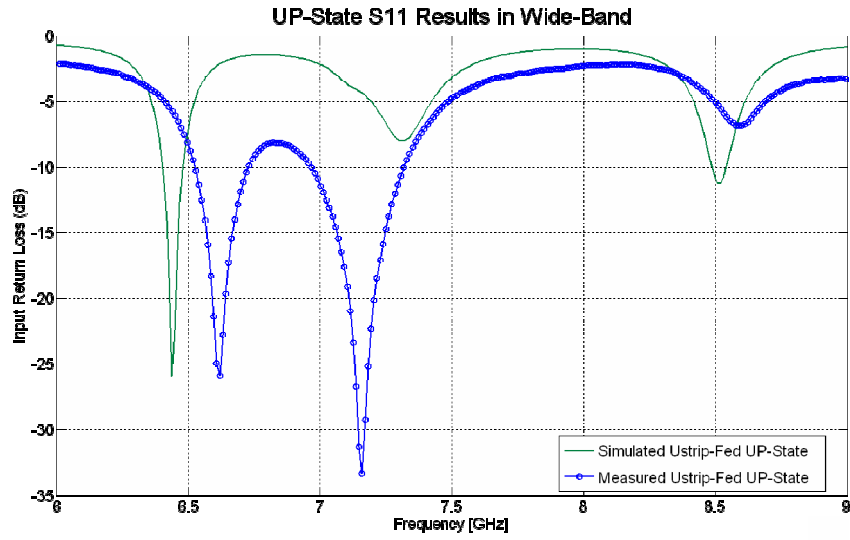
(a)



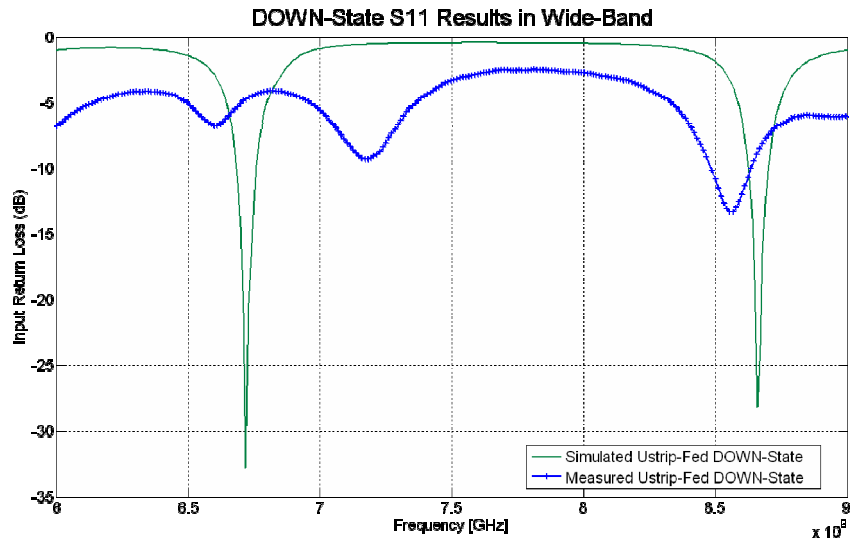
(b)

**Figure 4.12:** Simulation and measurement results of integrated re-configurable dual-frequency microstrip-fed microstrip patch antenna.

(a) Close look around 6.5 GHz, (b) Close look around 8.5 GHz,



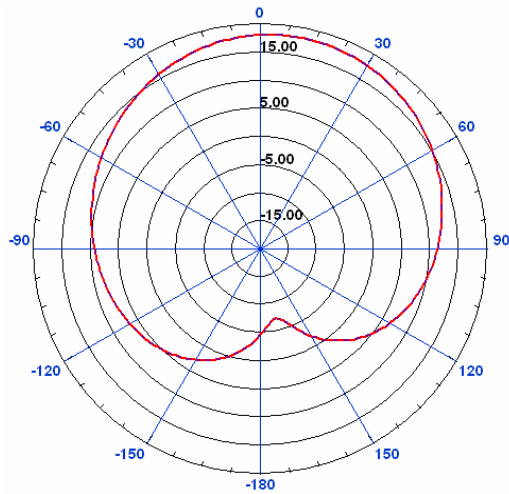
(c)



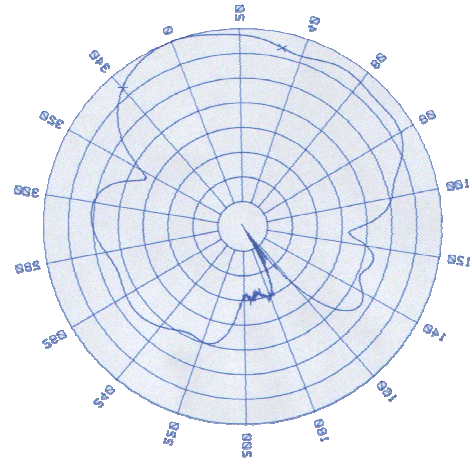
(d)

**Figure 4.12 (cont'd):** Simulation and measurement results of integrated re-configurable dual-frequency microstrip-fed microstrip patch antenna.

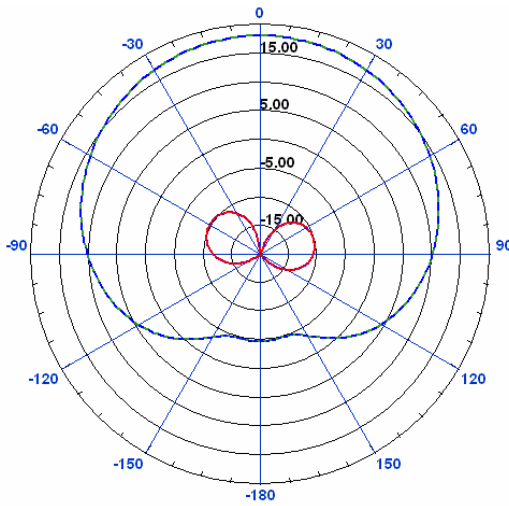
(c) Wide-band response at OFF State, (d) Wide-band response at ON State.



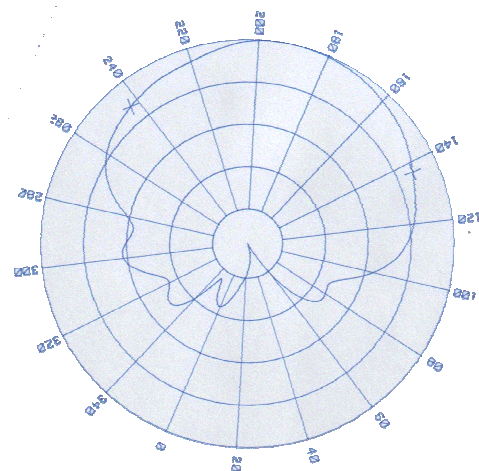
(a)



(b)



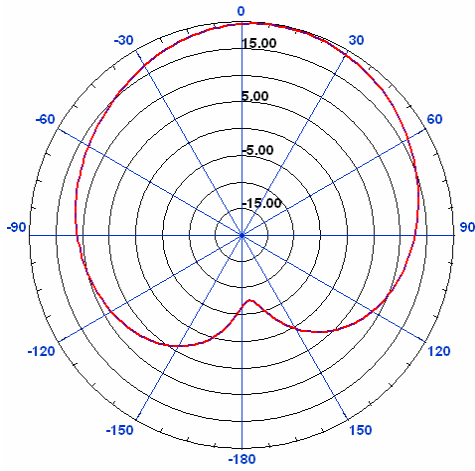
(c)



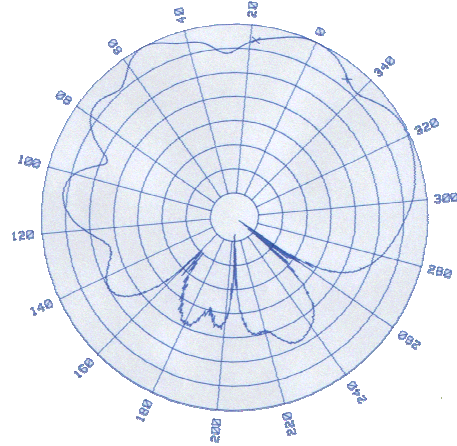
(d)

**Figure 4.13:** Radiation pattern simulation and measurement results of integrated reconfigurable dual-frequency microstrip-fed microstrip patch antenna.

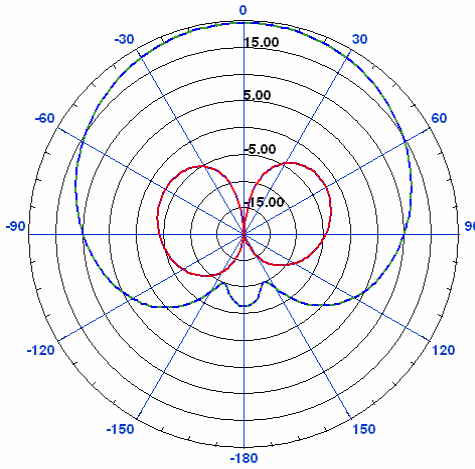
- (a) Simulated OFF-state E-plane @ 6.4 GHz, (b) Measured E-plane @ 6.9 GHz (5dB / div),  
(c) Simulated OFF-state H-plane @ 6.4 GHz, (d) Measured H-plane @ 6.9 GHz (5dB / div),



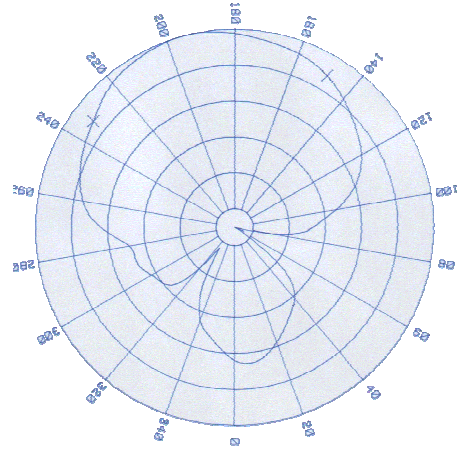
(e)



(f)



(g)



(h)

**Figure 4.13 (cont'd):** Radiation pattern simulation and measurement results of integrated re-configurable dual-frequency microstrip-fed microstrip patch antenna.

(e) Simulated ON-state E-plane @ 8.7 GHz, (f) Measured E-plane @ 8.9 GHz (5dB / div), (g) Simulated ON-state H-plane @ 8.7 GHz, (h) Measured H-plane @ 8.8 GHz (5dB / div).

**Table 4.1:** Simulated gain results of integrated re-configurable dual-frequency microstrip-fed microstrip patch antenna.

Antennas at:	Gain (dB):
OFF-State @ 6.44 GHz	1.11
ON-State @ 8.7 GHz	1.60

**Table 4.2:** 3-dB bandwidth measurement results of integrated re-configurable dual-frequency microstrip-fed microstrip patch antenna.

<b>E-Plane</b>	<b>3-dB BW:</b>	<b>H-Plane</b>	<b>3-dB BW:</b>
@ 6.9 GHz	52.9°	@ 6.9 GHz	106.0°
@ 8.9 GHz	32.2°	@ 8.8 GHz	84.0°

Gain of antennas from simulation and 3-dB bandwidths from radiation measurement results are shown in Table 4.1 and Table 4.2, respectively.

#### 4.4. Summary

In this study, two complete designs of a re-configurable dual frequency antenna structures including their integrated RF MEMS switches and their actuation lines are introduced. During the study, instead of utilizing the available RF MEMS switches in METU production line, brand new switches suitable for this application are designed. Two different switch configurations are studied. Although very good performance is obtained for both of these configurations, the switch set design consisting of two switches is preferred due to the lower DC voltage requirement for the actuation.

Based on the results above, there are a few noticed significant outcomes. One of them is simulation results show that there are two good resonances at both frequencies when switches are in ON state for microstrip-fed structure. This unexpected result, which was the driving point of this study, could be explained as the additional admittance of switch and coupling between stubs and patch. The switch impact could be because of the structure of switches: capacitive T-Wings. There is a certain layer of dielectric, which has a dominant role in admittance especially when switches are at ON state. The second and more dominant impact could be driven from the stubs and their groundings. Because from the graphs it is observed that only microstrip-fed structures have both well resonances at the same time but CPW-fed structure. As could be tracked, in spite of the feed and grounding

approaches are similar; the ground structures are different by its nature, which might result with different coupling to the patch.

Another observation from comparison of two different feed structure is that, with 1 MHz resolution, the 10-dB bandwidths are noteworthy different. Microstrip-fed structure has two or three times wider 10-dB bandwidth than CPW-fed antenna, in both frequencies. This result could be explained by taper structure. As it has been described before, for the optimum design effort grounding microstrip to CPW taper is designed as linear. This linear structure has a great advantage of presenting design easiness, in the cost of narrower bandwidth and increased phase vs. frequency slope. As the taper gets smoother or more exponential bending, such as polynomial tapers, wider bandwidths of impedance matching are expected to be achieved.

In both antenna structures, when switches are at up-state, it is observed that there is an additional resonance at mid-frequency: around 7.25 GHz. That resonance does not occur when each part of antenna (stubs, shorting pins of the stubs, switches, and slot) is excluded from the complete structure, one by one. Also, while examining the radiation pattern and radiation efficiency of the antenna at all resonance frequencies (including the mid-frequency), it is observed that both gain and radiation efficiency at this mid-frequency are much lower than the ones at the lower (6.5 GHz) and higher (8.5 GHz) frequencies. The conclusion regarding to that resonance is; there is a very good match of antenna at the specified frequency however radiation characteristics at mid-frequency are very poor, for both microstrip- and CPW-fed antenna structures. Therefore, that resonance at mid-frequency is not adequate for this application.

Both CPW-fed and microstrip-fed integrated re-configurable dual-frequency microstrip patch antennas are manufactured by RF MEMS group in METU – MET facility and microstrip-fed antenna is measured successfully to compare with the simulation results. When all graphs are concerned all together, all the performances expected from the antennas were not short in measurements. The good resonance at low frequency is achieved when switches are at OFF state. Also when switches are

ON, the low input return loss is obtained at high frequency but low frequency. This is, as a matter of fact, the true motivation of this study: not having good resonance at multi-frequencies at the same time. There are generally some frequency shifts between measurement and simulation results, but those shifts could be accepted within in experimental accuracies. Besides, in fact all structure is processed in MEMS manufacturing, the feeding and grounding is realized by large-scaled connector, bonding with some conductor: silver epoxy. That might cause some resonance shifts through the complete structure. Moreover, when radiation measurements are considered, the noticeable effect of antenna spinning structure and any forward- or back-scattering should not be unrewarded. Therefore there might be inevitable additional admittance introduced in the experimental environment, which cause slight excursions on the plots.

In addition, one other dominant reason for those differences could be antenna performance sensitivity on stubs dimensions. The stubs used in the structure are only 50  $\mu\text{m}$  wide, and the lengths are longer than 10 mm. There is a huge aspect ratio, which enables some fabrication difficulties or imperfections. Other than that dielectric thickness was a very critical parameter in switch design. Thus small changes in manufacturing might cause un-expected mismatches. But to sum up, all measurement results are interpreted as compatible with design simulation results.

## CHAPTER V

### HYBRID RE-CONFIGURABLE (TRIPLE FREQUENCY) MICROSTRIP PATCH ANTENNA

In this chapter the complete design and manufacturing details of two hybrid re-configurable triple-frequency microstrip patch antennas are introduced. The major difference on these antennas is complexity in insets; the first configuration has one stub in its inset, which offers two different effective inset lengths, one at a time. And the second configuration has two stubs in each inset, which procures finer matching at each of three frequencies. Moreover, in both configurations there is another switch placed on the slot for adjusting the slot size. All those implementations are investigated through design and manufacturing phase of that hybrid structures, which are all explained in this chapter. The operating frequency bands of these linearly polarized antennas are selected to be L – S bands, 1.8 GHz, 1.9 GHz and 2.4 GHz, as these three frequency bands are most commonly used frequencies in cellular phone and WLAN applications.

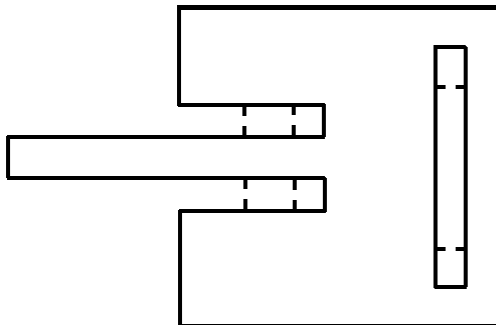


**Figure 5.1:** Hybrid Re-Configurable (Triple Frequency) Microstrip Patch Antenna

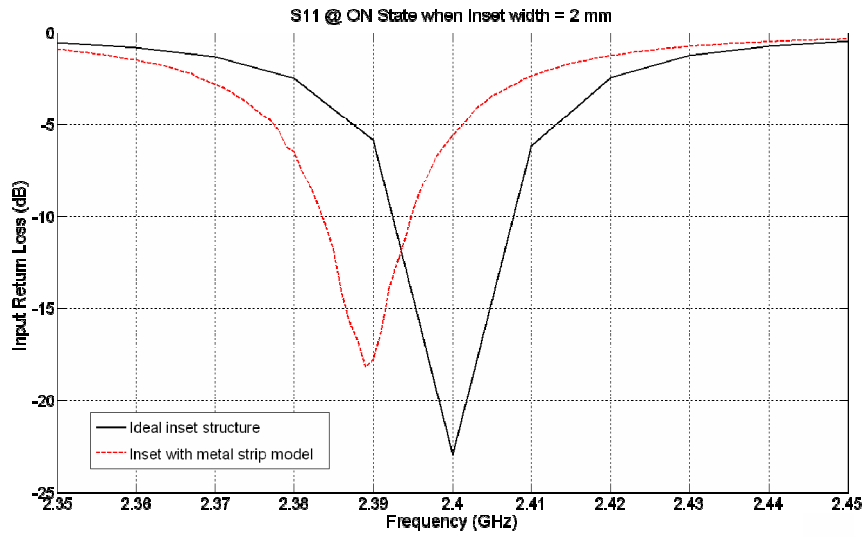
In the first section of chapter, the motivation and proposed performance for this particular antenna structure is pointed out. Then investigated patch antenna structure, both single and double stub configurations, is going to be explained. Next, the design details of RF MEMS switches that are planned to be used in this antenna are given. In the following section, separate MEMS and microstrip-patch manufacturing phases applied for this integrated structure are briefly introduced. Those phases are followed by hybridizing phase. Finally, simulation and measurement results are compared and discussed. Discussions are made for both S-parameter (input return loss) and radiation characteristics.

### **5.1. Antenna Design Details**

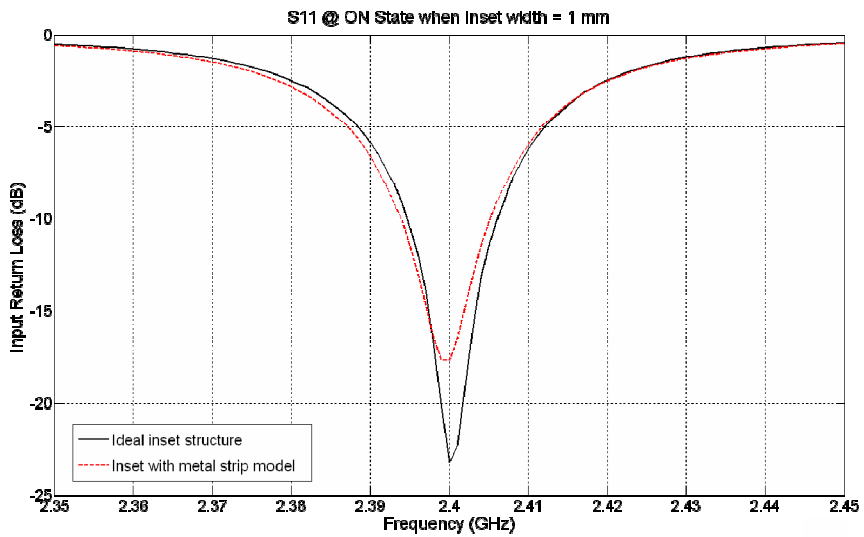
In this study, RO 4003 ( $\epsilon_r=3.38$ , Tangent loss is 0.0027) substrate with 1.52 mm thickness is chosen. Here the optimized dimensions of the dual frequency patch antenna are  $L = 40.8$  mm,  $W = 40.8$  mm,  $l = 1.3$  mm,  $l_i = 13.3$  mm,  $w = 1.1$  mm,  $l_s=1$  mm,  $l_f = 15.6$  mm,  $w_f = 3.52$  mm,  $w_i = 2$  mm.. Optimized inset lengths are found as 17.7 mm for 1.8 GHz, and 10.8 mm for 2.4 GHz. With those inset lengths, return losses decreased below -20 dB for both resonance frequencies.

Then when ON state metal strip model is applied even if the switch-to-switch spacing optimized, the best result had a resonance 11 MHz shift with almost 5 dB worse return loss Figure 5.2 (a). This impact is minimized by narrowing the inset width; therefore frequency shift sensitivity on inset length might be decreased.

Hence antenna inset width is changed from 2 mm to 1 mm; because of an expectation of less sensitivity on inset length, in the cost of leaving a smaller area to resolve possible switch related issues in following steps of hybrid structure design. New ideal inset lengths are determined as 19.1 mm and 11.5 mm, for 1.8 GHz and 2.4 GHz respectively. When ON state metal strip modelling is applied as same as before (switches are placed 1.1 mm apart to each other until the shorter ideal inset position), again mismatch degradation is observed but not any resonance frequency offset at all Figure 5.2(b). The deviations at ON state metal strip modelling for two



(a)



(b)

**Figure 5.2:** ON state metal strip model performance of two inset width alternatives.

(a) Inset width = 2 mm, (b) Inset width = 1 mm.

different inset widths are shown in Figure 5.2.

As seen from the graphs, when inset width is set to be 1 mm only, slide of the resonance frequency is avoided truly. Also, together with ON state impacts of

switches, OFF state impacts are also covered in antenna inset width design work. However the OFF state performance is effecting RF MEMS switch type selection. Therefore related design details in that topic are going to be discussed in *RF MEMS Switch Design Details* section, explicitly. In following paragraphs, antenna design is explained furthermore based on two serial connected SPST (T-Wing) switches.

This work continued on re-configurable triple-frequency microstrip patch antenna after above achievements in dual-frequency exercises. As stated in previous chapters, together with the dimensions of the patch, the length of the slot determine the resonance frequencies. Hence, in order to obtain the resonance at the third frequency, the length of the slot is adjusted by placing RF-MEMS switches at the end points of the slot. The third frequency is chosen to be 1.9 GHz.

The optimized dimensions for a good resonance at this frequency are  $L = 40.8$  mm,  $W = 40.8$  mm,  $l = 1.34$  mm,  $l_i = 16.9$  mm,  $w = 4.12$  mm,  $l_s = 1$  mm,  $l_f = 15.6$  mm,  $w_f = 3.52$  mm,  $w_i = 1$  mm. the corresponding input return loss performance is shown in Figure 5.3

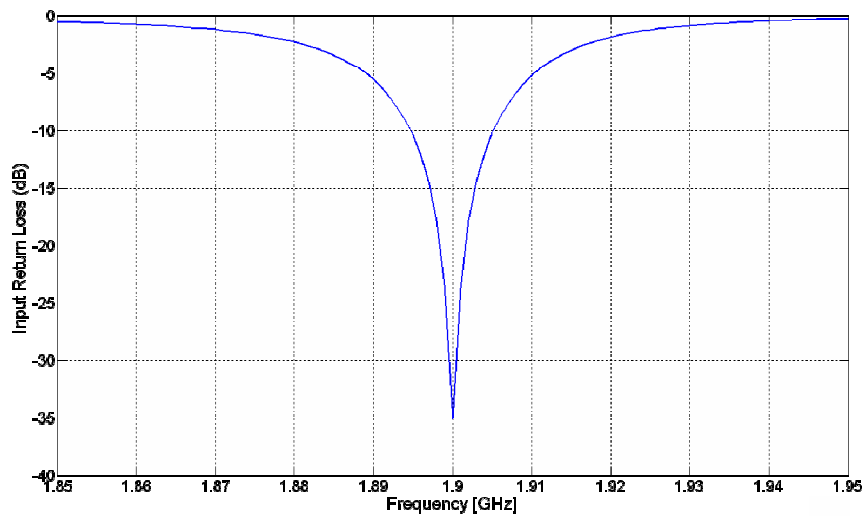


**Figure 5.3:** S11 performance of ideal antenna structure resonating at 1.9 GHz.

Up to here, listed first four-step work is also done in order for the new 1.9 GHz resonance. For better matching at 1.9 GHz, only single switch (the one in the deepest side of the inset) is operated at ON state in each inset, as requested inset length is already close to the 1.8 GHz one. Also in slot, two switches (one in one side and one in the other side to keep symmetry in the structure for radiation purposes) are used to shorten the effective slot-length. The simulation results of the whole structure is going to be shown later in this chapter.

In the following two sections, two configurations are going to be introduced. The goal in this study was implementing three different inset lengths for better matching at each resonance. However hybridizing an antenna with RF MEMS switches is a new topic to be investigated by this research group, therefore a single stub configuration is decided to be implemented first for understanding the behaviour of this hybrid antenna structure. After possibly having success in single stub configuration, a more complex inset structure (double stub), which provides two actuations resulting with matching at each frequency, is planned to be investigated.

### **5.1.1. Single Stub Configuration**

In single stub configuration there are two switch groups, in functional manner. The first group is placed in slot, which adjust the resonance frequency sweep from either 1.8 GHz & 2.4 GHz or 1.9 GHz, in OFF and ON state respectively. Other than that, another switch group is placed in inset for matching purposes. However as only single stub is planned to be used, there would be only two inset effective lengths. In non-conducting (OFF) state of switches, antenna should resonate at 1.8 GHz and 1.9 GHz with the best matching possible. In contrary, at conducting (ON) state of switches, antenna should have the requested matching performance at 2.4 GHz. In other words, OFF state is shared by two adjacent (1.8 GHz and 1.9 GHz) resonance frequencies, therefore it is expected to have a degradation in input return loss performance at those frequencies in the beginning of design phase of single stub configuration. But better matching goal is still valid for proposed resonance at 2.4 GHz.

To actuate serial connected SPST (T-Wing) switches used in slot of patch antenna, there has to be a DC-potential difference between serial-switch-intersection and centre conductors (signal line) of each switch, which establishes the connections to the patch. To supply that potential difference, DC-voltage is assumed to be pertained through microstrip feed together with RF. On the serial-switch intersection (carrier side of T-Wing), antenna structure might provide a DC-grounding with a stub connected to patch ground. Here a few stub approaches are investigated; some are shown in Figure 5.4.

The design study on type of grounding stub in the slot resulted in rectangular stub continued by radial stub Figure 5.4(d). The reasons for others not selected are briefly, in (a) and (b) approaches resonance at 1.9 GHz is either disappeared or moved so far away. The reason thought for that is even when quarter wavelength length is adjusted as stub length, due to the coupling with patch; the resonance is affected. Also in (b) a grounding path is opened on the radiating edge. Such a stub might have a negative impact on radiation pattern because of DC-grounding with

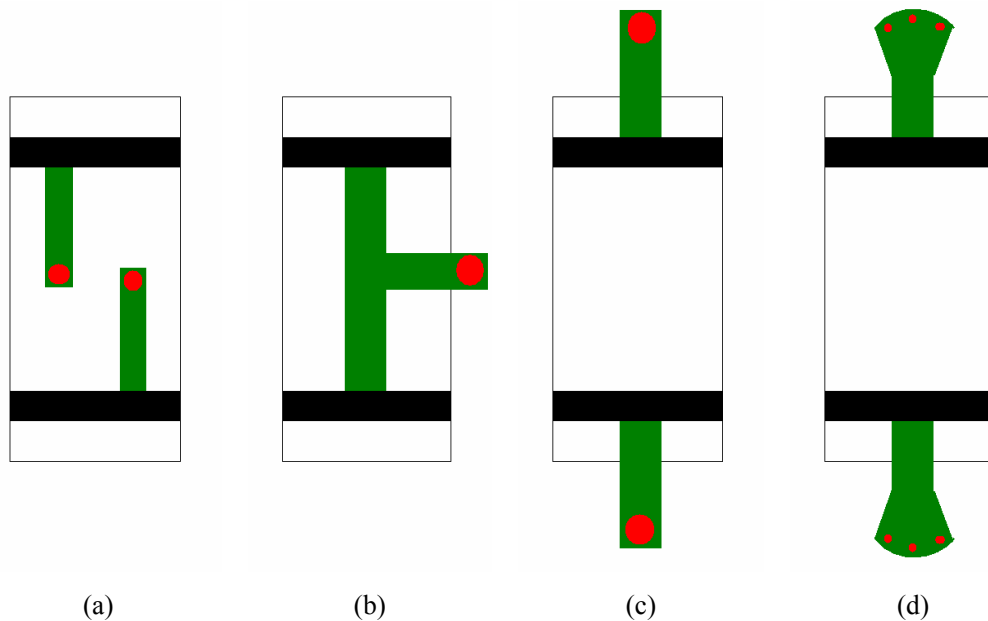


**Figure 5.4:** Slot switch grounding stub alternatives investigated in the study, where black colour represents switches, green stubs, and red via to ground plane.

RF-leakage. When slot approach (c), which is a regular rectangular stub and (d) is compared, radial (40° wide) stub ending is preferred as it is having wider and smoother phase characteristics, in the order of 100 MHz whereas rectangular stub does in the order of 10 MHz.

However the choice of (d) has an impact on the antenna physical structure, unfortunately (Figure 5.5) in contrary to (a-b). That impact is the need of a bridge over the stub, to connect the right hand side of the patch to the feed-side of the patch. Such a bridge type connection is not an ideal solution, which results with also some design criteria. Some important parameters in a design of such bridge are its elevation (z-axis) distance from stub, its cross section at the connections of patches. After tuning, that bridge size is obtained to be 1.3 mm x 0.96 mm, connected to each side of the patch by three via (r = 0.1 mm). The height resigned from the stub is 0.1 mm; the material between them is selected as air in simulations. This stub selection part of the study is almost same in both single and double stub configurations of hybrid re-configurable (triple-frequency) microstrip patch antenna.

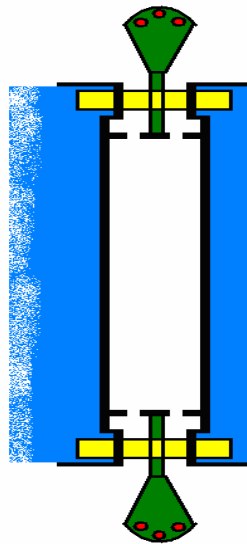


**Figure 5.5:** Impact of chosen radial stub

Green => Stub, Red => Via to ground plane, Black => Switch, Yellow => Bridge,  
Blue => Patch

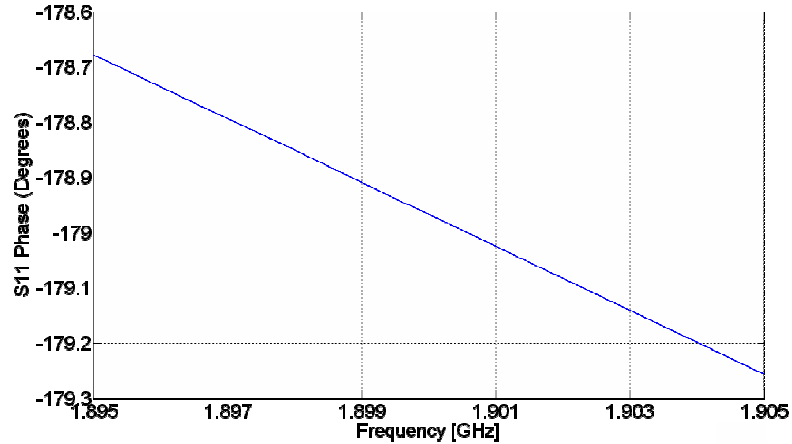


**Figure 5.6:** Phase performance of slot stub

**Table 5.1:** Dimensions of stubs in slot.

Stubs:	Rectangular Section		Radial Section	
	Length	Width	Length	Opening
<b>Slot Stub:</b>	5 mm	0.2 mm	9.5 mm	40°

Another impact of a rectangular stub followed by a radial stub is increasing the complexity of stub structure; again DC-short and RF-open for avoiding any RF-leakage to the ground. The total length is odd multiples of quarter-wave length. Here the stub is only used for 1.9 GHz application, therefore the quarter wavelength calculations are completed at 1.9 GHz. During all stub simulations, radial ends of stubs are not grounded but kept open, and stubs are expected to perform true short-circuit in rectangular end. The final dimension information and corresponding phase relation of the stub used in slot is shown in Figure 5.6 and Table 5.1, respectively.

Similar effort is spent for the grounding of switches placed in the inset. Again a rectangular followed by radial stub approach is embraced for inset stub. The rectangular stub is again tried to be kept as short as possible, for radial dominance as much as possible. So that, wider and smoother phase performance is achieved. In addition, during the antenna design a tilt of (20°) is realized on the inset stub to

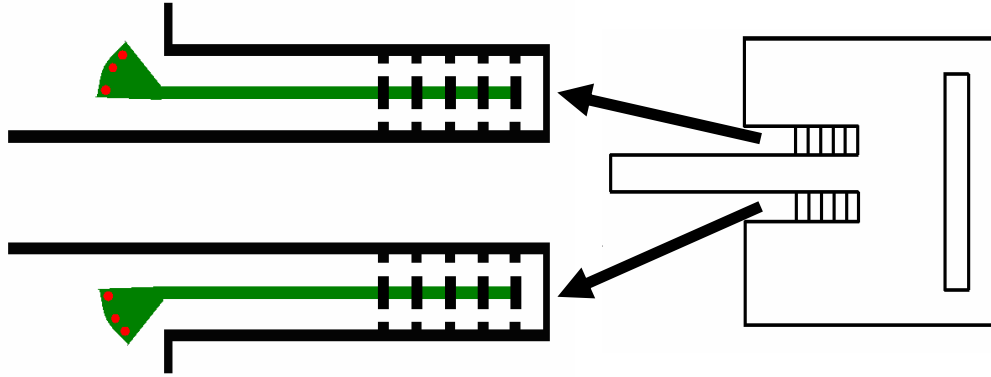


**Figure 5.7:** Inset stub in single stub in configuration.

**Table 5.2:** Dimensions of stubs in inset.

Stubs:	Rectangular Section		Radial Section	
	Length	Width	Length	Opening
<b>Inset Stub:</b>	17.5 mm	0.2 mm	2.65 mm	40°

avoid the radial stub and microstrip feed overlap (Figure 5.7), just after the radiating edge corner. The dimensions of stubs are represented in Table 5.2.

One of the major differences in the design of inset stub from the slot stub is the value of frequency used in quarter wavelength calculations. In inset, stub is used to actuate switches when antenna is utilized for 2.4 GHz resonance. Therefore RF-leakage to ground should be avoided only at 2.4 GHz, and at the other frequencies switch isolation is expected to be enough to prevent any leakage from patch to ground through stubs. The other difference in this inset stub from the slot stub design is reasoned by not being connected to a single switch. This particular stub is planned to be connected to a few switches at the same time, in each inset Figure 5.7. Thus calculated quarter wavelength length would not transform impedance exactly in real implementation of the structure. To minimize this deviation effect, average centre point of switches is taken into account. Again rectangular section of stub is kept as short as possible for phase bandwidth. Phase performance of designed inset stub is shown in Figure 5.8.

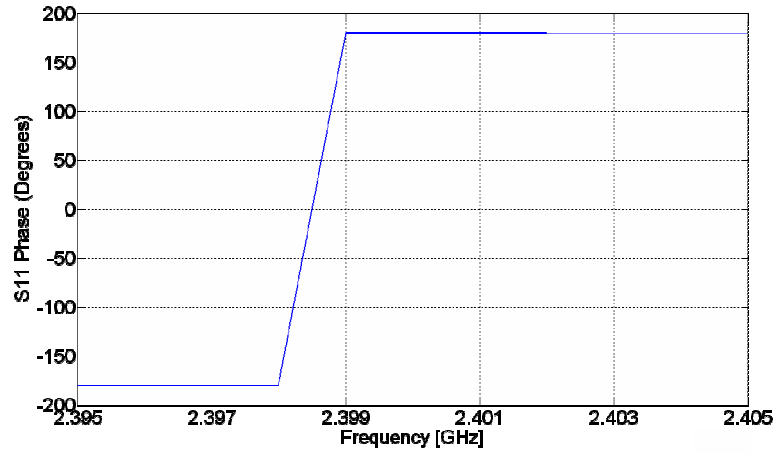


**Figure 5.8:** Phase performances of inset stub.

Finally the complete antenna structure (including inset lengths, slot position and lengths, switch positions) is optimized after partial designs are completed. Hence the coupling between stubs and patch, the bridge effect, as well as the switches are taken into account all together in simulation. Previously designed and manufactured (Hüseyin Sağkol, Kağan Topallı, Mehmet Ünlü) RF MEMS switches in METU facilities are included as black boxes in the antenna simulations, by using their S-parameters in the gaps within switch model. Simulation tool for this study was 2.5D EM simulator, Ansoft, Ensemble. Detailed information about used switches and hybrid antenna performance graphs are going to be given in later sections of this chapter.

### 5.1.2. Double Stub Configuration

The double stub configuration is the actual determined goal of this study to be achieved, from the beginning of the triple frequency idea. In this stub configuration each resonance frequency would be able to find its exact impedance matching, ideally. Achieved goals when metal strip model is implemented for this structure are shown in Figure 5.9. To achieve the goals, brand new switch sets are designed. It is proposed that single switch for each resonance matching would be enough if

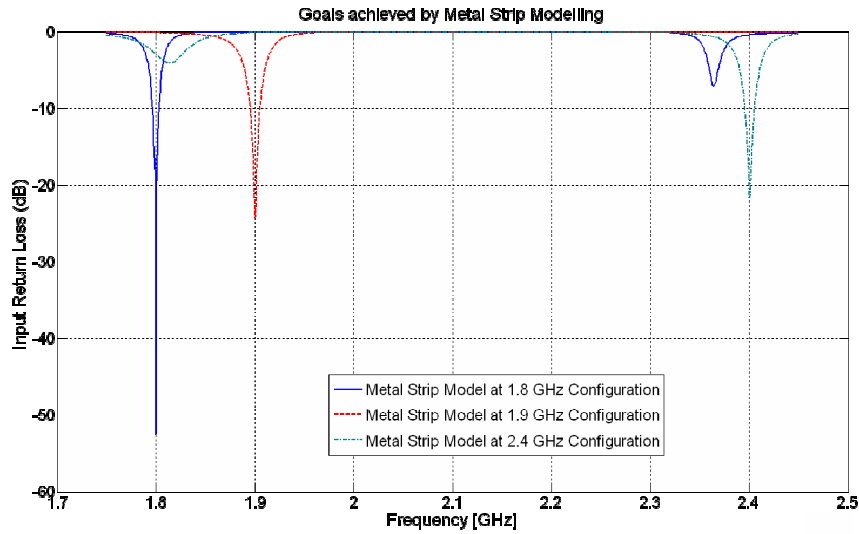


**Figure 5.9:** Metal strip model driven design goals of triple-frequency antenna.

switches are designed properly for this antenna use, in contrary to use of multiple re-manufactured switches. This switch work is going to be explained in detail in the next section. The impacts of designing brand new switches in inset and slot structures are explained next.

First, let's consider impact of inset stub. According to new inset structure approach, impedance matching is still assured for 1.8 GHz by default (the longest) inset length. However, now on there would be only two switches to be actuated individually for matching purposes at 1.9 GHz and 2.4 GHz. This time both for 1.9 GHz and 2.4 GHz switch actuations, the stubs are connected to each single switch. However, as there is going to be two stubs in same inset area, the stub widths and coupling between stub-to-stub and stub-to-patch is expected to increase.

For better visualization during the explanation of design effort, inset schematic of proposed double stub configuration is shown in Figure 5.10.

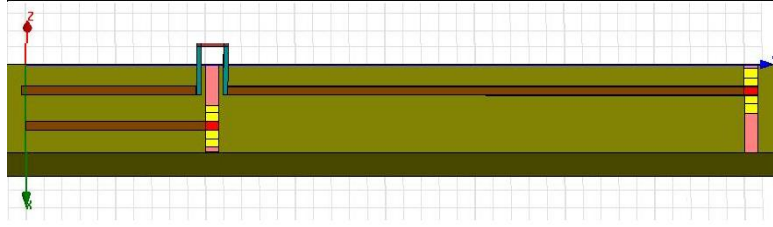


**Figure 5.10:** Close look into proposed inset structure in double stub configuration.

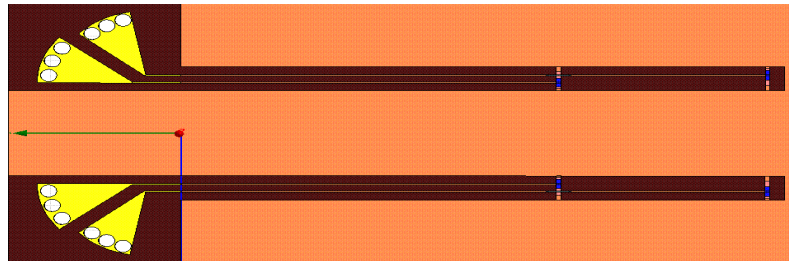


**Figure 5.11:** The proposed inset whole structure in double stub configuration

As it can be seen in Figure 5.10, there is a challenge to fit two stubs in the inset. The rectangular section of stubs has  $50\ \mu\text{m}$  widths, because smallest end-mil radius of in-house microstrip manufacturing capabilities is 10 mils. The gap between two stubs is adjusted as far as possible, around  $250\ \mu\text{m}$ . The stub-to-patch distance is kept over  $300\ \mu\text{m}$ . An interesting architecture in this inset is the bridge across the 2.4 GHz switch. That bridge is used to connect 1.9 GHz switch to the ground while jumping over the 2.4 GHz switch. This bridge models the wire-bond to connect two breakdowns of 1.9 GHz rectangular stub. That rectangular stub is followed by a radial stub as seen from Figure 5.11. When carefully looked at two stubs in each inset, it can be observed that the radial stub sizes are different. That's because these two stubs are designed individually. The outer most one is for 1.9 GHz switches DC-ground and an RF-open, whereas the inner most is for the same function at 2.4 GHz switches. The inset radial stubs have ground connections through via which are placed at the very end ( $r = 0.2\ \text{mm}$ ). The dimensions regarding the stubs and corresponding phase characteristics for those stubs are specified in Table 5.3.

**Table 5.3:** Dimensions of stubs in slot and inset

Stubs:	Rectangular Section		Radial Section		Frequency	Phase
	Length	Width	Length	Opening		
<b>Slot (1.9 GHz):</b>	6.0 mm	100 $\mu\text{m}$	8.3 mm	20°	1.9 GHz	-179.8
<b>Inset (1.9 GHz):</b>	19.0 mm	50 $\mu\text{m}$	2.65 mm	20°	1.9 GHz	-179.7
<b>Inset (2.4 GHz):</b>	13.0 mm	50 $\mu\text{m}$	2.9 mm	20°	2.4 GHz	179.2

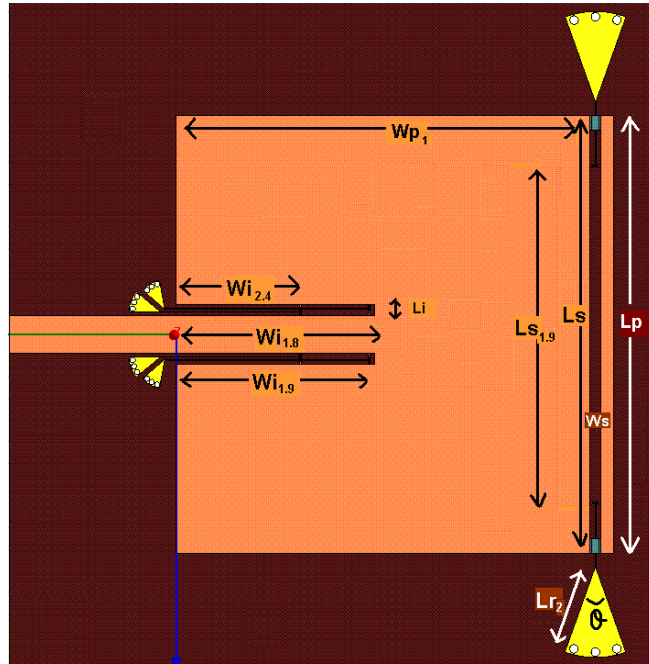


**Figure 5.12:** Overall proposed hybrid re-configurable (triple-frequency) microstrip patch antenna with double stub configuration.

In addition, there are also some impacts of using brand new switches in slot, particularly for this antenna. They are the re-tuning of switch position on the slot, and change in dimension of the stub that connects to the ground. A change in switch position is obligatory, based on change in its insertion loss. Another expected improvement is on switch electrical characteristics. Also, because of the change of carrier width of slot switches from 0.2 mm to 0.1 mm, the stub length for DC-ground and RF-open, is also changed. An overall schematic of the proposed hybrid re-configurable (triple-frequency) microstrip patch antenna with double stub configuration is shown in Figure 5.12.

## 5.2. RF MEMS Switch Design Details

During the single stub configuration design, a capacitive SPST RF MEMS switch is selected from METU Electrical & Electronics Engineering Department RF MEMS switch gallery, to be used in antenna design. Switch configurations are evaluated for the best performance. For that purpose, a detailed work is carried out for switches along the inset.

As explained in the very beginning of this chapter, ON state metal strip modelling is performed for determining goals in the study. Also an OFF state metal strip modelling in dual-frequency mode of this study, for understanding whether enough isolation is achieved from single SPST switch at OFF state, or two SPST switches connected is needed. Basically, the switch is thought to be placed either once or twice into the gaps in inset (Figure 5.13). Switches are expected to be placed on a 1 mm x 0.1 mm area. The simulation results of those investigated alternatives among metal strip modelling are shown in Figure 5.14 (a).

As it is observed from Figure 5.14 (a), there is not a design driven difference from metal strip modelling analysis. That's why similar work is performed by including the measured S-parameter data for both OFF and ON states (Figure 5.14 (b), (c)).

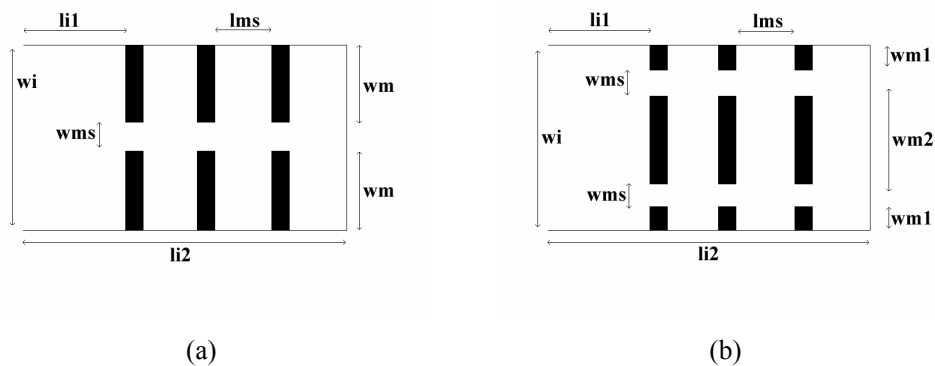
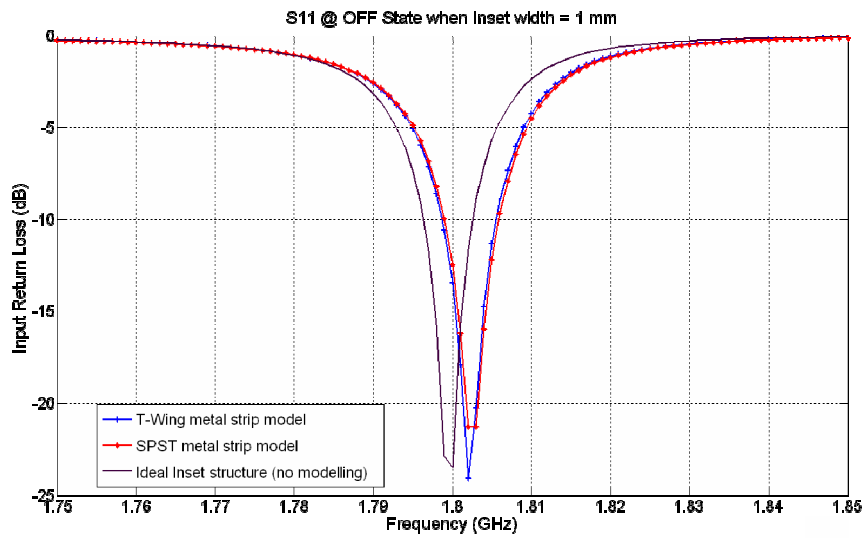
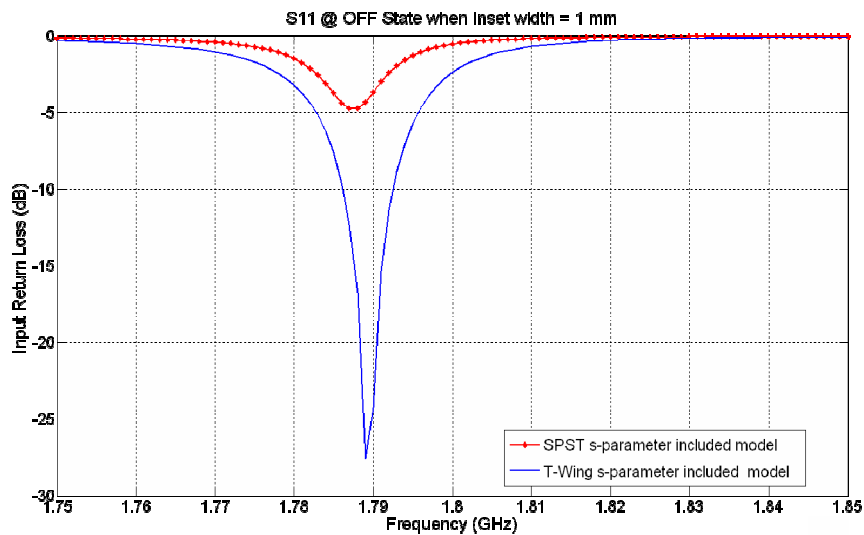


**Figure 5.13:** Inset switch alternatives (a) Single SPST, (b) Serial connected SPSTs, where  $li1 = 11.5$  mm,  $li2 = 19.1$  mm,  $wi = 1$  mm,  $lms = 1.1$  mm,  $wms = 0.1$  mm,  $wm = 0.45$  mm,  $wm1 = 0.1$  mm,  $wm2 = 0.6$  mm.

Especially at OFF state, with single SPST a great matching degradation is interpreted, compared to metal strip case. However the two-serial-switch (T-Wing) approach gave very close result to both metal strip and ideal cases. So the antenna design with single stub configuration continued on having two serial connected (T-Wing) switches in inset and slot.



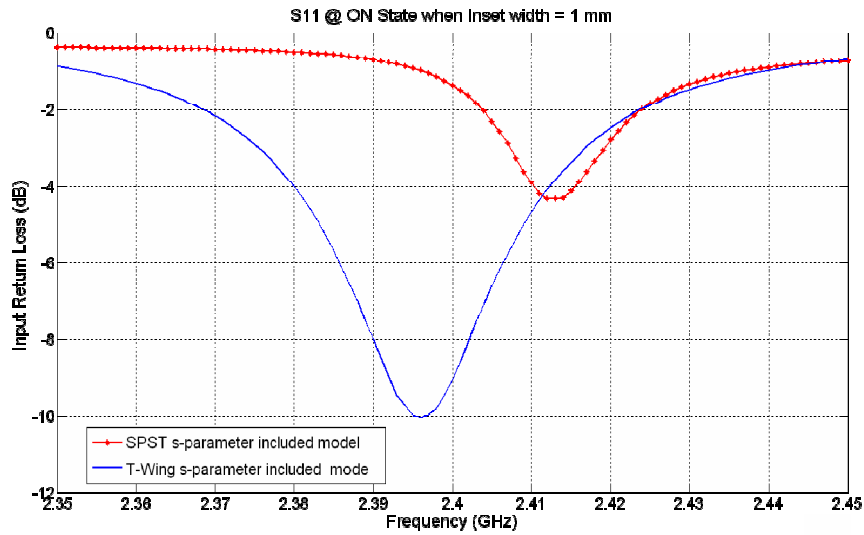
(a)



(b)

**Figure 5.14:** Switch type alternative simulation results to be used in antenna structure.

(a) Metal strip modelling at OFF state, (b) S-parameter included OFF state,



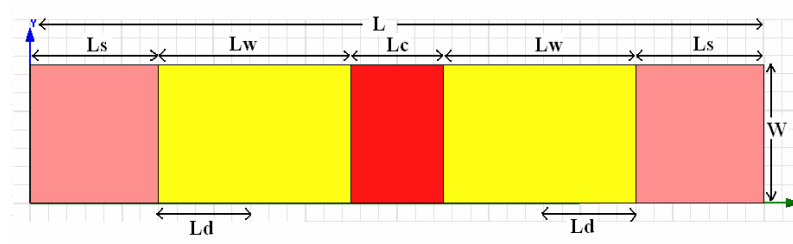
(c)

**Figure 5.14 (cont'd):** Switch type alternative simulation results to be used in antenna structure. (c) S-parameter included ON state.

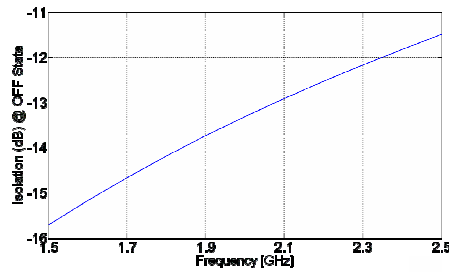
In double stub configuration however, as 1 mm x 0.1 mm area can not be reserved for each resonance frequency switch set due to the lack of space, a switch design is performed. This new switch type is chosen to be T-Wing, in consistency with serial connected SPST switches used in single stub configuration. T-Wing switch is expected to behave like serial connected SPST switches but provides a gain in space, as being an integrated SPDT structure. In the next two sections individual design efforts spent for T-Wing switches in slot and inset are explained.

### 5.2.1. Slot Switches

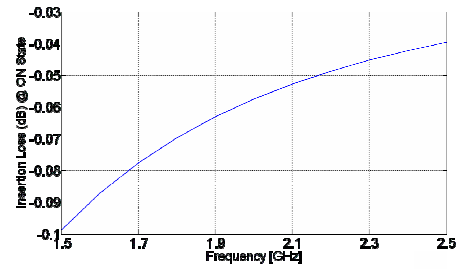
Three individually designed switches exist in several areas of proposed hybrid re-configurable (triple-frequency) microstrip patch antenna with double stub configuration. Therefore a performance requirement study for a single switch is not applicable in this configuration in contrary to the switch design work in integrated re-configurable (dual-frequency) microstrip patch antenna. However, through the experience achieved from previous design, it is still useful to determine electrical



(a)



(b)



(c)

**Figure 5.15:** Designed slot switches (1.9 GHz) for double stub configuration of hybrid re-configurable (triple-frequency) microstrip patch antenna

(a) Schematic, (b) Isolation at OFF state, (c) Insertion Loss at ON state,

where  $W = 150 \mu\text{m}$ ,  $L = 1 \text{ mm}$ ,  $L_c = 100 \mu\text{m}$ ,  $L_s = 140 \mu\text{m}$ ,  $L_w = 210 \mu\text{m}$ ,  $L_d = 110 \mu\text{m}$ .

requirement goals of T-Wing switches. The design goals for T-Wing switches at OFF and ON states are defined as  $> 11 \text{ dB}$  of isolation and  $< 0.7 \text{ dB}$  of insertion loss, respectively.

The space allocated for slot switches is 1 mm long (as long as slot width), which is fairly enough and that's why it makes the switch design easy compared to inset switches. As OFF and ON switch states and design assumptions are already described in Chapter 4, it is not needed to repeat switch states and related electrical functional information in this chapter. The schematic and corresponding OFF and ON state electrical characteristics of double stub configuration slot switch are shown in Figure 5.15.

### 5.2.2. Inset Switches

Same goals specified for slot switch are also valid for inset RF MEMS switches. Again similar design effort is spent for both for 1.9 GHz and 2.4 GHz inset switches. The schematic are shown in Figure 5.16 and Figure 5.17.

As it can easily be interpreted from last two figures, inset switches are not as symmetric as slot switch. The main reason for that is lack of space in inset. For best fit in inset including stubs, switches needed to have different length signal lines. However wing and dielectric lengths are kept the same for all switches therefore the

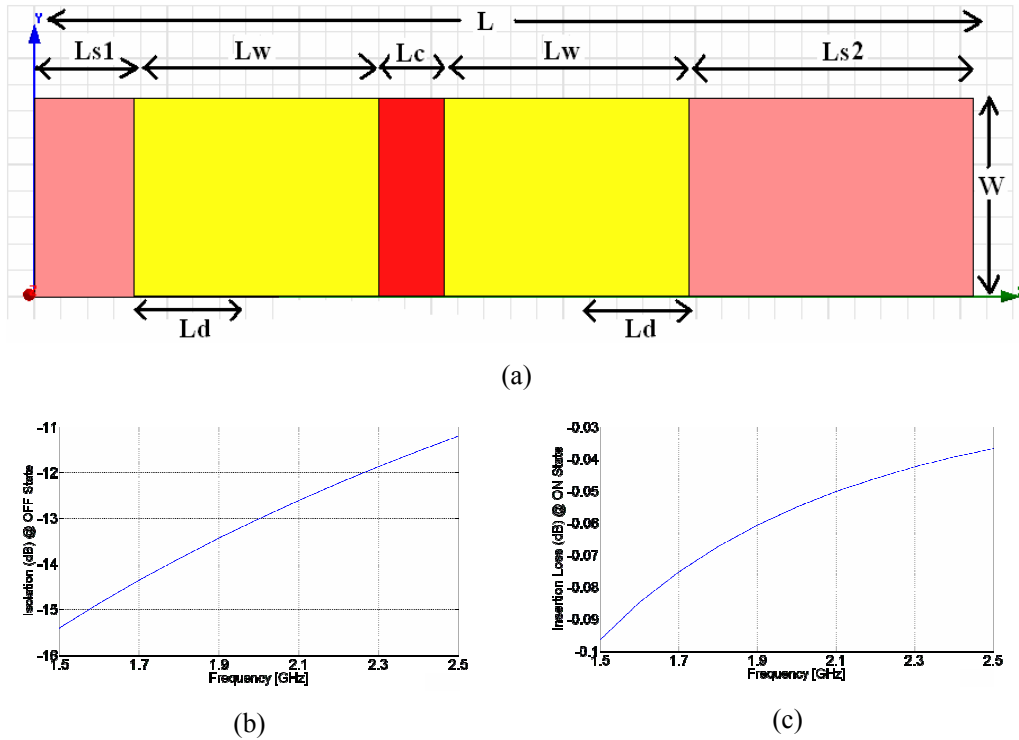
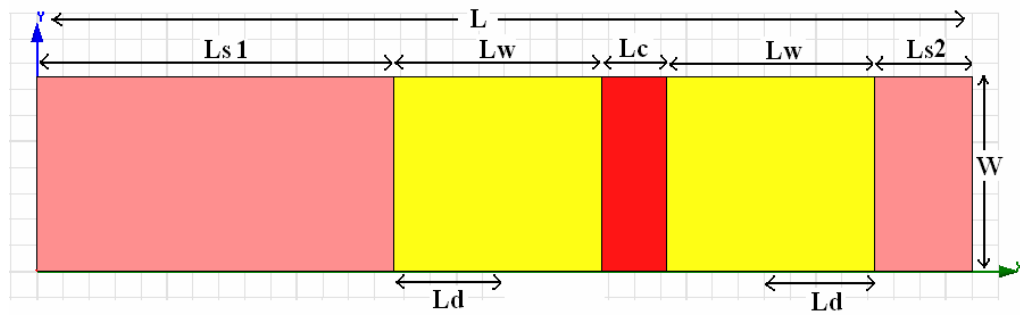


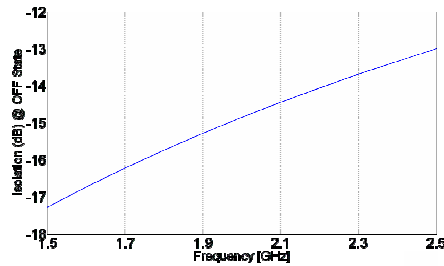
**Figure 5.16:** Designed inset switches (1.9 GHz) for double stub configuration of hybrid re-configurable (triple-frequency) microstrip patch antenna

(a) Schematic, (b) Isolation at OFF state, (c) Insertion Loss at ON state

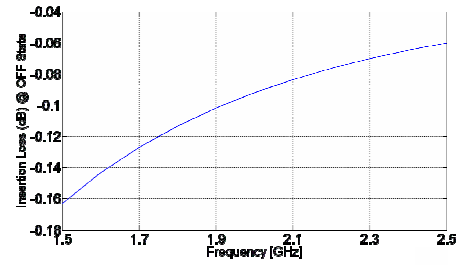
where  $W = 150 \mu\text{m}$ ,  $L = 1 \text{ mm}$ ,  $L_c = 50 \mu\text{m}$ ,  $L_{s1} = 75 \mu\text{m}$ ,  $L_{s2} = 215 \mu\text{m}$ ,  $L_w = 185 \mu\text{m}$ ,  
 $L_d = 110 \mu\text{m}$ .



(a)



(b)



(c)

**Figure 5.17:** Designed inset switches (2.4 GHz) for double stub configuration of hybrid reconfigurable (triple-frequency) microstrip patch antenna

(a) Schematic, (b) Isolation at OFF state, (c) Insertion Loss at ON state

where  $W = 150 \mu\text{m}$ ,  $L = 1 \text{ mm}$ ,  $L_c = 50 \mu\text{m}$ ,  $L_{s1} = 255 \mu\text{m}$ ,  $L_{s2} = 75 \mu\text{m}$ ,  $L_w = 160 \mu\text{m}$ ,  $L_d = 85 \mu\text{m}$ .

actuation voltage shall be same for both cantilevers of switches. An additional important remark about the design of switches is; for double stub configuration antenna two different switches are designed, in fact only one prototype could be enough if only OFF and ON state electrical performance is required. In other words, a single switch could be designed which would satisfy all electrical requirements for all frequency bands. However that is not preferred, instead two different inset switches are designed. That preference is related with switch actuation order, different actuation voltage levels is requested while antenna is switching from one frequency to other. This order shall be as follows; when no DC voltage is applied to the antenna, all inset switches are supposed to be at OFF state (wings are UP). At that configuration, the longest (default) inset length is effective inset length. When DC voltage is applied, inset 1.9 GHz switches are actuated first and only they switch

to ON state, but 2.4 GHz switch still stay at UP (OFF) state. So inset length is shortened to 1.9 GHz switch position. Next, when DC voltage is increased, inset 2.4 GHz switch is also actuated, and switched to ON state and meantime inset 1.9 GHz switch is still ON but does not ‘burn’ (dielectric is not overloaded). So current effective inset length is now the shortest inset length, which is the 2.4 GHz switch position. When DC-voltage is decreased switches are supposed to switch to OFF state in similar reverse order.

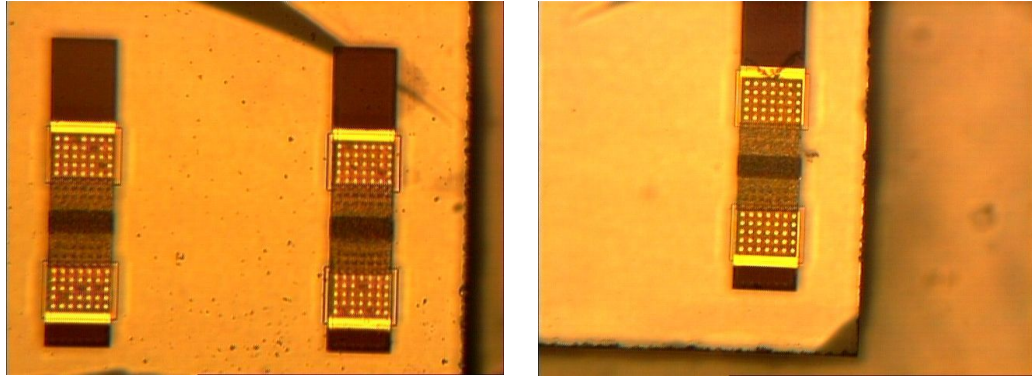
In summary, antenna working principle is extremely depending on actuation voltage levels of switches. That particular reason increases the importance of RF MEMS switch design for this study. The most challenging point during the switch design is adjusting the capacitive cross-section area of inset switches; it should be close enough to avoid breakdown but also different to actuate in functionally requested order. That’s why for this configuration, inset 2.4 GHz switch has to have larger capacitive cross-section area than inset 1.9 GHz switch; switches having larger capacitive cross-section area actuates with less voltage.

### **5.3. Manufacturing Details**

After design work is successively completed, antennas are manufactured to observe measurement deviations from simulations results. The manufacturing phase of this study is also very challenging because small scaled devices (RF MEMS switches) are manufactured individually, and large scaled (patch antenna including stubs) is manufactured by itself. Finally they are all combined in a single structure to work as a hybrid re-configurable (triple-frequency) microstrip patch antenna.

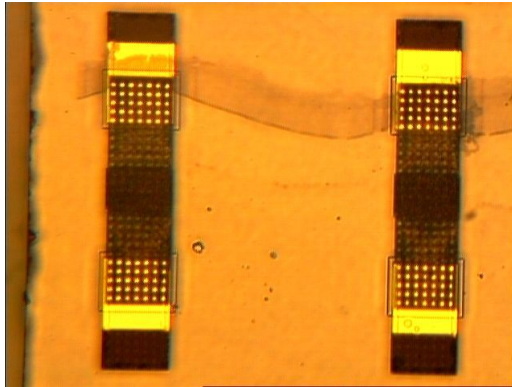
#### **5.3.1. RF MEMS Fabrication**

In this study, only RF MEMS switches are the small scaled components. Therefore only these switches are manufactured along MEMS fabrication flow, in METU facilities. The fabrication is pretty much similar to the flow specified in Chapter 4, that’s why the process flow is not repeated in this chapter. Indeed, capacitive SPST



(a)

(b)



(c)

**Figure 5.18:** Manufactured double stub RF MEMS switches

(a) Inset 1.9 GHz switch, (b) Inset 2.4 GHz switch, (c) Slot 1.9 GHz switch

switches planned to be used in single stub configuration has a dielectric thickness of roughly  $0.5 \mu\text{m}$  (depends on the MEMS fabrication).

Also the T-Wing switches designed for double stub configuration are processed on Corning Glass substrate ( $\epsilon_r = 4.6$ , Loss Tangent = 0.005), with the same thickness (0.5 mm) in METU MET facility. However the corresponding dielectric thickness is around  $0.3 \mu\text{m}$ . Some pictures of manufactured RF MEMS switches are shown in Figure 5.18.

### 5.3.2. Microstrip-patch Manufacturing

All microstrip patch antennas are planted on substrate RO 4003 ( $\epsilon_r = 3.52$ , Loss Tangent = 0.0027) with 1.52 mm thickness. LPKF, computer controlled

(CAM) mechanical RF and PCB prototyping device, is used to manufacture the large scaled parts of both hybrid re-configurable (triple-frequency) microstrip patch antenna configurations. As specified before the narrowest end-mil used in this manufacture has a radius of 10 mil (254  $\mu\text{m}$ ). Some pictures of the manufactured patch antenna configurations are shown in Figure 5.19.

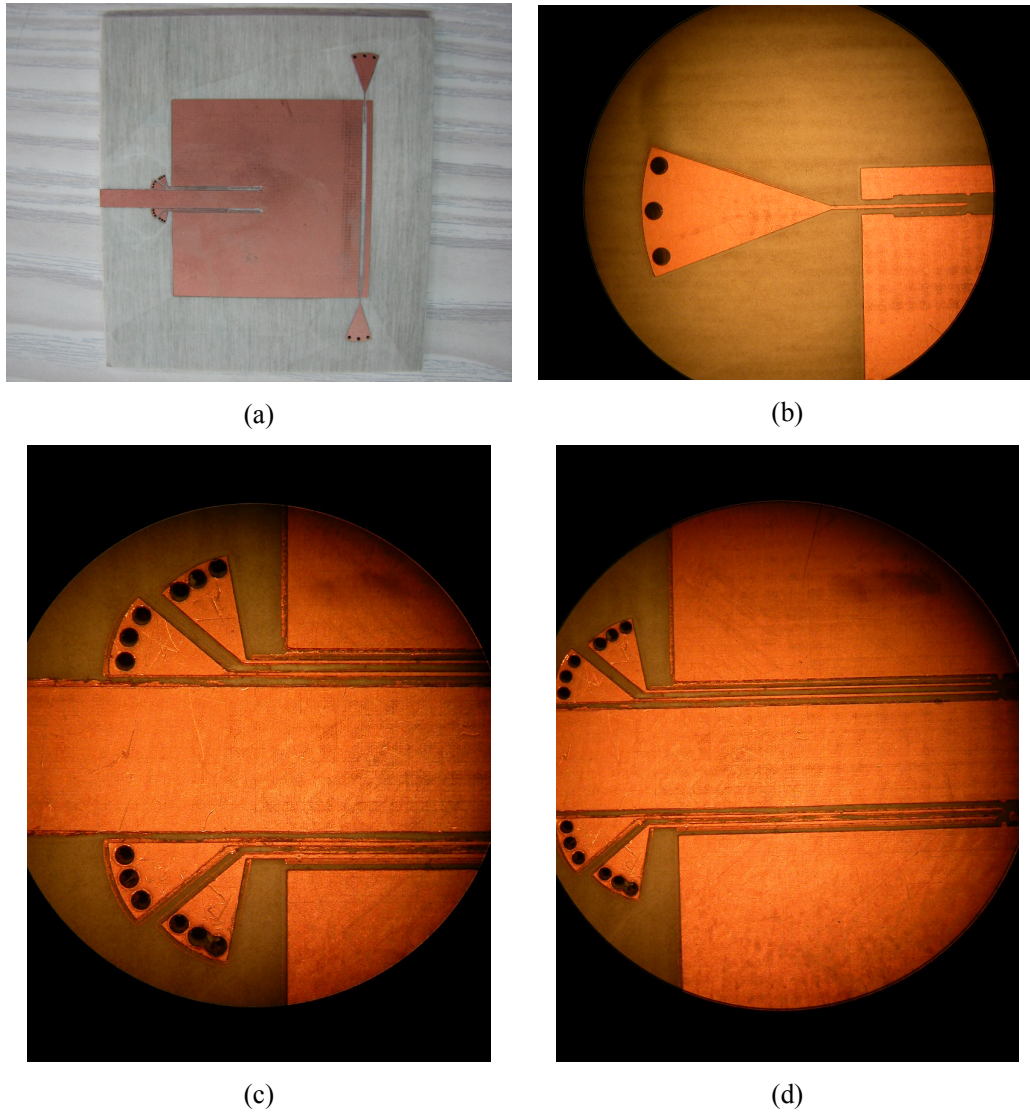


**Figure 5.19:** Manufactured double stub configuration of hybrid re-configurable (triple-frequency) microstrip patch antenna

(a) Whole structure, (b) Close look into slot,  
(c) Close look into inset radial stubs, (d) Close look into inset

Here two extra modifications are made on manufactured (by Mustafa Seçmen) patch antennas. First, all via connections from top face to ground plane placed in inset and slot stubs are assured by inner-hole-solder, by hand. The second modification is placing bridges which connect two sides of slot, and inset 1.9 GHz stub. In both single and double stub configurations slot bridges are realized as a 0.96 mm x 1 mm sized metal plate, which is placed over an isolating tape layer and soldered from edges to the patch gently. Inset bridges are planned to be realized through wire bond, in double stub configuration only. More detailed information about wire-bonding is given in the next section.

### **5.3.3. Hybridizing the Structure**

Hybridizing is one of the most highlighted manufacturing phases of this study, because very small scaled (micron-sized) devices are aimed to be integrated on a very large scaled component. By the word “hybridizing”, it is meant that these two different scaled objects (RF MEMS switches and the patch) are connected by some bonding, such as wire bonding in this case. With a wire bond, it is thought that switches and patch will be combined and act as a single hybrid structure. So that, when each switch is actuated, the patch would behave differently, perform different radiation characteristics. Theoretically there should not be any problem or surprising performance through those connections however the practical cases are also one of the objectives of this study. Those connections are assumed to be implemented well enough through wire-bonding.

Wire-bonding technology is common method to connect sensitive surfaces. In this study the sensitive surface is generally RF MEMS signal lines. A true and strong bonding should be valid on switch side to allow RF input signal flow on T-Wing switch. Additional use of wire-bond in the second part of this study is in double stub configuration, which is for supplying a connection along inset 1.9 GHz stub, as a bridge across inset 2.4 GHz switch. In this study a 25  $\mu\text{m}$  diameter gold wire-bond is planned to be used to connect the proposed surfaces.

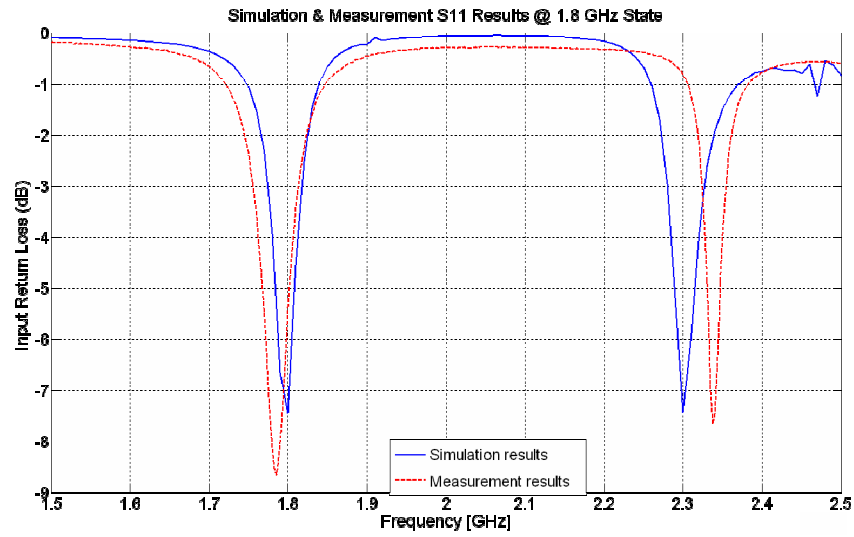
## **5.4. Simulation and Measurement Results**

After design of two hybrid re-configurable (triple-frequency) microstrip patch antenna configurations, antennas are built in METU facilities, as specified above. Then antennas are all measured individually by using metal strips to replace RF MEMS switches, as in model explained previously. Next two sections will be introducing the simulation and measurement results for both configurations. The simulators used for these configurations are Ansoft Ensemble and Ansoft HFSS, respectively.

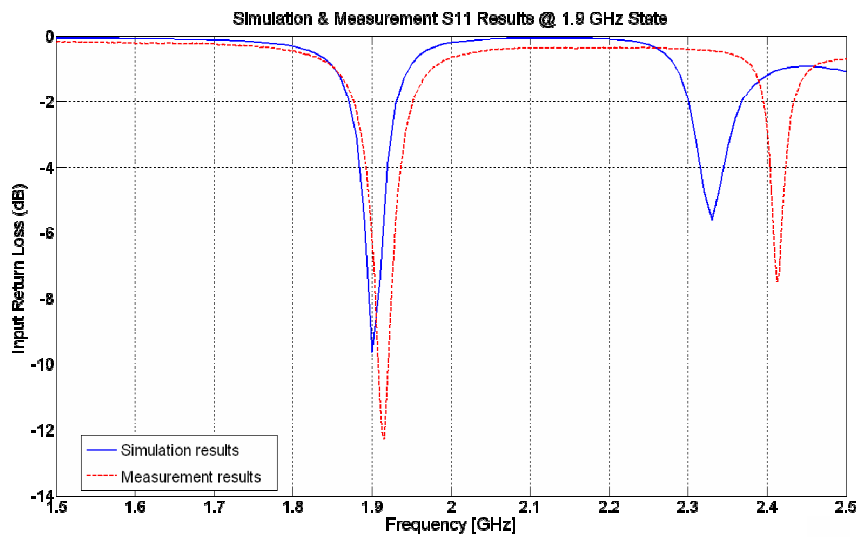
### **5.4.1. Single Stub Configuration**

In this configuration, re-configurability (triple-frequency) is obtained by exact individual matching at 2.4 GHz, but shared matching at 1.8 GHz and 1.9 GHz, as inset length kept same for these two frequencies whereas ideally they are different. The simulation and measurement results of this configuration using metal strip modelling are shown in Figure 5.20. As a remark, simulation results are s-parameter characteristics of switches are included, but during the measurements switches are realized as similar sized metal (copper) strips.

Also, radiation pattern simulation results at each resonance frequency for optimized hybrid re-configurable (triple-frequency) microstrip patch antenna single stub configuration with metal strip modelling are shown in Figure 5.21.

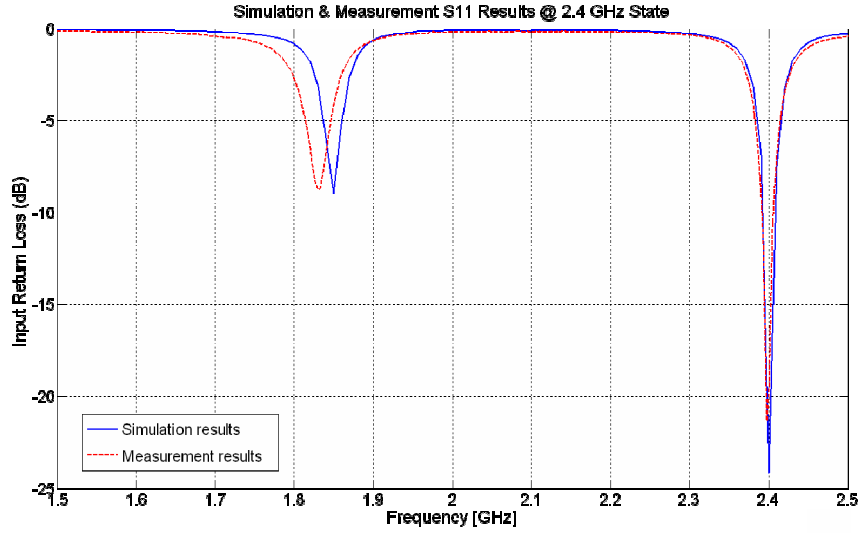


(a)



(b)

**Figure 5.20:** Simulation and measurement results of optimized hybrid re-configurable (triple-frequency) microstrip patch antenna single stub configuration with metal strip modelling. (a) At 1.8 GHz state (all switches are at OFF state)  
 (b) At 1.9 GHz state (inset switches are at OFF state, slot switches are at ON state)



(c)

**Figure 5.20 (cont'd):** Simulation and measurement results of optimized hybrid re-configurable (triple-frequency) microstrip patch antenna single stub configuration with metal strip modelling. (c) At 2.4 GHz state (all switches are at ON state)

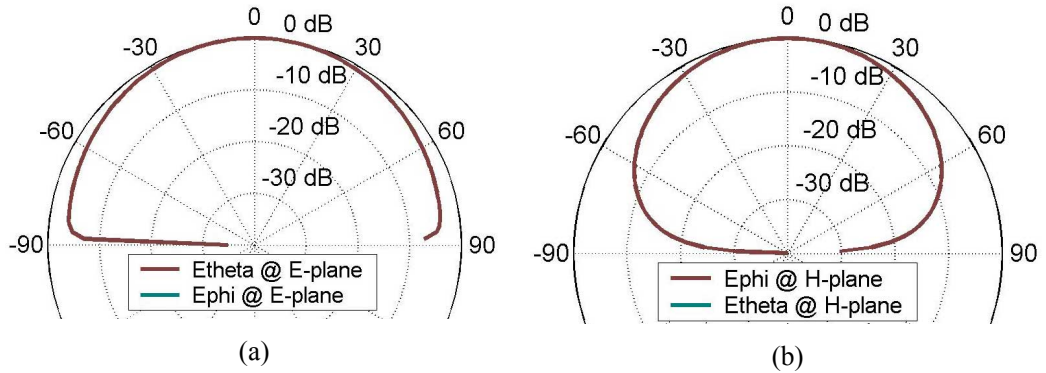


**Figure 5.21:** Radiation pattern simulation results optimized hybrid re-configurable (triple-frequency) microstrip patch antenna single stub configuration with metal strip modelling, (a) 1.8 State E-plane @ 1.8 GHz, (b) 1.8 State H-plane @ 1.8 GHz,

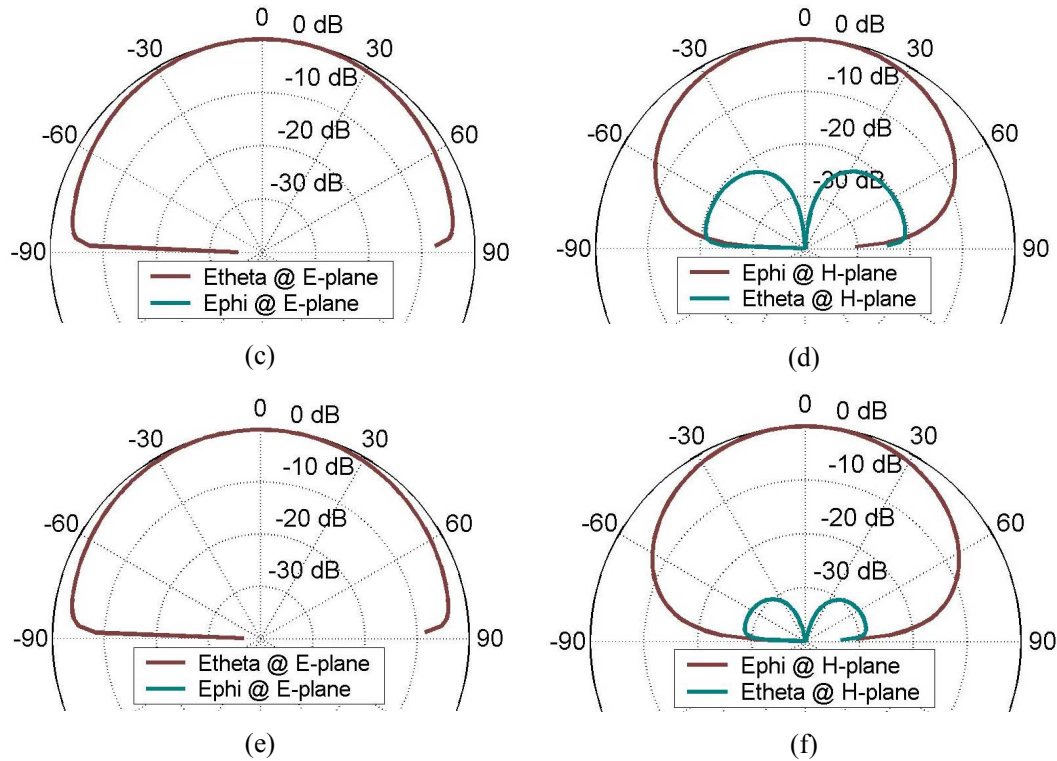


**Figure 5.21 (cont'd):** Radiation pattern simulation results optimized hybrid re-configurable (triple-frequency) microstrip patch antenna single stub configuration with metal strip modelling,

(c) 1.9 State E-plane @ 1.9 GHz, (d) 1.9 State H-plane @ 1.9 GHz,  
(e) 2.4 State E-plane @ 2.4 GHz, (f) 2.4 State H-plane @ 2.4 GHz.

#### 5.4.2. Double Stub Configuration

Hybrid re-configurable (triple-frequency) microstrip patch antenna with double stub configuration is an even more complex structure. This configuration has a dimensions starting from 50  $\mu\text{m}$  to 40.8 mm, in only azimuth plane. In elevation the sizes changes from 0.2  $\mu\text{m}$  to 2  $\mu\text{m}$ . The huge aspect ratio in azimuth challenges the stability of simulations. Up to now only single frequency state simulation of this hybrid structure configuration could be completed (Figure 5.22). And antenna structure could not be measured yet in spite of all parts are manufactured but hybridized as a single structure.

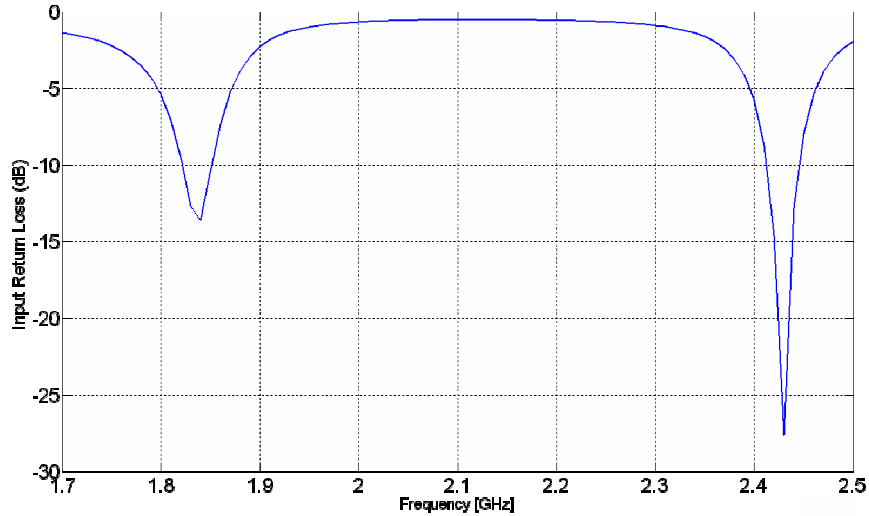


**Figure 5.22:** Simulation results of optimized hybrid re-configurable (triple-frequency) microstrip patch antenna double stub configuration including RF MEMS switches at 2.4 GHz state (all switches are at ON state)

### 5.5. Summary

Yet two hybrid re-configurable (triple-frequency) microstrip patch antenna structures including its switches and corresponding stubs are studied with a lot of research and design effort. The inset length is electronically changed like in integrated re-configurable (dual-frequency) microstrip patch antenna design. Furthermore, in these antennas the slot effective length is changed to add the third frequency to multi-frequency structure.

In this study the main objective was implementing two different scaled devices together as a ‘hybrid’ structure. It was expected that there would be some difficulties till designs and fabrications are completed. As it is explained in this chapter exhaustively, at almost each step (including the manufacturing) in the study, there were some difficulties to be overcome, and some to be lived with, as best as possible.

To sum up, in addition to the design-detail-highlights summarized in Chapter 4, especially in re-configurable multi-frequency microstrip patch antenna designs like this, switch actuation architecture is very important. In other words, the actuation architecture becomes more challenging as number of resonance frequencies to operate increases. Here in this structure only three resonance frequencies are valid but it is still very challenging to operate in each one individually when switch actuations are concerned. Therefore one should consider frequency switching architecture from the beginning of such a design effort.

When graphs are examined, it can be observed in Figure 5.20 that there is a quite good agreement with simulation and measurement results. In fact, as an antenna working principle, only 2.4 GHz State could be realized, which is the only actual design goal case. And even in that state, the better proposed matching (-24 dB) is accomplished as -21 dB. In addition, although matching values of 1.8 GHz and 1.9 GHz States could not be designed because of shared inset matching situation in single stub configuration, the measurement results are still very close to simulation results.

If radiation pattern results are evaluated, it could be observed that there is not any cross-polarization at 1.8 GHz resonance and there is a very little cross-polarization at 2.4 GHz and enough but still a noticeable cross-polarization at 1.9 GHz resonances. The main reason for the lowest and highest resonance has unnoticeable cross coupling is the switches on the slot are at OFF state. When those switches are at OFF state, there is a valid isolation and thus not any current flow through corresponding stub, which has a perpendicular path to signal flow to the radiation edge. That perpendicular current flow when slot switches are ON ends up with an increase in E-theta at H-plane, in spite of being followed by an effective-quarter-wavelength long grounded stub. In ideal case, that stub is at a length that from the switch, there is a true open circuit so that there would be no leakage at all to cross-couple the radiation. One of the suggested methods to decrease the effect of that radial stub could be lengthening the rectangular section more and increasing the distance from sides of the patch.

Moreover on radiation characteristics; note that HFSS is a 3D EM simulator that employs FEM whereas Ensemble is a 2.5D EM simulator employing MOM. Therefore HFSS results in a larger number of unknowns compared to Ensemble in the analysis of same structure. The antenna structure studied in this section is quite complex and HFSS fails to simulate this structure due to memory limitations. Hence, radiation characteristics of the antenna are simulated by Ansoft Ensemble rather than Ansoft HFSS. While simulating the radiation pattern in HFSS, the size of the ground plane is defined by the designer. And the antenna is enclosed by a box to limit the solution space. However the ground plane is assumed to be infinite in Ensemble. Besides that the excitation port should be defined on one of the faces of bounding box in HFSS. These differences in the simulation setup might have caused the symmetrical pattern in the E-plane obtained by Ensemble, as opposed to the tilted pattern obtained by HFSS for the integrated antenna.

Similar well simulation – measurement agreement is also expected for hybrid re-configurable (triple-frequency) microstrip patch antenna double stub configuration. In this configuration, also input return losses are supposed to be better, as the structure is being much closer to the ideal model. As soon as wire-bonding process is completed in that configuration, the measurements are going to be completed.

## CHAPTER VI

### CONCLUSION AND FUTURE WORK

In this thesis work, main objective was to demonstrate complete design – manufacture and test phases of re-configurable multi-frequency microstrip antennas. This study mainly focussed on re-configurability by impedance matching, because it was very challenging to obtain good impedance matching at more than one frequency at all and same time. Here RF MEMS switches are used to change the effective length of the inset, to adjust the admittance of the complete structure while operating at two separate frequency bands with the same input impedance, polarization, directivity, radiation characteristics within these bands. Thus, it has been shown that better resonances could be achieved by re-configurability in microstrip patch antennas with some modifications, especially within inset on the patch, one at a time.

In addition, a group of RF MEMS switch is placed in the slot to add another resonance frequency as in triple-frequency microstrip patch antenna study. This provides new opportunities to change slot dimensions and shapes, presented in Chapter 2. Therefore different frequency ratios within different frequency bands could be achieved with this suggested method. Let's remember that, these re-configurable structures are good for saving space, as better and many resonances are achieved by smaller structures in size without any other degradation in polarization, directivity and radiation characteristics.

In Chapter 4, included measurement results proved that design simulation results are in good agreement, which are finalized with expected results. This also shows that

the design studies are not only utopia, but could easily be realized with correct and fine fabrication. However the main concern would be stub dimension and position dependencies and sensitivity on better resonance and radiation characteristics.

Another outcome in this study was, experiencing two different manufacturing approaches: integrated and hybrid structures. Besides the different feed techniques, the achieved experience from these two methods suggests some cons and pros of each type. Main advantage of integrated structure is, not having any connection problems during the fabrication, whereas wire bonding is required in hybrid structure. This is very important, because wire-bonding is a special technique to connect two surfaces, which needs a very unique fine engineering. On the other hand, as MEMS fabrication in integrated structure is applied, antenna design is restricted by fewer substrate type and smaller dimensions; especially thickness is the biggest concern. The most important advantage of hybrid structure is, the wide catalogue of substrate is applicable together with smaller / bigger dimensions, both in azimuth and elevation. This opportunity relaxes the antenna designer more, and leaves the RF MEMS switches as only a third party device to change effective- slot and inset-lengths, which is the most critical driving point in integrated structure because of same restricting fabrication steps.

Moreover, in this research two different scaled devices are studied (Chapter 5) and tried to be implemented together for re-configurability purpose. Although the metal strips used in stead of RF MEMS switches in triple frequency antenna during the measurements, good agreements with simulation and measurement results are observed. Of course, there are still works to be completed and developed, such as microstrip manufacturing and wire-bonding between RF MEMS switches and the patch in triple-frequency antenna. One other future work, especially in design, is decreasing the dimension dependency which causes unexpected measurement results and less repeatability. This could be achieved by wider stubs or finer manufacturing capabilities, mainly. Also better switch actuation architectures should be arranged for more complex antenna performances (such as modes, or more resonances etc.). Another future work is, having more control on stub effects on

resonances, with or without switches. Also, no need to specify, more switches for different effective lengths would increase resonance frequencies together with better matches.

To conclude, it would be meaningful to emphasize that although publishing date is December 2006, this two year long thesis research started in the end of 2002; all the design effort spent by writer presented here are continued until 2004 together with their fabrication and measurements (by Kağan Topallı, Mehmet Ünlü, İpek İstanbulluoğlu, Halil İbrahim Aksoy, Ufuk Temoçin, Mustafa Seçmen). One of the biggest accomplishments during the research was the experience achieved during the design and fabrication of the antennas while employing RF MEMS switches both in hybrid and as integrated, at that time [33, 35, 37 – 39]. That is gladsome that at the time when this research is first published, same remarks are experienced, similar conclusions are observed by the other researchers in the literature for several similar applications – studies [28 – 31]. This thesis is truly a design study and could be classified as one of the first series of re-configurable antenna studies with RF MEMS switches employed in the literature, as the design and manufacturing year is considered. Today, there are many journals and books in the literature, together with some on going researches on antenna re-configurability using RF MEMS switches. Hopefully more practical designs in the future and the theoretical modelling of this and other studies would continue in the next research phase with more support together with new or continuing sponsors or partners.

## REFERENCES

- [1] Porath R., "Theory of Miniaturized Shorting-Post Microstrip Antennas," IEEE Trans. on Antennas and Propagation, Volume 48, Issue 1, Page(s): 41 – 47, Jan 2000.
- [2] Wong K. L., "Compact and Broadband Microstrip Antennas," John Wiley & Sons, Inc. 2002.
- [3] Bafrooei P.M., Shafai L., "Characteristics of Single- and Double-Layer Microstrip Square-Ring Antennas," IEEE Trans. on Antennas and Propagation, Volume 47, Issue 10, Page(s): 1633 – 1639, Oct. 1999.
- [4] Chen W. S., Wu C. K., Wong K. L., "Novel Compact Circularly Polarized Square Microstrip Antenna," IEEE Trans. on Antennas and Propagation, Volume 49, Issue 3, Page(s): 340 – 342, Mar. 2001.
- [5] Wong K. L., Hsu W.H., "A Broad-Band Rectangular Patch Antenna with a Pair of Wide Slits," IEEE Trans. on Antennas and Propagation, Volume 49, Issue 9, Page(s): 1345 – 1347, Sept 2001.
- [6] Erdemli Y.E., Sertel K., Gilbert R.A., Wright D.E., Volakis J.L., "Frequency-Selective Surfaces to enhance Performance of Broad-Band Reconfigurable Arrays," IEEE Trans. on Antennas and Propagation, Volume 50, Issue 12, Page(s): 1716 – 1724, Dec. 2002.
- [7] Lu J. H., Tang C. L., Wong K. L., "Novel Dual-Frequency and Broad-Band Designs of Slot-Loaded Equilateral Triangular Microstrip Antennas," IEEE Trans. on Antennas and Propagation, Volume 48, Issue 7, Page(s): 1048 – 1054, July 2000.

- [8] Sze J. Y., Wong K. L., "Slotted Rectangular Microstrip Antenna for Bandwidth Enhancement," IEEE Trans. on Antennas and Propagation, Volume 48, Issue 8, Page(s): 1149 – 1152, Aug. 2000.
- [9] Wang B., Lo Y., "Microstrip Antennas for Dual-Frequency Operation," IEEE Trans. on Antennas and Propagation, Volume 32, Issue 9, Page(s): 938 – 943, Sep. 1984.
- [10] Maci S.; Gentili G.B., "Dual Frequency Patch Antennas," IEEE Antennas and Propagation Magazine, Volume 39, Issue 6, Page(s): 13 – 20, Dec. 1997.
- [11] Yang K. P., Wong K. L., "Dual-Band Circularly-Polarized Square Microstrip Antenna," IEEE Trans. on Antennas and Propagation, Volume 49, Issue 3, Page(s): 377 – 382, March 2001.
- [12] Aissat H., Cirio L., Grzeskowiak M., Laheurte J.-M., Picon O., "Reconfigurable Circularly Polarized Antenna for Short-Range Communication Systems," IEEE Trans. on Microwave Theory and Techniques, Volume 54, Issue 6, Part 2, Page(s): 2856 – 2863, June 2006.
- [13] Sor, J., Chang C. C., Yongxi O., Itoh, T., "A Reconfigurable Leaky-Wave / Patch Microstrip Aperture for Phased-Array Applications," IEEE Trans. on Microwave Theory and Techniques, Volume 50, Issue 8, Page(s): 1877 – 1884, Aug 2002.
- [14] Yang S.-L.S., Luk K.M., "Design of a Wide-Band L-Probe Patch Antenna for Pattern Reconfiguration or Diversity Applications," IEEE Trans. on Antennas and Propagation, Volume 54, Issue 2, Part 1, Page(s): 433 – 438, Feb 2006.
- [15] Gianvittorio J.P., Rahmat-Samii Y., "Reconfigurable Patch Antennas for Steerable Reflectarray Applications," IEEE Trans. on Antennas and Propagation, Volume 54, Issue 5, Part 1, Page(s): 1388 – 1392, May 2006.
- [16] Cetiner B.A., Akay E., Sengul E., Ayanoglu E., "A MIMO System with Multifunctional Reconfigurable Antennas," IEEE Antennas and Wireless Propagation Letters, Volume 5, Issue 1, Page(s): 463 – 466, Dec 2006.
- [17] Aberle J.T., Oh S. H., Auckland D.T., Rogers S.D., "Reconfigurable Antennas for Wireless Devices," IEEE Antennas and Propagation Magazine, Volume 45, Issue 6, Page(s): 148 – 154, Dec 2003.

- [18] Brown E.R., "On the Gain of a Reconfigurable-Aperture Antenna," IEEE Trans. on Antennas and Propagation, Volume 49, Issue 10, Page(s): 1357 – 1362, Oct 2001.
- [19] Jin N., Yang F., Rahmat-Samii Y., "A Novel Patch Antenna with Switchable Slot (PASS): Dual-Frequency Operation with Reversed Circular Polarizations," IEEE Trans. on Antennas and Propagation, Volume 54, Issue 3, Page(s): 1031 – 1034, March 2006.
- [20] Langer J.-C., Zou J., Liu C., Bernhard J.T., "Micromachined Reconfigurable Out-of-Plane Microstrip Patch Antenna Using Plastic Deformation Magnetic Actuation," IEEE Microwave and Wireless Components Letters, Volume 13, Issue 3, Page(s): 120 – 122, March 2003.
- [21] Huff G.H., Feng J., Zhang S., Bernhard J.T., "A Novel Radiation Pattern and Frequency Reconfigurable Single turn Square Spiral Microstrip Antenna," IEEE Microwave and Wireless Components Letters, Volume 13, Issue 2, Page(s): 57 – 59, Feb. 2003.
- [22] Huff G.H., Bernhard J.T., "Integration of Packaged RF MEMS Switches with Radiation Pattern Reconfigurable Square Spiral Microstrip Antennas," IEEE Trans. on Antennas and Propagation, Volume 54, Issue 2, Page(s): 464 – 469, Feb 2006.
- [23] Yang F., Rahmat-Samii Y., "Switchable Dual-Band Circularly Polarised Patch Antenna with Single Feed," IEEE Antennas and Propagation Letters, Volume 37, Issue 16, Page(s): 1002 – 1003, Aug 2001.
- [24] Yang F., Rahmat-Samii Y., "Patch Antenna with Switchable Slot (PASS): Dual-Frequency Operation," IEEE Microwave and Optical Technology Letters, Volume 31, Issue 3, Page(s): 165 – 168, Nov 2001.
- [25] Yang F., Rahmat-Samii Y., "A Reconfigurable Patch Antenna Using Switchable Slots for circular Polarization Diversity," IEEE Microwave and Wireless Components Letters, Volume 12, Issue 3, Page(s): 96 – 98, March 2002.
- [26] Cetiner B.A., Qian J.Y., Chang H.P., Bachman M., Li G.P.; De Flaviis F., "Monolithic Integration of RF MEMS Switches with a Diversity Antenna on PCB Substrate," IEEE Trans. on Microwave Theory and Techniques, Volume 51, Issue 1, Part 2, Page(s): 332 – 335, Jan. 2003.

- [27] Goteti R.V., Jackson R.E. Jr., Ramadoss R., "MEMS-Based Frequency Switchable Microstrip Patch Antenna Fabricated Using Printed Circuit Processing Techniques," IEEE Antennas and Propagation Letters, Volume 5, Page(s): 228 – 230, 2006.
- [28] Yang F., Rahmat-Samii Y., "Patch Antennas with Switchable Slots (PASS) in Wireless Communications: Concepts, Designs, and Applications," IEEE Antennas and Propagation Magazine, Volume 47, Issue 2, Page(s): 13 – 29, April 2005.
- [29] Pringle L.N., Harms P.H., Blalock S.P., Kiesel G.N., Kuster E.J., Friederich P.G., Prado R.J., Morris J.M., Smith G.S., "A Reconfigurable Aperture Antenna Based on Switched Links Between Electrically Small Metallic Patches," IEEE Trans. on Antennas and Propagation, Volume 52, Issue 6, Page(s): 1434 – 1445, June 2004.
- [30] Jung C. W., Lee M. J., Li G.P., De Flaviis F., "Reconfigurable Scan-Beam Single-Arm Spiral Antenna Integrated with RF-MEMS Switches," IEEE Trans. on Antennas and Propagation, Volume 54, Issue 2, Part 1, Page(s): 455 – 463, Feb 2006.
- [31] Anagnostou D.E., Zheng G., Chryssomallis M.T., Lyke J.C., Ponchak G.E., Papapolymerou J., Christodoulou C.G., "Design, Fabrication, and Measurements of an RF-MEMS-Based Self-Similar Reconfigurable Antenna," IEEE Trans. on Antennas and Propagation, Volume 54, Issue 2, Page(s): 422 – 432, Feb 2006.
- [32] Balanis C. A., Antenna Theory, 3rd ed., Wiley, New York, 2005.
- [33] Onat S., Demir Ş., Alatan L., "Farklı Yarık Şekilli Çift-Frekanslı Mikroşerit Yama Anten Yapıları", URSI-Türkiye'2004 İkinci Ulusal Kongresi, Ankara, Türkiye, p.354-356, Eylül 08-10 2004 (in Turkish).
- [34] Zhang L. X., Zhao Y.-P., "Electromechanical model of RF MEMS Switches," Microsystems Technologies, Volume 9, Page(s): 420 – 426, 2003.
- [35] Topallı K., Sağkol H., Ünlü M., Onat S., Aydın Çivi Ö., Demir Ş., Koç S., Alatan L., Akın T., "Microwave Circuit Components and Reconfigurable Antennas Using RF MEMS Technology," Proceeding of 4th COST284 Management Committee Meeting & Workshop with INICA, Berlin-Germany, 19 September 2003.

- [36] Temoçin E. U., Topallı K., Ünlü M., İstanbulluoğlu İ., Atasoy H. İ., Bayraktar Ö., Demir Ş., Aydın Çivi Ö., Koç S., Akın T., “Eşdüzlemsel Dalga Klavuzundan Mikroşerit Hatta Geçiş Üzerine Çalışmalar”, URSI Ulusal Konferansı 2006, Hacettepe, Ankara, Türkiye, p. 448-450, 6-8 Eylül 2006. (in Turkish).
- [37] Onat S., Ünlü M., Alatan L., Demir Ş., Akın T., “Design of a re-configurable dual frequency microstrip antenna with integrated RF MEMS switches, 2005 IEEE International Antennas and Propagation Symposium, Washington, DC-USA, vol.2A p.384-387, July 3-8 2005.
- [38] Onat S., Alatan L., Demir Ş., “RF MEMS Anahtar Kontrollü Çoklu-Frekans Anten”, URSI-Türkiye’2004 İkinci Ulusal Kongresi, Ankara, Türkiye, P.99-101, Eylül 08-10 2004 (In Turkish).
- [39] Onat S., Alatan L., Demir Ş., “Design Of Triple-Band Re-Configurable Microstrip Antenna Employing RF-MEMS Switches”, 2004 IEEE International Antennas and Propagation Symposium, Monterey, California-USA, vol.2 p.1812-1815, June 20-25 2004.
- [40] Sagkol H., “A Phase Shifter Using RF MEMS Technology,” M. Sc. Thesis, Middle East Technical University, September 2002.
- [41] Unlu M., “An Adjustable Impedance Matching Network Using RF MEMS Technology,” M. Sc. Thesis, Middle East Technical University, September 2003.
- [42] Rebeiz G., “RF MEMS Theory, Design, and Technology,” John Wiley & Sons, 2003.
- [43] Temoçin E. U., “Design and Implementation of Microwave Lumped Components and System Integration Using MEMS Technology,” M. Sc. Thesis, Middle East Technical University, September 2006.